

https://dspace.org/

A study of burden movement In submerged-arc furnaces

Dyason, Gavin John

2015-03-10
http://hdl.handle.net/10539/17217

Downloaded from a DSpace repository. https://dspace.org/

A Study of Burden Movement in Submerged-arc Furnaces

GAVIN JOHN DYASON

A dissertation submitted to the Faculty of Engineering, University of the Witwatersrand, Johannesburg for the Degree of Master of Science in Engineering.

Johannesburg, 1977.

UNDERTAKING

I certify that this is my own work and has not been submitted for a Master of Science degree at any other University.

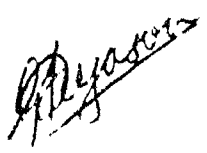

G.J. DYASON

November, 1977.

ACKNOWLEDGEMENTS

The author wishes to record his sincere appreciation for the assistance given by his supervisor, Dr. J.B. See.

Sincere thanks are extended to Professor R.P. King for his assistance and advice in the development and computer implementation of the mathematical models used in the investigation.

The National Institute for Metallurgy and the Ferro-Alloy Producers Association of South Africa provided the financial assistance which enabled the research to be undertaken and this financial support is gratefully acknowledged.

The assistance of the South African Atomic Energy Board, and in particular that of Mr. S.W. Smith, in the development and implementation of the experimental technique is gratefully acknowledged.

The assistance and co-operation provided by the production staff of Metalloys Limited, and in particular Messrs. Z. van der Walt, J.S. Stanbury, D. Hennessey, G. De Toit and W.A. Gericke made this investigation possible and this help is also gratefully acknowledged.

ABSTRACT

The mechanism of burden movement was investigated in two large industrial submerged-arc furnaces for the production of high-carbon ferromanganese. Detailed knowledge of the mechanism of burden movement and the influence of operating conditions on this movement will help to suggest means to increase the efficiency of the furnace.

The experimental technique was the stimulus-response technique using a radio-tracer input as the stimulus. Irradiated hematite or Hotazel manganese ore was used as the radio-tracer and the source of radio-activity in both these ores was the radioisotope Fe^{59}. This radioisotope was suitable for measurement of residence time distributions for the alloy phase but was not suitable for measurement of the residence time distributions for the slag phase. Consequently the analysis of the experiments was limited to the alloy phase.

Different techniques were used to introduce the radio-tracer to selected sites in the furnace. The response was determined by collection of samples during tappings and the radio-activity levels of these samples were then measured at the South African Atomic Energy Board to give the residence time distributions for each experiment. During each experiment the average values of the furnace operating parameters were recorded to indicate variations in furnace operation during the experiment.

The residence time distributions obtained were analysed by various techniques. Due to truncation of most of the residence time distributions, single parameter description of these distributions was only possible in three experiments. This analysis involved determination of the mean and variance of the residence time distributions. Comparison of experimentally measured mean residence times and calculated nominal mean residence times for these experiments verified the existence of stagnant zones within the furnace volume. The variance for these three residence time distributions showed that burden movement through the furnace could not be described by either of the two idealized patterns of flow - plug flow and mixed flow.

A composite model was developed to describe burden movement through the furnace. This model was developed by considering the mechanism and position of heat generation within the furnace, a qualitative picture of the inner structure of the furnace, the general form of the measured residence time distributions, and practical observations of the mode of burden descent through the furnace. The composite model consisted of a dispersed plug flow region in the upper regions of the furnace discharging into a constantly stirred tank reactor beneath the electrode tips.

Non-linear regression analysis of equations developed from the composite model permitted the selection of optimum values of model parameters to give computed curves which approximated the residence time distributions. Since the computed results used realistic values of the model parameters it was concluded

that the model was a valid representation of burden movement through the furnaces.

Attempts were made to determine quantitative correlations between operating parameters and the optimum model parameters. No important correlations were obtained and this appeared to be due to insufficient data and the complexity of furnace operation.

The rôle of factors such as the position of radiotracer addition, the energy input to the furnace, the mode of heat distribution in the furnace and variations in raw material feed rate was analysed to describe the influence of furnace operating conditions on the value of the model parameters. Although this qualitative analysis did not reveal any trends it did provide a means of analysing the results.

CONTENTS

	Page No.
LIST OF SYMBOLS AND ABBREVIATIONS	i
1. INTRODUCTION	1
2. THE PRODUCTION OF HIGH-CARBON FERROMANGANESE	
2.1. The production of high-carbon ferromanganese in the submerged-arc furnace	3
2.1.1. Basic chemistry of process	3
2.1.2. Electrical considerations	5
2.2. The production of high-carbon ferromanganese at Metalloys Limited	7
3. RADIO-TRACER TECHNIQUES FOR FLOW ANALYSIS	9
3.1. Application of radio-tracer techniques in pyrometallurgy	9
3.2. Residence time distributions in processing equipment	12
3.2.1. Single parameter descriptions of residence time distributions	15
3.3. Description of residence time distributions by flow models	16
3.3.1. The dispersion model	16
3.3.2. The tanks-in-series model	18
3.3.3. Composite models	18

Page No.

4. THE DEVELOPMENT OF A THEORETICAL MODEL FOR BURDEN MOVEMENT IN THE SUBMERGED-ARC FURNACE 21

4.1. The generation of heat in submerged-arc furnaces 21

4.2. The inner structure of the submerged-arc furnace for the production of high-carbon ferromanganese 25

4.3. The theoretical model of burden movement in submerged-arc furnaces producing high-carbon ferromanganese 28

4.4. The general shape of the experimentally determined residence time distributions 31

4.5. Mathematical description of the theoretical model of burden movement in the submerged-arc furnace 33

5. EXPERIMENTAL 37

5.1. Description of furnaces 37

5.1.1. Design parameters 37

5.1.2. Charging of raw materials 38

5.1.3. Tapping of furnaces 39

5.1.4. Removal and treatment of waste gases 39

5.2. The radio-tracer input to the furnace 40

5.2.1. Choice of suitable radio-tracer material 40

5.2.2. Introduction of the radio-tracer into the furnace 42

5.3. Monitoring of the furnace response to the radio-tracer input 45

5.4. Data logging during each experiment 47

5.5. The experimental campaign 48

5.5.1. Experiments on furnace M11 with 48 MVA transformers 48

5.5.2. Experiments on furnace M10 with 48 MVA transformers 49

5.5.3. Experiments on furnace M11 with 75 MVA transformers 49

		Page No.
6.	RESULTS	51
7.	ANALYSIS OF RESULTS	53
	7.1. Introduction	53
	7.2. Correlations between the average operating parameters recorded during the experimentation	56
	7.3. Single parameter description of residence time distributions	60
	7.4. Description of residence time distributions by means of a theoretical model	63
	7.4.1. Experiments on furnace M11 with 48 MVA transformers	66
	7.4.2. Experiments on furnace M10 with 48 MVA transformers	66
	7.4.3. Experiments on furnace M11 with 75 MVA transformers	66
	7.5. Correlations between model parameters and average furnace operating parameters	67
8.	DISCUSSION	68
	8.1. Introduction	68
	8.2. The experimental procedure	70
	8.3. Correlations between average furnace operating parameters	72
	8.4. Single parameter description of residence time distributions	74
	8.4.1. The mean residence time, $\bar{t}a$	74
	8.4.2. The variance, σ^2	76

Page No.

8.5. Description of residence time distributions by means of a theoretical model 77

8.5.1. Introduction 77

8.5.2. Sensitivity of model parameters to regression analysis 78

8.5.3. Analysis of model parameters 79

8.5.4. Effect of position of radio-tracer input on mean residence times 80

8.5.4.1. The dispersed plug flow region of the furnace 81

8.5.4.2. The C.S.T.R. region of the furnace 84

8.5.5. Influence of operating conditions on mean residence time in dispersed plug flow region 85

8.5.5.1. Radio-tracer inputs to charging shafts 89

8.5.5.2. Radio-tracer inputs to furnace bunkers 91

8.5.6. The alloy inventory volume in the furnace hearth and the mean residence time in the C.S.T.R. region of the furnace 93

8.5.7. The overall mean residence time in the furnace, $\bar{t}_{fce}$ 95

8.5.8. Significance of analysis of the model parameters 96

8.6. Future Work 97

Page No.

9. CONCLUSION 100

APPENDIX A. Computer program for single parameter evaluation of residence time distribution

APPENDIX B. Computer optimization of parameters in equations to describe residence time distributions

APPENDIX C. Estimation of mass capacity of furnaces M10 and M11

REFERENCES

LIST OF SYMBOLS AND ABBREVIATIONS

The more important symbols employed in the text are as follows:-

C	Concentration of radio-tracer.
Co	Initial concentration of radio-tracer.
D	The dispersion number.
K	Heat distribution factor.
t	Time (hours).
$\bar{t}n$	Nominal mean residence time (hours).
$\bar{t}r$	True mean residence time (hours).
$\bar{t}a$	Experimentally calculated mean residence time using the technique of moments (hours).
$\bar{t}$	Computed mean residence time in the dispersed plug flow region of the furnace (hours).
$\bar{t}inv$	Computed mean residence time in the constantly stirred tank reactor region of the furnace (hours).
$\bar{t}fce$	Computed overall mean residence time of the furnace ($= \bar{t} + \bar{t}inv$) (hours).
V	Volume (m^3).

Vinv	Computed alloy inventory volume (m^3).
θ	Dimensionless time in units of nominal mean residence time ($= t/\bar{t}$).
ν	Volumetric feedrate (m^3/hour).

The more important abbreviations employed in the text are:-

C.S.T.R.	Constantly stirred tank reactor.
e, exp	Exponential.
erf	Error function.

1. INTRODUCTION

This investigation was undertaken to study burden movement in two large industrial submerged-arc furnaces for the production of high-carbon ferromanganese. The mechanism of burden movement in industrial submerged-arc furnaces for the production of high-carbon ferromanganese was considered an important area for research since South Africa is one of the major producers of high-carbon ferromanganese in the Western World.[1]

The objectives of this investigation were:-

(i) To establish an experimental technique for measurement of residence time distributions for a submerged-arc furnace.

(ii) To determine time constants for the furnace by analysis of the residence time distributions.

(iii) To develop flow models to describe burden movement through the furnace and interpret the physical meaning of the model parameters.

(iv) To assess the effect of operating conditions on burden movement through the furnace.

The stimulus-response technique, using a radio-tracer input as stimulus, was used to measure the residence time distributions. By application of the technique of moments the time constants for the furnace were calculated from the residence time distributions. By consideration of the mechanism of heat generation within the furnace, and observation of burden movement during

furnace operation, composite models to describe burden movement through the furnace were developed. These composite models consisted of a network system of ideal flow reactors in series and parallel. Wherever possible the physical meaning of the values obtained for the model parameters were determined in terms of conditions of furnace operation.

The information obtained in the investigation has provided the basic technique for extensive investigation into the mechanism of burden movement through submerged-arc furnaces. Once the mechanism of burden movement through submerged-arc furnaces is known, process control may be improved and furnace throughput may be optimized.

To achieve the objectives of the investigation a series of radio-tracer experiments were performed on two submerged-arc furnaces operated by Metalloys Limited, Meyerton, Transvaal.

2. THE PRODUCTION OF HIGH-CARBON FERROMANGANESE

2.1. The production of high-carbon ferromanganese in the submerged-arc furnace

The discard slag process and the enriched slag process are used to produce high-carbon ferromanganese in the submerged-arc furnace.[2] The chemical analysis of the high-carbon ferromanganese, in mass per cent, is 70 to 80 Mn, 6 to 8 C, less than 0,5 Si, usually less than 0,1 P, with the balance Fe.

Discard slags contain 12 to 14 mass per cent Mn whilst enriched slags contain 25 to 40 mass per cent of the Mn present.[2] In the discard slag process the desired slag properties are achieved by fluxing additions of lime in contrast to the enriched slag process in which the burden is largely self fluxing with MnO fulfilling the same function as the lime. Small additions of quartzite may be made in the enriched slag process. The enriched slag is used as a raw material in the production of silico-manganese alloy.

2.1.1. Basic chemistry of process

Manganese oxides thermally decompose on heating as follows:-[2]

$2MnO_2 \rightarrow Mn_2O_3 + \frac{1}{2}O_2$ at 527°C

$3Mn_2O_3 \rightarrow 2Mn_3O_4 + \frac{1}{2}O_2$ at 940°C

$Mn_3O_4 \rightarrow 3MnO + \frac{1}{2}O_2$ at 1560°C (the melting point of Mn_3O_4)

Hence only MnO is involved in the actual reduction processes.

Only elemental carbon will reduce MnO. The products of the reduction of MnO are either metallic manganese and CO or manganese carbide and CO. These reactions become thermodynamically favourable at 1420°C for metallic manganese production and at 1280°C for Mn_7C_3 production.[2] Since carbide formation is thermodynamically more favourable it is not possible to produce a low-carbon ferromanganese by carbo-thermic reduction. From the manganese-carbon phase diagram it may be observed that other carbides such as $Mn_{23}C_6$ may also be formed.[2]

Hematite present in the ore is reduced in the upper regions of the burden by stepwise reduction to FeO. The FeO is then reduced by either CO or elemental carbon to the metallic state or the carbide, Fe_3C. The metallic and carbide phases produced combine to form the primary alloy.

Most of the phosphorus in the burden is reduced to elemental phosphorus, but only about 30 per cent enters the alloy, and the balance is volatilized.[2] The small amounts of silicon in the alloy are produced by the reduction of silica with carbon. Most of the sulphur enters the slag or is lost in the furnace gases.[3]

If localized overheating occurs metallic manganese (boiling point 2095°C) evaporates. This vapour may either recondense on reaching the upper, cooler furnace regions or be reoxidized to MnO. If this fine MnO leaves the furnace brown manganese "smoke" results.[4]

The unreduced oxides combine in the lower regions of the burden to form the slag phase. This phase should have

a low melting point, be fluid, and have a high basicity.[2, 5]

In practice slags are required to have a classical basicity ratio, $\frac{CaO + MgO}{SiO_2}$, greater than 1,1.[2] High basicity ensures a low MnO content in the slag and results in a low silicon content in the alloy.[2, 6] However high basicity also results in a high slag melting point.[2] Hence to achieve optimum slag properties it is necessary to compromise between a low melting point and high basicity. The slag composition, and hence its properties may be controlled by flux additions and by varying the extent of reduction of MnO.

2.1.2. Electrical considerations

Submerged-arc furnaces are cylindrical, three electrode, 3-phase, low shaft electric furnaces. The furnaces have either open, semi-closed, or fully closed tops. The three electrodes are sited at the vertices of an equilateral triangle and are of the continuous self-baking Söderberg type.

Electrical energy is delivered to the electrodes via power transformers which step down the supply voltage from 33 kV to voltages between 100 to 400 V. In modern large furnaces three single phase transformers are usually used. These are either star- or delta-connected on the primary side and usually delta-connected on the secondary side to reduce the current flowing through the secondary windings.[7]

From the electrodes heat is generated along various conduction paths. This heat generation will be discussed

in greater detail in Section 4.1.

It is important to maintain the correct temperature profile within the electrode to ensure correct electrode baking and to prevent oxidation of the electrode paste.[8] For a given rate of electrode consumption, paste quality, and electrode cross-sectional area, the electrode current density determines the temperature profile. Hence each particular electrode has a maximum current carrying capacity.

To avoid excessive arc formation which results in overheating and manganese evaporation, operational voltages must be kept relatively low.[2] Hence the desired power input can only be achieved with relatively high electrode currents. Since current density is limited, these furnaces require electrodes of greater diameter than are required for similar furnaces producing high-carbon ferrochromium.

The operating resistance of the furnace is determined by the burden resistivity, the electrode penetration and the depth and properties of the slag layer.

2.2. The production of high-carbon ferromanganese at Metalloys Limited

The total rated MVA of high-carbon ferromanganese furnaces in South Africa is 207 MVA.[9, 10] The furnaces at Metalloys Limited have a total rated MVA of 169,4 MVA in two separate plants which are both situated at the Kookfontein Works near Meyerton, Transvaal. In the older plant there are four high-carbon ferromanganese furnaces with design ratings from 10 to 13,2 MVA and in the newer plant there are two furnaces both of which were initially equipped with 48 MVA transformers. The two large new furnaces have superior instrumentation and control, and hence the radio-tracer experiments were limited to these furnaces.

At Metalloys Limited high-carbon ferromanganese is produced by both the discard and the enriched slag processes. As this investigation was limited to furnaces producing a discard slag, only this process will be described.

Local raw materials are used. Ores are the "jasperlite" type from the Kuruman-Postmasburg area[11] and the most important carbonaceous reducing agent, coal, is from the Delmas area.[12] Metallurgical coke from various sources is also used as a reducing agent. Small fluxing additions of either quartz or dolomite are made. When the slag-to-alloy ratio drops below 0,5 high-grade slag is returned to the furnace to improve this ratio.[12] The return high-grade slag increases the furnace resistance. Small amounts of unsaleable ferromanganese are returned to the furnace.

Only ore with the minimum amount of fines is used and

raw material preparation is limited to screening out the -3 mm fraction of the Delmas coal.[13]

The low cost of manganese ore means that discard slags may contain as much as 22 mass per cent manganese. Manganese recovery is sacrificed to yield maximum output and the lowest conversion costs per tonne of alloy.[14] Blending of South African ores and this practice produces an essentially self-fluxing burden.

If coal is used as the primary reducing agent the burden resistance is increased and the electrodes penetrate more deeply, decreasing the losses of manganese vapour. However the high volatile content of the coal does create problems in treatment of the waste gas.

Operation is carried out with a constant depth of slag. The constant depth is maintained by positioning the slag tap hole about one metre vertically above the alloy tap hole. Under these conditions manganese evaporation and the formation of brown MnO "smoke" is eliminated.

3. RADIO-TRACER TECHNIQUES FOR FLOW ANALYSIS

3.1. Application of radio-tracer techniques in pyrometallurgy

It is of interest to summarize the applications of radio-tracer techniques to pyrometallurgical processes. These applications include investigation of burden movement in rotary kilns,[15-19] iron and steelmaking furnaces,[20-36] reverberatory furnaces,[23, 37] and submerged-arc furnaces.[39, 40]

Several aspects related to material movement in rotary kilns have been investigated.[15-19] These include measurements of; the rate of passage of material through the kiln, the extent of longitudinal mixing along the kiln length, the effect of lifters and baffles on material movement, the extent of formation of dust and the extent of recirculation of components of the charge.

Blast furnaces used for production of pig iron have been extensively investigated by means of radio-tracer techniques. Overall residence time distribution measurements have been used to measure the retention times of various burden components and the variation of the rate of descent of the burden with the position of the radio-tracer input.[20-26] The factors influencing the degree of mixing of molten products in the hearth crucible have been determined by means of mixing studies using radio-tracers.[21, 22, 27] Transit times between various levels in the furnace[20, 21, 25] and blast-air movement within the furnace[20, 26] have been monitored.

Radio-tracer techniques have shown that the operation

of furnaces for continuous production of sponge iron pellets is very stable and that the rate of burden descent along different verticals is relatively uniform.[15, 25, 28]

Several processes for the production and refining of steel have been investigated. In open hearth furnaces metal movement has been shown to be mainly parallel to the hearth floor.[25, 29] This movement has been described by the dispersion model.[30, 31] The flow of steel in the WORCRA steel refiner has been studied using radio-tracer techniques and has been modelled using both dispersion and tanks-in-series models.[32-34] Mixing studies in the vacuum refining processes known as the R.H.-Vacuum process[26, 35] and the ASEA-SKF process[22, 36] have been performed using radio-tracers.

Radio-tracer techniques have shown that ideally the first half of a reverberatory furnace smelting copper concentrates should act as a perfect mixer with the balance of the furnace volume acting as a plug flow reactor.[23, 37] For the smelting of copper-nickel concentrates in the six-in-line electric furnace radio-tracer techniques have shown that electromagnetic stirring results in a greater degree of mixing than in the reverberatory furnace which serves the same function.[38]

Submerged-arc furnaces have been investigated using radio-tracer techniques. Time constants and residence time distributions have been measured for a furnace producing ferrochromium.[39] The movement of "alloy forming" components of the burden was modelled using a composite model consisting of a plug flow reactor in series with a perfect mixer. The movement of "slag forming" components

of the burden was modelled using a dispersed plug flow model. Total residence time distributions for lime and coke have been measured for a submerged-arc furnace producing calcium carbide.[40]

Other applications of radio-tracer techniques include:-

(i) Measurement of the movement of coal in continuous vertical retorts.[41]

(ii) Study of the behaviour of metals during fractional distillation.[42]

(iii) Study of the movement of aluminium in an aluminium reduction cell.[43]

(iv) Measurement of furnace lining wear.[44-46]

The application of radio-tracer techniques to pyrometallurgy is more fully described elsewhere.[47] Consideration of these applications of radio-tracer techniques to pyrometallurgy, provided valuable information which was used in development of the experimental technique for this investigation.

3.2. Residence time distributions in processing equipment

The concept of age distribution functions was introduced to deal with non-ideal flow in processing equipment. Functions relevant to this investigation are defined and briefly described. A complete description and full derivation of these functions is readily available.[48-51]

The nominal mean residence time, $\bar{t}n$, of fluid flowing through a closed vessel under steady state conditions is;

$$\bar{t}n = V/v \qquad (1)$$

where

V = volume of fluid in the vessel,
and
v = volumetric flowrate of fluid through the vessel.

Time, t, may be expressed in units of nominal mean residence time giving a dimensionless measure of time, θ, viz.,

$$\theta = t/\bar{t}n \qquad (2)$$

If age is defined as the time spent by an element of fluid in the vessel the following age distribution functions may be defined;

(i) F(θ) which gives the fraction of fluid having ages between 0 and θ at the moment of leaving the vessel.

(ii) $E(\theta)d\theta$ which gives the fraction of fluid having ages between θ and $\theta+d\theta$ at the moment of leaving the vessel.

(iii) $I(\theta)d\theta$ which gives the fraction of fluid in the vessel having ages between θ and $\theta+d\theta$.

The following relationships hold for these functions:-

$$F(\infty) = 1 \tag{3}$$

$$\int_0^\infty E(\theta)d\theta = 1 \tag{4}$$

$$E(\theta) = dF(\theta)/d\theta = -dI(\theta)/d\theta \tag{5}$$

The forms of the age distribution functions define the residence time distribution of fluid in the vessel. These functions may be measured for a vessel by means of the stimulus-response technique.

Assume a property of the inlet fluid to a vessel changes to a new value for an instant before returning to its original value. If the initial concentration in the vessel of fluid with the new property is Co, and the concentration of fluid with the new property in the outflow at time θ latter is $C(\theta)$,

$$E(\theta) = C(\theta)/Co \tag{6}$$

It can be shown that

$$Co = \int_0^\infty C(\theta)d\theta \tag{7}$$

A "pulse" change of property of fluid in the inflow may be mathematically described by the Dirac Delta function, $\delta(\theta)$, which has the following properties;

$\delta(\theta) = \infty$ at $\theta = 0$,

$\delta(\theta) = 0$ elsewhere, and

$\int_{-\infty}^{+\infty}\delta(\theta)d\theta = 1.$

It follows that the "pulse" change of property of fluid in the inflow is given by $Co.\delta(\theta)$.

If the change in property of the inflowing fluid is from non radio-active to radio-active, and this change is described by $Co.\delta(\theta)$, measurement of the radio-activity level of the outflowing fluid as a function of time, θ, gives $C(\theta)$ and hence $E(\theta)$. Using this technique the residence time distributions $C(\theta)$, of any processing equipment may be measured.

Often either the true mean residence time, $\bar{t}r$, for a vessel is not equal to the nominal mean residence time, $\bar{t}n$, or $\bar{t}n$ cannot be accurately calculated. Inequality between $\bar{t}r$ and $\bar{t}n$ may arise due to short circuiting and/or stagnant regions within the vessel. In these instances the procedure adopted is to measure the residence time distribution as a function of time, t, giving $C(t)$. It can be shown that

$$\bar{t}r = \frac{\int_o^\infty C(t)tdt}{\int_o^\infty C(t)dt} \qquad (8)$$

and,

$$C(\theta) = \bar{t}r.C(t) \qquad (9)$$

The use of radioisotopes as tracer materials has the advantages that the radio-tracer often satisfies the condition of chemical identity with the material to be traced,[15, 16] and measurement of the response is relatively simple and may be achieved at low concentrations of radioisotope.[50, 52, 53]

3.2.1. Single parameter descriptions of residence time distributions[50]

The function E(θ) can be fully described in terms of its moments. The kth moment of E(θ) about the origin is defined as

$$M'_k = \int_0^\infty \theta^k E(\theta)\,d\theta \qquad (10)$$

The kth moment of E(θ) about the mean is defined as

$$M_k = \int_0^\infty (\theta-1)^k E(\theta)\,d\theta \qquad (11)$$

The mean of E(θ) is given by M'_1 (=1) and the variance of E(θ) is given by M_2.

3.3. Description of residence time distributions by flow models

Mathematical models are frequently used to describe the flow through processing equipment. The dispersion model, the tanks-in-series model, and composite models will each be described in turn. This description is warranted since these models were incorporated in the model developed to describe the experimental results obtained in this investigation.

3.3.1. The dispersion model[49-51, 54]

In this one-dimensional model a degree of mixing in the direction of flow is superimposed on a plug flow vessel. If the degree of mixing is independent of position the basic differential equation representing this model is,

$$\frac{\partial C}{\partial t} = D'\frac{\partial^2 C}{\partial x^2} - U\frac{\partial C}{\partial x} \qquad (12)$$

where D' = axial dispersion coefficient,
x = position in the direction of flow,
U = mean velocity through the vessel,
C = concentration, and
t = time.

Rewriting in terms of the dimensionless forms of time, θ, and position z, gives

$$\frac{\partial C}{\partial \theta} = \left(\frac{D'}{UL}\right)\frac{\partial^2 C}{\partial z^2} - \frac{\partial C}{\partial z} \qquad (13)$$

where $\theta = tU/L$,
$z = x/L$, and
L = length of the vessel.

The vessel dispersion number, D = (D′/UL), measures the extent of axial dispersion and as D tends to zero plug flow is approached.

The analytical solution of equation (13) has been obtained for a wide variety of boundary conditions.[49] An approximate solution that is valid for small values of the dispersion number is

$$C(\theta) = Co \cdot \left(\frac{1}{2\sqrt{\pi D}}\right) \cdot \exp\left(\frac{-(1-\theta)^2}{4D}\right) \qquad (14)$$

when the tracer is injected as an impulse, $Co.\delta(\theta)$, at $z = 0$.[49]

Rewriting this solution in terms of time, t,

$$C(t) = Co \cdot \left(\frac{1}{2\sqrt{\pi D}}\right) \cdot \exp\left(\frac{-(1-\frac{U}{L}t)^2}{4D}\right) \qquad (15)$$

when the tracer is injected as an impulse, $Co.\delta(t)$, at $x = 0$.[54]

The mean of the distribution given by equation (14) is unity while the mean for the distribution given by equation (15) is L/U. Equations (14) and (15) neglect the effect of the boundaries at each end of the vessel as well as the spread of the tracer pulse while it passes the observation point, $z = x/L = 1$.

The error in equations (14) and (15) depends on the value of D. When D is less than 0,001 the error is less than 0,5 per cent and when D is less than 0,01 the error is less than 5 per cent.

3.3.2. The tanks-in-series model[49-52]

Consider the flow of fluid through a series of ideal stirred tanks which are equal in size. For an input of tracer to the first tank given by $Co.\delta(0)$ the response in the discharge from the Nth tank is given by,

$$C_N(0) = Co(N^N/(N-1)!)\theta^{N-1}e^{-N\theta} \qquad (16)$$

This model is useful for considering recirculation.[49, 55]

3.3.3. Composite models[49-51, 56]

When single parameter flow models do not satisfactorily account for non-ideal flow more complicated models must be used. In these models the processing equipment is considered to be subdivided into discrete flow regions. In each of these regions there is a well-defined type of flow and the regions are interconnected to form a composite model. Such composite models can usually be applied most satisfactorily to physical equipment that itself has an interconnected flow structure. If distinct physical regions that conform to one of the well-defined types of flow exist in the equipment then the natural model structure is the composite one.

It is often possible to conclude that, if the experimental response measured in the equipment conforms very closely to that predicted by a composite model, the actual flow structure in the equipment does have many of the specific features included in the model. Thus the comparison between the experimental response and

that predicted by a composite model can provide very valuable insight into the pattern of material movement inside process equipment. This concept is examined fully later in connection with the experimental results obtained in this study.

However caution must always be advised because the measured response curve does not always conform to only one composite model - often many different models will fit to a comparable level of satisfaction and the conclusions regarding flow patterns are not unique. It is always wise to draw strongly on what is known about the physical equipment before drawing conclusions regarding flow patterns from the response curves.

The types of well-defined flow include plug flow, ideal mixing, dispersed plug flow and deadwater.

The definition of deadwater or stagnant regions cannot be reconciled with the assumption of steady state flow through the equipment. Even in small stagnant regions, the calculated mean age of the vessel contents would be infinite.

In practice deadwater regions do not occur but equipment may contain regions where fluid movement is sufficiently slow to be considered stagnant. In composite models these regions are considered to contribute to the vessel volume but are ignored in determination of age distribution functions.

Bypass flow, recycle flow and cross flow may also be included in the model. The various flow regions and flow mechanisms are combined to form the composite model.

By consideration of the forms of the response curves obtained for processing equipment, and the physical nature of the equipment, the most feasible composite model may be developed. The greater the number of flow regions and flow mechanisms considered in the model the more general the composite model becomes. However the more complex the model, the more unwieldy the mathematics. It is therefore best to aim for the simplest model which can reproduce the response and can possibly represent the physical nature of the processing equipment.

4. THE DEVELOPMENT OF A THEORETICAL MODEL FOR BURDEN MOVEMENT IN THE SUBMERGED-ARC FURNACE

To develop and interpret a theoretical model for the mechanism of burden movement in the submerged-arc furnace it is necessary to consider the mode and position of heat generation within submerged-arc furnaces and the inner structure of submerged-arc furnaces. The mode and position of heat generation within submerged-arc furnaces is important because it determines the position of alloy and slag formation and contributes to the stirring of the molten phases.

4.1. The generation of heat in submerged-arc furnaces

In carbo-thermic reduction processes heat is as important as carbon, as a deficiency of heat, or carbon, or both, results in incomplete reduction.[57] The major portion of heat generated in submerged-arc furnaces is required for reduction.[58]

Heat for the process is generated along the current paths in the furnace and the extent of current transfer along each of the current paths has a critical effect on furnace operation. This is best illustrated by considering Westly's principle of heat distribution[57, 59] in which the furnace is divided into a charge zone in the upper furnace region with electrical resistance R_c, and a reaction zone in the vicinity of the electrode tips with electrical resistance R_r. In both regions star and delta connected inter-electrode conduction may occur.[60]

If it is assumed that the resistive load connections

in both regions are either star or delta only, this assumption having no effect on the generality of the treatment,[61] then the furnace operating resistance R, is

$$\frac{1}{R} = \frac{1}{R_r} + \frac{1}{R_c}$$

For ohmic resistance heating in the current paths the heat distribution factor, K, is

$$K = \frac{Q_c}{Q} = \frac{v^2/R_c}{v^2/R} = \frac{R_r}{R_r+R_c}$$

where Q_c = heat generated in the charge zone,
Q = total heat generated
v = voltage drop.

Smaller values of K mean that more heat is available for reduction. Consequently for stable furnace operation K must be controlled to a value which provides the correct distribution of the total heat available, to smelting and to reduction processes. This implies control of the extent of current transfer along the different current paths by adjustment of the relative values of R_c and R_r. It can be shown that this is best achieved by selection of the optimum burden composition for the process, thereby fixing R_c (R_c is determined by burden resistivity), and adjustment of R_r to desired levels by control of the electrode tip-to-alloy bath distance.

Since K must be significantly smaller than 0,5 it follows that R_r must be significantly smaller than R_c and so most of the current transfer must occur from the electrode tips. Urquhart[62] has calculated that in the production of high-carbon ferrochromium, 50 per cent of the heat is generated at the electrode tips and 25 per cent is generated along the lower 300 mm of the electrode.

In slag-free silicon reduction processes the electrode tips operate in a crater void and heat is generated by arcing from the electrode tips.[63-65] The mode of heat generation is not as clearly understood for the production of high-carbon ferrochromium and ferromanganese.

In these two processes there is a slag phase between the electrode tip and the alloy bath, and a coke bed floats on, and is partially immersed in, this slag phase.[57, 66] Similar behaviour has been observed in electric pig iron furnaces.[67] In these processes the electrode tip may operate either immersed beneath the slag layer or in a tightly packed coke bed.

For a primary slag typical of those produced in the manufacture of high-carbon ferrochromium, an experimental study of the mechanism of current transfer from a graphite electrode immersed in the slag showed that at 1500°C arcing occurred at electrode current densities above 12A/cm^2 when using 50 Hz current.[68] At current densities below 12A/cm^2 ohmic conduction occurred. In industry electrode current densities are usually about 5A/cm^2 so if the electrodes are immersed in the slag layer ohmic conduction probably occurs.

If the electrode tip operates in the tightly packed coke bed conduction within each particle is ohmic. Conduction between particles in the coke bed probably occurs by the mechanism postulated by Urquhart.[62] In this mechanism ohmic conduction occurs across the interparticle contact zones. The contact resistance causes heating which results in reaction at the interface. Reaction results in the formation of a gap between the particles

and liberation of CO(g). The voltage drop across the gap is sufficiently large to strike an arc in the CO(g) atmosphere. This arcing results in further reaction and an increase in gap size until the prevailing voltage drop is too small for the gap and the arc is extinguished. Hence interparticle conduction occurs by a combination of ohmic conduction and unstable micro-arcing.

Conduction from the electrode tips and the high temperatures which prevail in this region result in strong electromagnetic and convective stirring effects at and beneath the electrode tips.

4.2. The inner structure of the submerged-arc furnace for the production of high-carbon ferromanganese

To develop a qualitative picture of the inner structure of the submerged-arc furnace for the production of high-carbon ferromanganese the following observations must be taken into account:-

(i) Raw materials usually descend rapidly in a "clover leaf" pattern around the electrodes as shown in Figure 1.

(ii) During dig-out of furnaces crust build-up along the furnace walls in the hearth region has been observed. This crust obstructs the even descent of the burden giving rise to the "clover leaf" pattern of rapid burden descent.

(iii) Under certain conditions only the electrode directly above the alloy tapping hole moves in response to the alloy tapping process. This behaviour occurs when the alloy bath is broken down into discrete pools due to accretion build-up on the hearth floor.

(iv) During conditions of normal furnace operation the slag and alloy phases separate into two layers on the hearth floor. During normal furnace operation extensive entrapment of alloy in the slag phase, and slag in the alloy phase, has not been observed to occur to any marked extent during tapping. This shows that slag/alloy separation does occur in the hearth region.

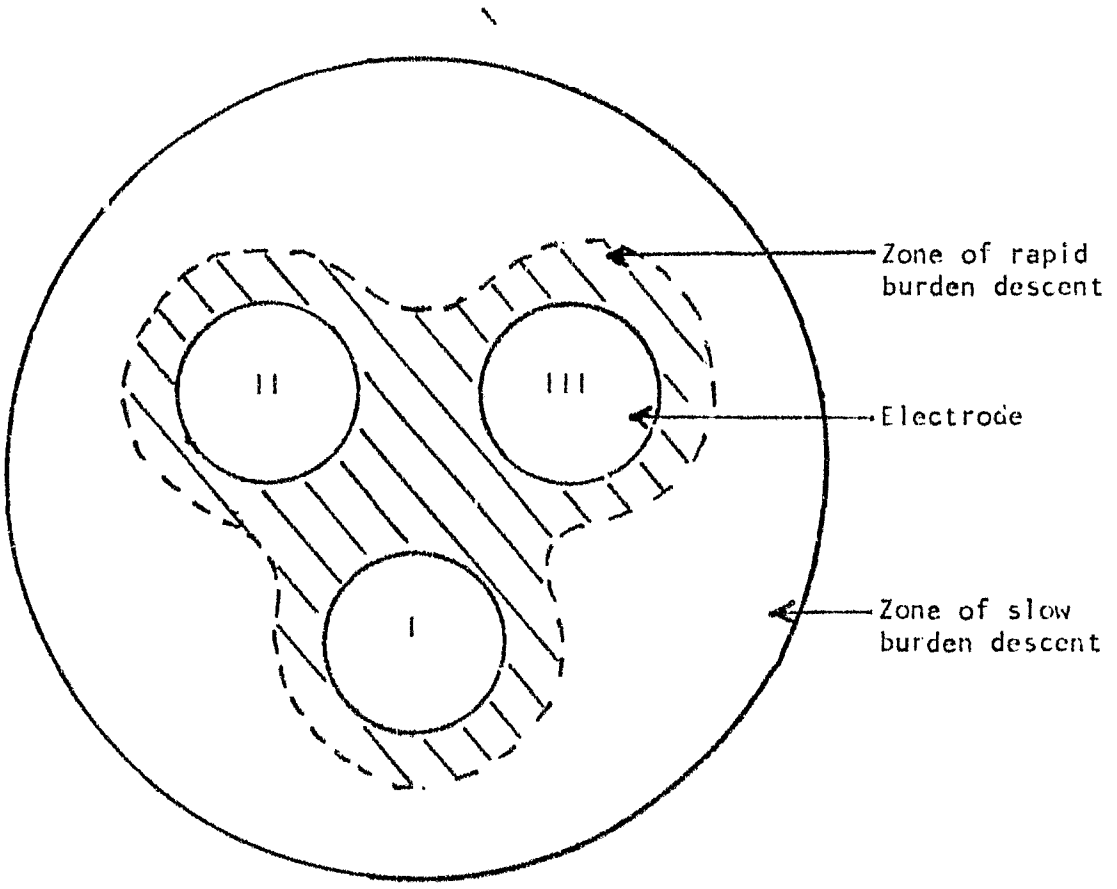

Figure 1. Schematic plan view of the furnace at stockline level showing the "clover leaf" pattern of rapid burden descent

Within the furnace volume where the burden is solid there are two zones. In the active zone, which surrounds the electrodes and which is delineated at stock level by the "clover leaf" pattern, rapid burden movement occurs. In the inactive zone, which makes up the balance of the furnace volume occupied by solid burden, movement is very slow.

Thus the major portion of solid material entering the furnace descends towards the electrode tips through the active zone. As the burden descends it is progressively heated until, in the vicinity of the electrode tips, the slag and alloy forming components of the burden melt and combine to form the slag and alloy phases respectively. These two phases are immiscible and, under the influence of gravity, the heavier alloy phase tends to separate from the slag phase. However at the electrode tips, where mixing effects are most intense, these two phases are probably well mixed. Further beneath the electrode tips mixing effects are less intense and so the two phases separate into a slag bath floating on the alloy pool on the hearth floor. Alloy droplets are probably constantly settling through the slag layer. Within each layer mixing effects are probably still sufficiently strong to ensure a homogeneous composition within each layer. Hence the slag and alloy layers may both be considered mixed zones.

The solid carbonaceous reducing agents within the burden do not become molten but descend to the electrode tips where they form the "coke" bed which floats on the slag layer. The electrode tips are either immersed within the coke bed or protrude through the coke bed into the slag layer.

Under certain conditions solid accretion build-up on the hearth floor may result in breakdown of the alloy bath into discrete pools.

Figure 2 represents the postulated inner structure of the submerged-arc furnace.

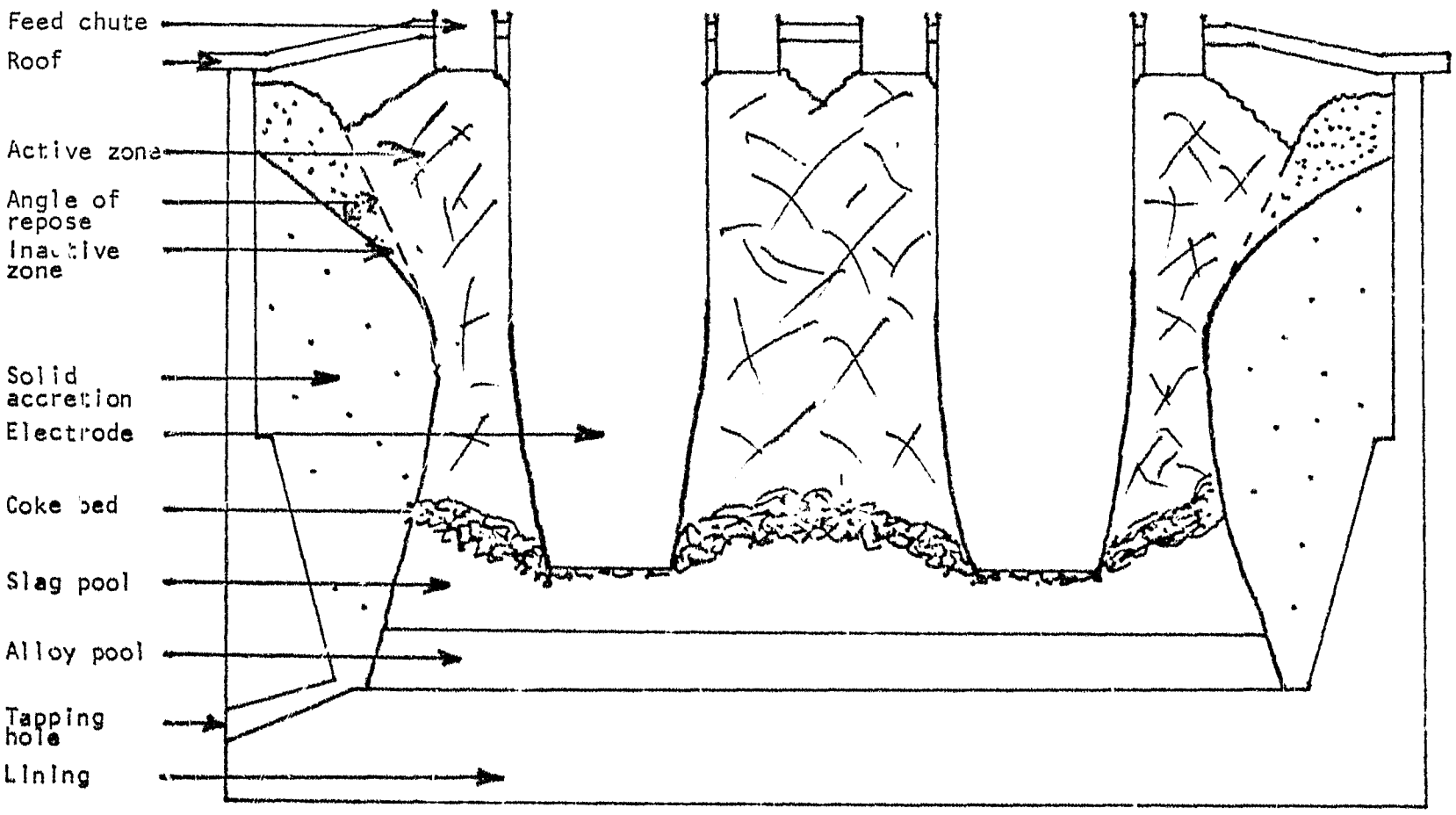

Figure 2. Schematic representation of the inner structure of a Submerged-Arc Furnace.

4.3. The theoretical model of burden movement in submerged-arc furnaces producing high-carbon ferromanganese

The qualitative picture of the inner structure of the submerged-arc furnace postulated in Section 4.2 may form the basis for a model of the movement of the slag and alloy forming components of the burden through the furnace.

Three flow regions within the furnace may be identified. These are the active zone, the inactive zone, and the zone wherein molten phases exist. Consequently the physical structure within the furnace lends itself to a composite model of the form described in Section 3.3.3.

The most feasible type of flow within each zone must be considered. Consider the active and inactive zones where the burden is solid. Here the most feasible type of "flow" for a burden element consisting of a number of particles is plug flow with some dispersion. This type of "flow" was successfully used to describe movement of the solid burden in the production of high-carbon ferrochromium in the submerged-arc furnace.[39] Beck *et al.*[69] showed for an experimental rotary kiln that the "flow" of granular solids (sand) could be described by a dispersion model with small dispersion coefficients (order of magnitude 10^{-5} m/s).

It is possible to differentiate between the active and inactive zones in one of two ways. The inactive zone can be considered to be stagnant in which case the furnace volume occupied by the inactive zone is not considered in the flow model. Alternatively the inactive zone can be considered to be represented by a dispersed plug flow region with large mean residence times. The latter

approach has been adopted as it permits mathematical description of the response due to radio-tracer inputs to both the active and the inactive zones. Consequently each burden element entering the furnace "sees" a dispersed plug flow reactor with dispersion number D and mean residence time $\bar{t}$. Burden elements entering inactive zones will "see" dispersed plug flow reactors with much larger mean residence times than will burden elements entering active zones.

The dispersed plug flow region is assumed to include the regions in the furnace in which the slag and alloy forming components soften and begin to melt.

Within the zone containing the molten phases, the most likely type of flow is mixed flow. This takes into account the intense mixing at the electrode tips and the less intense mixing in the slag and alloy baths once they have separated in the hearth floor region. Since the flow of each phase is considered independently, mixed flow can be considered to occur for each phase in the region of slag and alloy separation.

Raw materials are fed to the furnace continuously but liquid products are discharged intermittently. This may be taken into account by assuming that this region is represented by a constantly stirred tank reactor. Hence molten material is fed to this zone continuously but is discharged intermittently by tapping.

All solid-liquid phase changes are assumed to occur in the dispersed plug flow region because it is unlikely that mixed flow can occur where both solid and liquid phases are present. Therefore the constantly stirred tank reactor

is assumed to include only the molten phases and the dispersed plug flow region is assumed to include the balance of the furnace burden.

Consequently the movement of the slag and alloy forming components of the burden through the furnace may be described by a network of dispersed plug flow reactors in parallel feeding a constantly stirred tank reactor. This model is illustrated in Figure 3.

In an alternative model the zone represented by the constantly stirred tank reactor, (C.S.T.R.), has been divided into three continuous flow mixers, one at each electrode tip, feeding a single settler with the following properties:-

(i) The first material to arrive in the settler is the first material to leave the settler.

(ii) Discharge from the settler occurs only during tapping.

This model differentiates between the intense mixing at the electrode tips and the less intense mixing in the regions of separation of the slag and alloy and is illustrated in Figure 4.

The latter model is a mathematically more complex description of burden movement in the furnace. The existence of a settler in the hearth region in which no mixing occurs, and from which intermittent plug flow discharge occurs, is physically not as likely as is the existence of a constantly stirred tank reactor. For these reasons this model was not applied.

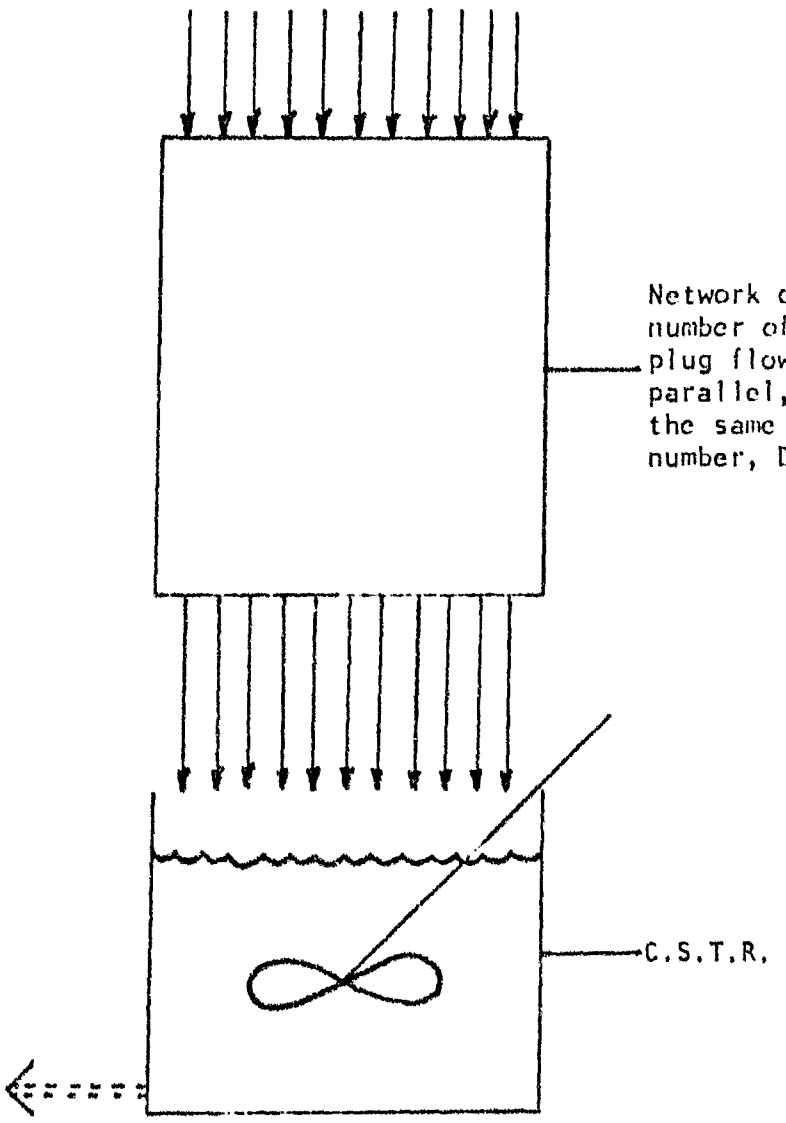

Figure 3. Schematic representation of the theoretical model for burden movement in the Submerged-Arc Furnace

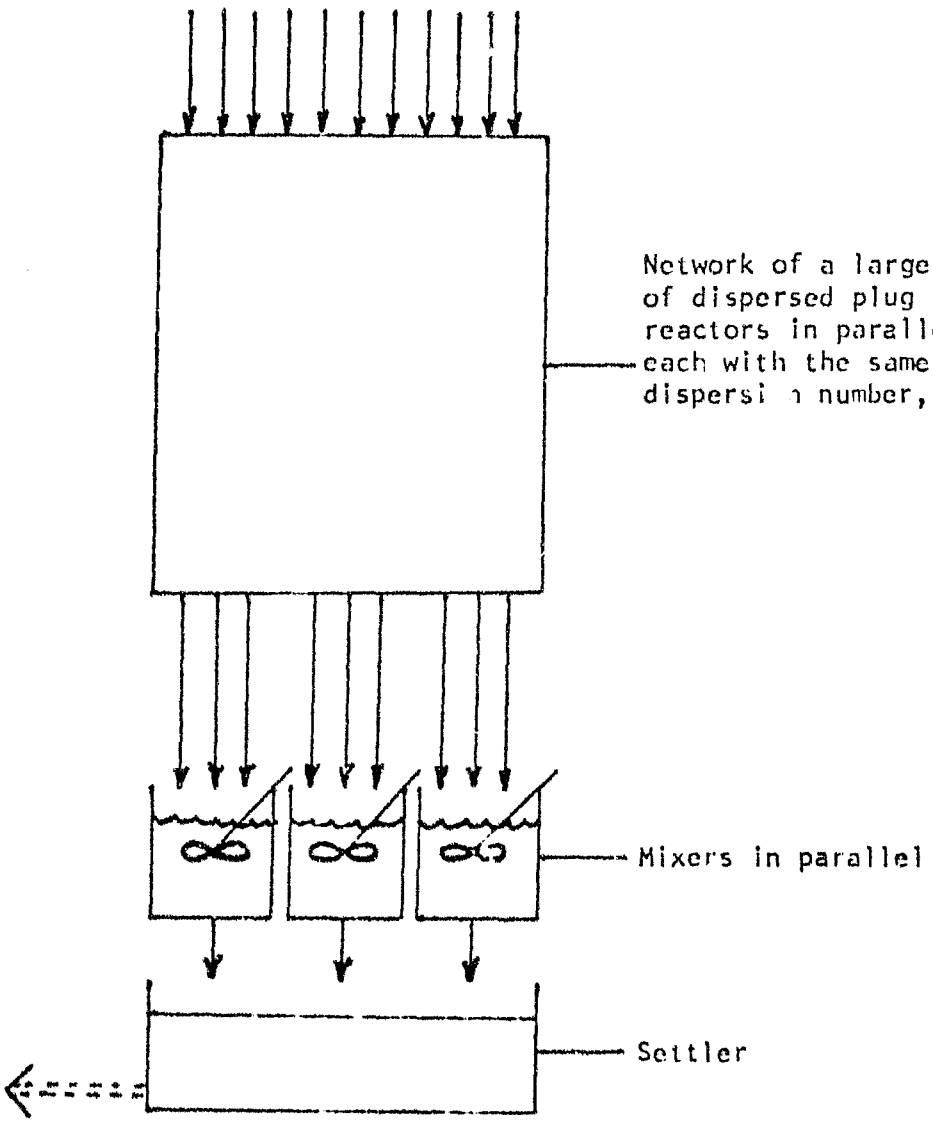

Figure 4. Schematic representation of an alternative model for burden movement in the Submerged-Arc Furnace

4.4. The general shape of the experimentally determined residence time distributions

Several qualitative c lusions may be drawn from the general shape of the experimentally measured residence time distributions. These are shown in Figures 18 to 33 and their general shape is shown in Figure 5. Superimposed on this curve is the ideal plug flow - C.S.T.R. pattern. Several zones may be identified on the general curve as shown. The significance of each of these zones will be discussed in turn.

(i) Zone A.

This portion indicates a delay in the response due to the material passing through a succession of well mixed regions or due to the material passing through a plug flow region.

(ii) Zone B.

The comparatively sharp rise in this zone indicates that the delay in the response shown by Zone A arises due to material passing through a plug flow region. The shallow "S" shape indicates slight dispersion in the plug flow region as must be the case in any real system. When the radio-tracer is introduced beneath the electrode tips (experiment 6 on furnace M11 with 75 MVA transformers) Zones A and B are absent as expected. This is shown in Figure 33.

(iii) Zone C.

The sharp peak in this zone indicates that there is only one mixed region, or that any other mixed regions are very small. For some of the results this peak

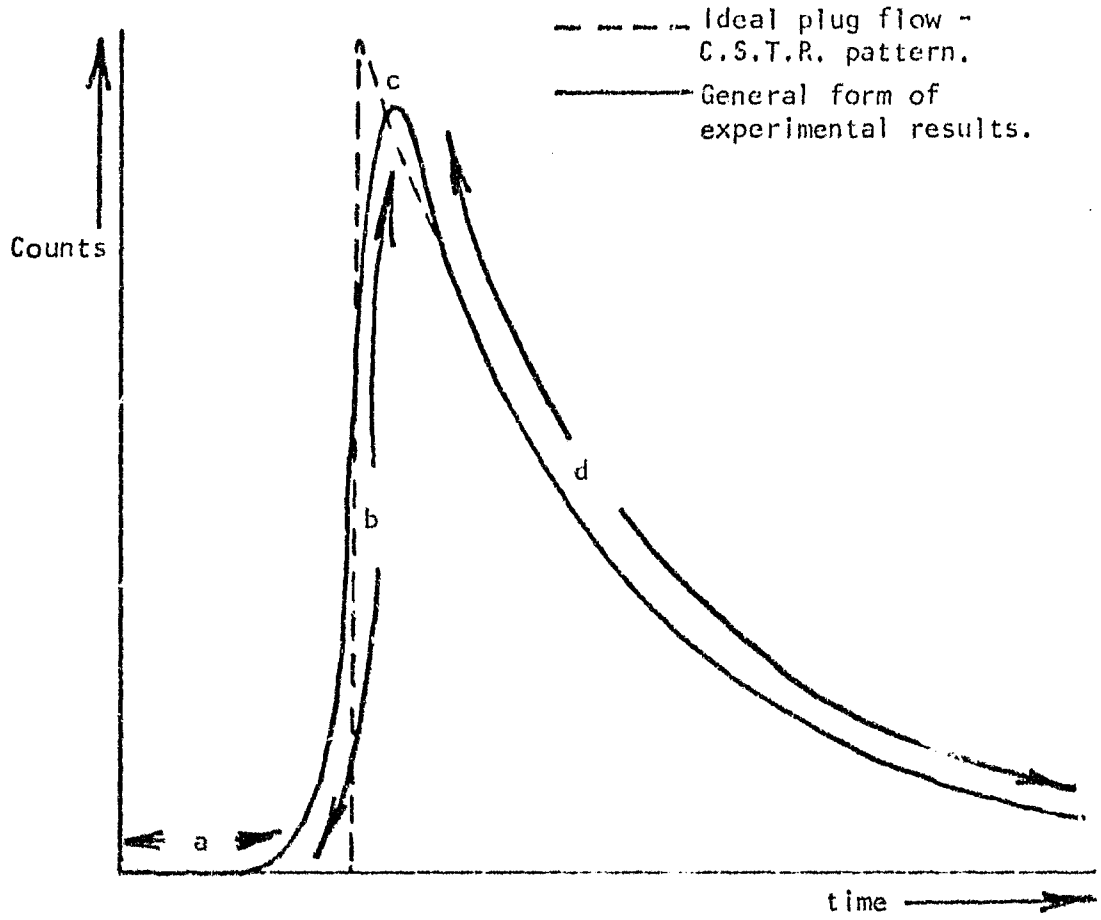

Figure 5. The general form of the experimentally measured residence time distributions with the ideal plug flow - C.S.T.R. pattern superimposed.

overshoots the ideal plug flow - C.S.T.R. pattern, indicating a bypass channel to the tap hole.

(iv) Zone D.

This portion of the curve is exponential showing that the alloy pool is very well mixed.

The postulated theoretical model fits in well with the above observation with the exception that a possible bypass channel to the tap hole is not considered. Inclusion of a possible bypass channel in the theoretical model was beyond the scope of the investigation since this would introduce significantly more complex mathematics into the model.

4.5. Mathematical description of the theoretical model of burden movement in the submerged-arc furnace

Consider the input of a radio-active burden sample into the furnace at time t = 0. This represents a "pulse" input of radio-tracer to a dispersed plug flow region at time t = 0. The concentration of radio-tracer in the discharge from the dispersed plug flow region as a function of time, t, is given by;[54]

$$C = \frac{Co}{2\sqrt{\pi D}} \cdot \exp\left(-\frac{1}{4D}\right) \cdot \exp\left(\frac{t}{2\bar{t}D} - \frac{t^2}{4\bar{t}^2 D}\right) \qquad (17)$$

where, Co = initial tracer concentration
D = dispersion number. (= D′/UL)
$\bar{t}$ = mean residence time.

This equation represents the concentration of radio-tracer in the feed to the constantly stirred tank reactor. The following assumptions are made about the C.S.T.R.

(i) Immediately before tapping a particular phase from the C.S.T.R. the volume of that phase present is a constant, Vinv.

(ii) Only a portion of Vinv is tapped from the C.S.T.R. at each tapping. This takes the permanent inventories of alloy and slag in the furnace into consideration.

(iii) Discharge from the C.S.T.R. is instantaneous and occurs at the middle of the time for each tapping.

(iv) The volumetric feedrate to the C.S.T.R. is constant for each tapping cycle, and for the cycle leading to the *ith* tapping after radio-tracer input is given by ν_i where

$$\nu_i = \frac{V_i}{(t_i - t_{i-1})},$$

V_i = volume tapped at the i*th* tapping

$t_i - t_{i-1}$ = time lapse between the $i-1$*th* and i*th* tapping.

For the first tapping after radio-tracer input

$$\nu_1 = \frac{V_1}{(t_o + t_1)}$$

where, t_o = time between the final tapping prior to radio-tracer input and radio-tracer input.

The tracer concentration in the discharge from the C.S.T.R. at the first tapping after tracer input is

$$C_1 = \frac{1}{Vinv} \int_o^{t_1} \nu_1 C dt = \frac{V_1}{Vinv(t_o + t_1)} \int_o^{t_1} C dt$$

Immediately after the first tapping the amount of tracer in the C.S.T.R. is

$$A_1 = C_1 \ (Vinv - V_1)$$

The tracer concentration in the discharge from the C.S.T.R. at the second tapping after tracer input is

$$C_2 = \frac{A_1}{Vinv} + \frac{V_2}{Vinv(t_2 - t_1)} \int_{t_1}^{t_2} C dt = C_1 \left(1 - \frac{V_1}{Vinv}\right) + \frac{V_2}{Vinv(t_2 - t_1)} \int_{t_1}^{t_2} C dt$$

The amount of tracer in the C.S.T.R. immediately after the second tapping is

$$A_2 = C_2 \ (Vinv - V_2)$$

Hence the tracer concentration in the discharge from the C.S.T.R. at the nth tapping after tracer input is

$$C_n = \frac{A_{n-1}}{Vinv} + \frac{V_n}{Vinv(t_n - t_{n-1})} \int_{t_{n-1}}^{t_n} Cdt = C_{n-1}\left\{1 - \frac{V_{n-1}}{Vinv}\right\} + \frac{V_n}{Vinv(t_n - t_{n-1})} \int_{t_{n-1}}^{t_n} Cdt$$

Consider the integral,

$$\int Cdt = \frac{Co}{2\sqrt{\pi D}} \cdot \exp\left(-\frac{1}{4D}\right) \cdot \int \exp\left(\frac{t}{2\bar{D}t} - \frac{t^2}{4D\bar{t}^2}\right) dt.$$

From tables,[70]

$$\int Cdt = \frac{Co}{2\sqrt{\pi D}} \cdot \exp\left(-\frac{1}{4D}\right) \cdot \sqrt{\pi D}\,\bar{t} \cdot \exp\left(\frac{1}{4D}\right) \cdot \operatorname{erf}\left(\frac{t}{2\sqrt{D}\bar{t}} - \frac{1}{2\sqrt{D}}\right)$$

Simplifying,

$$\int Cdt = \frac{Co\bar{t}}{2} \operatorname{erf}\left(\frac{t}{2\sqrt{D}\bar{t}} - \frac{1}{2\sqrt{D}}\right)$$

Introducing limits of integration,

$$\int_0^{t_1} Cdt = \frac{Co\bar{t}}{2}\left\{\operatorname{erf}\left(\frac{t_1}{2\sqrt{D}\bar{t}} - \frac{1}{2\sqrt{D}}\right) - \operatorname{erf}\left(-\frac{1}{2\sqrt{D}}\right)\right\}$$

$$\int_{t_{i-1}}^{t_i} Cdt = \frac{Co\bar{t}}{2}\left\{\operatorname{erf}\left(\frac{t_i}{2\sqrt{D}\bar{t}} - \frac{1}{2\sqrt{D}}\right) - \operatorname{erf}\left(\frac{t_{i-1}}{2\sqrt{D}\bar{t}} - \frac{1}{2\sqrt{D}}\right)\right\}$$

Substituting these values into the relevant equations gives,

$$C_1 = \frac{V_1 C_o \bar{t}}{2\,\mathrm{Vinv}\,(t_o+t_1)} \left\{ \mathrm{erf}\left(\frac{t_1}{2\sqrt{D\bar{t}}} - \frac{1}{2\sqrt{D}}\right) - \mathrm{erf}\left(-\frac{1}{2\sqrt{D}}\right)\right\} \qquad (18)$$

$$C_i = \frac{V_i C_o \bar{t}}{2\,\mathrm{Vinv}\,(t_i - t_{i-1})} \left\{ \mathrm{erf}\left(\frac{t_i}{2\sqrt{D\bar{t}}} - \frac{1}{2\sqrt{D}}\right) - \mathrm{erf}\left(\frac{t_{i-1}}{2\sqrt{D\bar{t}}} - \frac{1}{2\sqrt{D}}\right)\right\} + C_{i-1}\left(1 - \frac{V_{i-1}}{\mathrm{Vinv}}\right) \qquad (19)$$

Equation (18) gives the tracer concentration in the discharge from the C.S.T.R. at the first tapping after radio-tracer input and equation (19) gives the tracer concentration at all subsequent tappings.

Equations (18) and (19) hold for a single, pulse input of radio-tracer to the furnace. For several simultaneous inputs to the furnace the tracer concentration in the discharge is given by the sum of the tracer concentrations due to each input. Hence for m simultaneous inputs of radio-tracer to the furnace the tracer concentration in the discharge is given by,

$$C_1 = \sum_{k=1}^{m} C_{1,k} \qquad (20)$$

$$C_i = \sum_{k=1}^{m} C_{i,k} \qquad (21)$$

where the values of $C_{1,k}$ and $C_{i,k}$ are given by equations (18) and (19) respectively using the relevant values of D, and $\bar{t}$. If all these inputs experience the same values of D and $\bar{t}$ then equations (18) and (19) apply directly.

These expressions may be used to determine the tracer concentration in both the slag and the alloy discharge from the furnace.

5. EXPERIMENTAL

5.1. Description of furnaces

The furnaces used in this investigation, designated M10 and M11, are identical in design and construction. Each furnace has a fully closed refractory roof which contains the gas off-takes, explosion hatches, raw material charging shafts, and observation ports. A plan view of furnace M11 is sketched in Figure 6. The water-cooled, steel shell of each furnace is lined with refractory bricks covered by electrode paste. The hearth lining is refractory bricks supporting carbon blocks which are covered by a layer of electrode paste. The base of the furnace is air cooled using fans.

5.1.1. Design parameters

Furnace dimensions of interest are:-[9]

Nett furnace volume		405,284 m^3
Internal depth		5,265 m
Internal diameter	- roof level	12,600 m
	- floor level	9,900 m
Electrodes: diameter		1,900 m
spacing	- p.c.d.	5,429 m
	- centre-to-centre	4,702 m
	- side-to-side	2,802 m

Initially the furnaces were each equipped with 3 single phase 48 MVA transformers. These have the following design electrical characteristics:-[9]

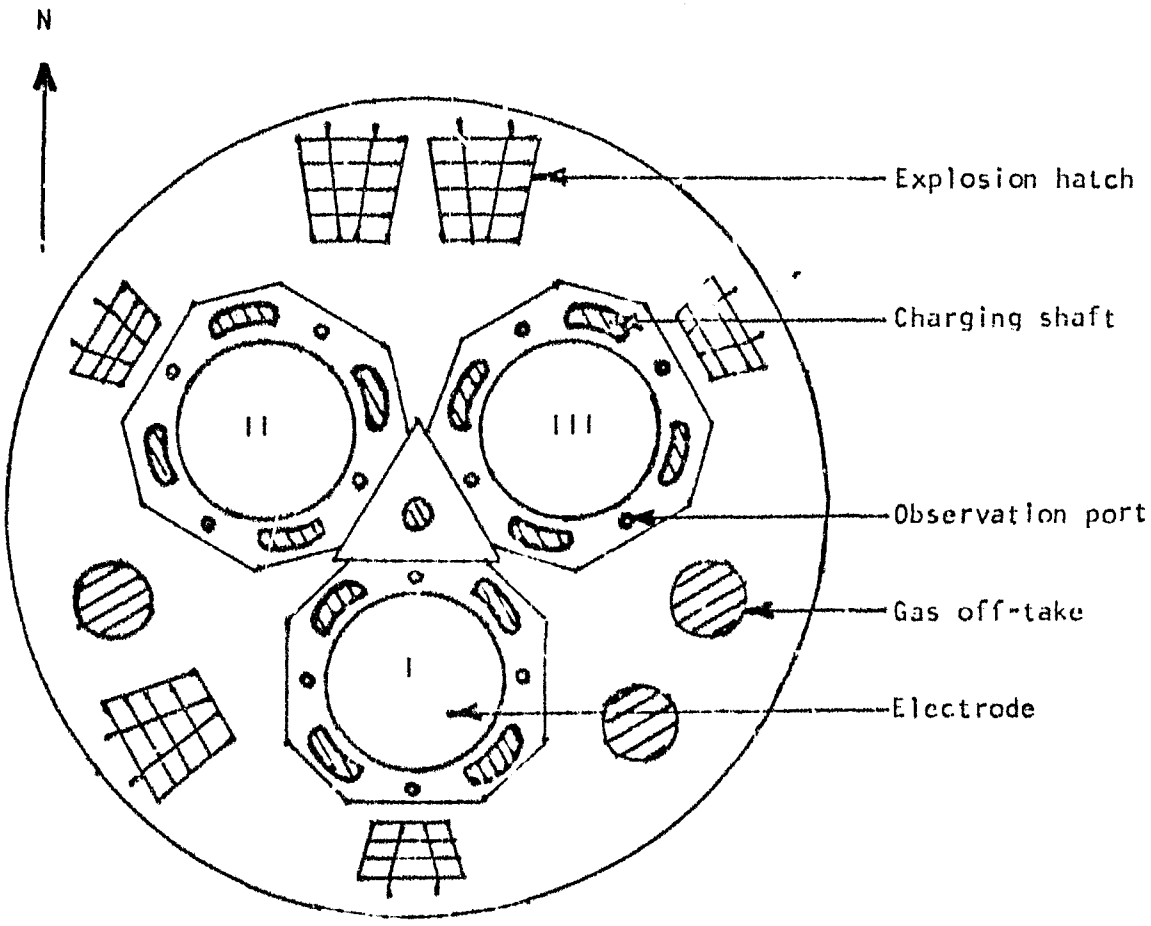

Figure 6. Plan view of the roof of furnace MII

Transformer rating	48 MVA
Line primary voltage	33 kV
Line primary current	840 A
Number of transformer taps	22
Secondary voltage range	176-300 V

In October 1975 the 48 MVA transformers on M11 were replaced by 75 MVA transformers with the following design electrical characteristics:-

Transformer rating	75 MVA
Line primary voltage	33 kV
Line primary current	1312 A
Number of transformer taps	35
Secondary voltage range	183,5-430,5 V

5.1.2. Charging of raw materials

The correctly proportioned mixture of ore, reducing agent and flux is delivered to each choke-fed charging shaft via a feed bunker and feed chute. The 13 feed bunkers, each feeding a single charging shaft, are sited in the furnace building, directly above the furnace installation. This raw material charging configuration permits the charging of burden mixtures with different compositions to different furnace zones if desired. When the mix level in any bunker falls below a certain point, a gamma-ray sensor activates the charging system and additional mix of the correct composition is automatically delivered to the bunker.

5.1.3. Tapping of furnaces

Alloy is tapped from one of two tap-holes both of which are beneath electrode I. Slag is tapped from a single tap-hole. In furnace M10 slag is tapped from beneath electrode III whilst in furnace M11 slag is tapped from beneath electrode II. The location of the electrodes for both these furnaces are the same as shown on the plan view of furnace M11 sketched in Figure 6. The slag tap-hole on each furnace is about 1 metre above the alloy tap-holes.

The time between alloy tappings is determined by the cumulative energy consumption which is usually 70 or 80 MWh. The slag is usually tapped 40 MWh after alloy tapping. Each alloy tapping yields approximately 25 to 30 tonnes of alloy but once a day between 50 to 60 tonnes are tapped.

5.1.4. Removal and treatment of waste gases

Raw waste gases may be passed through two identical gas cleaning plants or vented directly to atmosphere via the raw gas stacks. Each gas cleaning plant consists of two venturi scrubbers in series coupled to a cyclone. A dust hood and stack remove any dust and gas from above the furnace roof. The furnace pressure is controlled to a slightly positive value to prevent infiltration of air.

5.2. The radio-tracer input to the furnace

5.2.1. Choice of a suitable radio-tracer material

The choice of a suitable radioisotope involved satisfying the requirements of ease of generation, safety in handling, and true chemical identity with the material to be traced.

The element had to be present in the ore as an oxide which underwent a degree of reduction, with the oxide and its reduction product reporting in the slag and alloy phases respectively. The elements Mn, Fe and Si all meet this requirement of true chemical identity but Mn and Si were both eliminated because they did not meet the requirements of ease of generation and handling. The radioisotope used was Fe^{59} with a half-life of 45 days.

Initially the choice of ore in which to generate the Fe^{59} represented a problem. Due to the high Mn content of manganese ores, the Atomic Energy Board were at first not prepared to activate these ores. Therefore a high grade hematite iron ore was used for several tests. During this period trial activation of Hotazel manganese ore showed that it could be used. The problem of the high activity of Mn^{56} was overcome by allowing it to decay before handling the activated ore. (Mn^{56} has a half-life of 2,5 hours). Consequently in later tests activated Hotazel ore was used.

The radioisotope was produced in a mild steel rod for one experiment in which the radio-tracer was introduced beneath the electrode tip. This procedure ensured rapid

dissolution of the radioisotope in the alloy pool.

For experiments using radioactive ore, a 900 g sample was irradiated. Each 900 g sample was made up of ore particles approximately 1,5 cm in diameter. Thus each sample of Hotazel ore consisted of at least 300 particles whilst each sample of hematite ore contained at least 250 particles. This procedure should have ensured a statistically representative illustration of the behaviour of the ore in the process.

In experiments requiring more than one tracer input the 900 g sample was split into the required number of fractions of equal weight prior to irradiation. These fractions were isolated from one another using aluminium foil.

The radio-tracer was produced by irradiating the sample in the Safari 1 reactor of the South African Atomic Energy Board at Pelindaba, Transvaal, at 20 MW for a predetermined period.

Samples to be irradiated were sealed in an aluminium container which was attached to a spindle and inserted into the reactor pool for a predetermined period at a short distance from the core. During irradiation the spindle and container were rotated. Once irradiated the container was removed from the reactor pool and allowed to stand for one week to permit the short lived radio-isotopes present in the sample to decay fully. (At this stage the activity of the sample was calculated to be 0,5 mCi due to the Fe^{59} present). The radioactive sample was then sealed in a plastic bag.

As a precaution against contamination by fines ore samples were wrapped in aluminium foil prior to irradiation. This foil was removed once the irradiation and decay period was completed.

Prior to irradiation of Hotazel ore the ore was calcined at 700°C for 16 hours to prevent calcination and gas liberation during irradiation. An additional precaution with this ore was to seal the sample in the container by welding rather than by the screw-on lid used for other samples.

Where multi-addition experiments were performed each irradiated ore fraction was sealed in a separate plastic bag. In later multi-addition experiments the relative activity of each fraction was measured before addition to the furnace.

The chemical analysis of the ore samples used is given in Table 1.

5.2.2. Introduction of the radio-tracer into the furnace

The radio-tracer was added to the furnace in a feed bunker, in a charging shaft at furnace roof level, in a burden "valley" beneath the furnace roof, and beneath an electrode tip.

For radio-tracer addition in the furnace feed bunker, the sample was placed on the burden in the bunker "by-pass" when the burden level in the "by-pass" was about 0,6 m below the "by-pass" top. The bunker was then completely filled.

Element	MASS PER CENT	
	HEMATITE	HOTAZEL ORE
Fe	66,08	11,4
Mn	-	44,8
MgO	< 0,1	1,58
SiO_2	2,64	5,23
CaO	< 0,05	5,29
Al_2O_3	0,70	-

Table 1. Chemical analysis of process materials activated

For radio-tracer addition to the furnace via a charging shaft at roof level the sample was introduced into the burden through the gap of about 0,2 m between the charging shaft and its corresponding feed chute. In two initial experiments a stoppered steel cylinder containing the sample was driven into the burden to a depth of about 0,1 m. The stopper and sample were then "injected" into the burden by means of a plunger and the cylinder was removed. In subsequent experiments of this type a shovel was used to lift the burden in the charging shaft and the sample was introduced into the resultant hollow.

A feed bunker, feed chute and charging shaft, and the two sites of radio-tracer inputs are sketched in Figure 7.

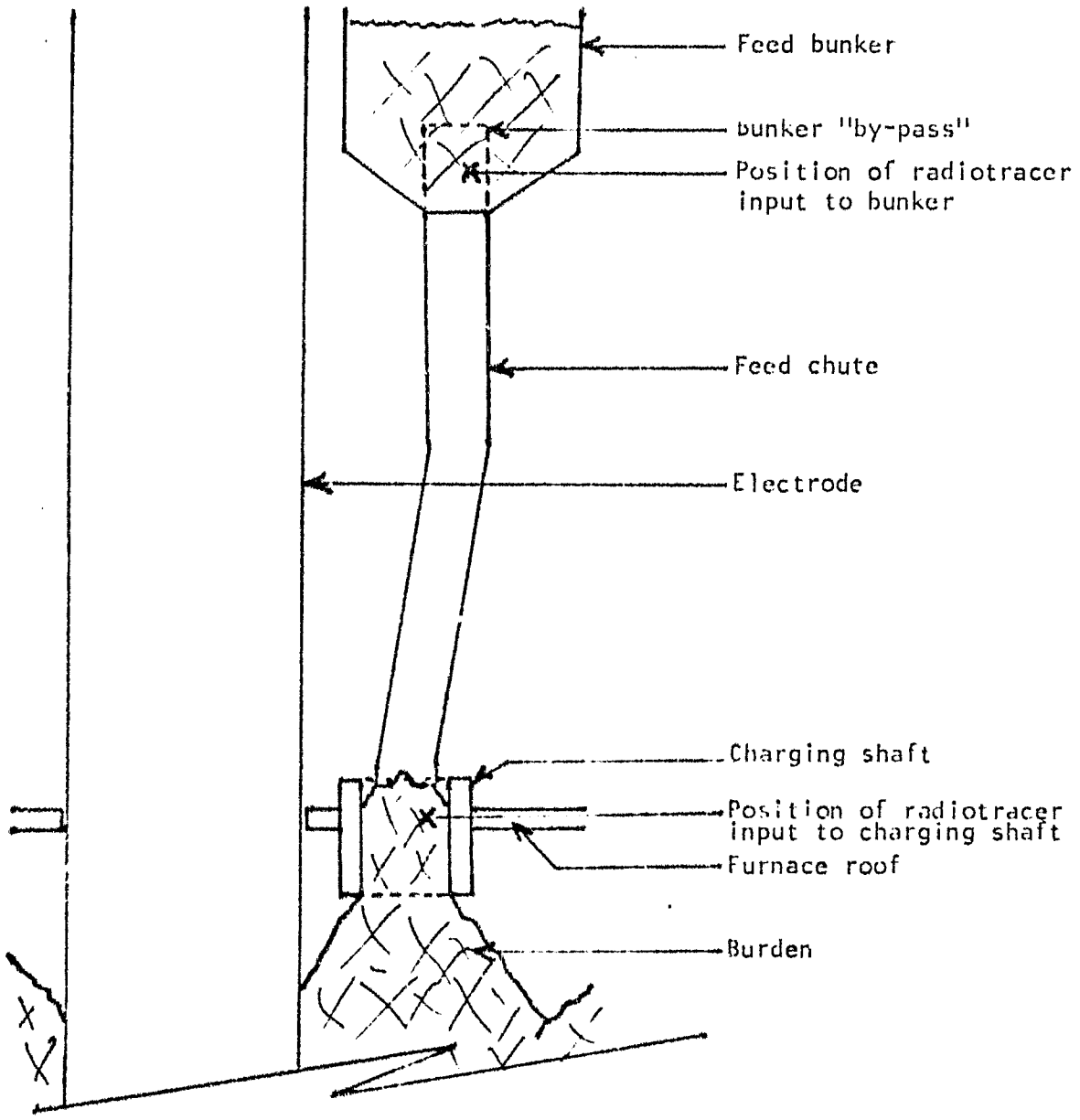

Figure 7. Feed Bunker, Feed chute, and Charging Shaft showing two sites of radiotracer input

To introduce the radio-tracer into a burden "valley", the sample was thrown through an observation port into the valley against the electrode. The site of the radio-tracer input for this experiment is sketched in Figure 8.

In one experiment a radio-tracer sample was introduced beneath the electrode tip. A stoppered, cylindrical probe was used to contain the radio-tracer sample. Once the probe tip was driven beneath the electrode tip, a plunger was used to "inject" the sample and stopper into the burden.

The furnace was switched out during introduction of the radio-tracer for all the experiments other than for introduction of radio-tracer into a feed bunker.

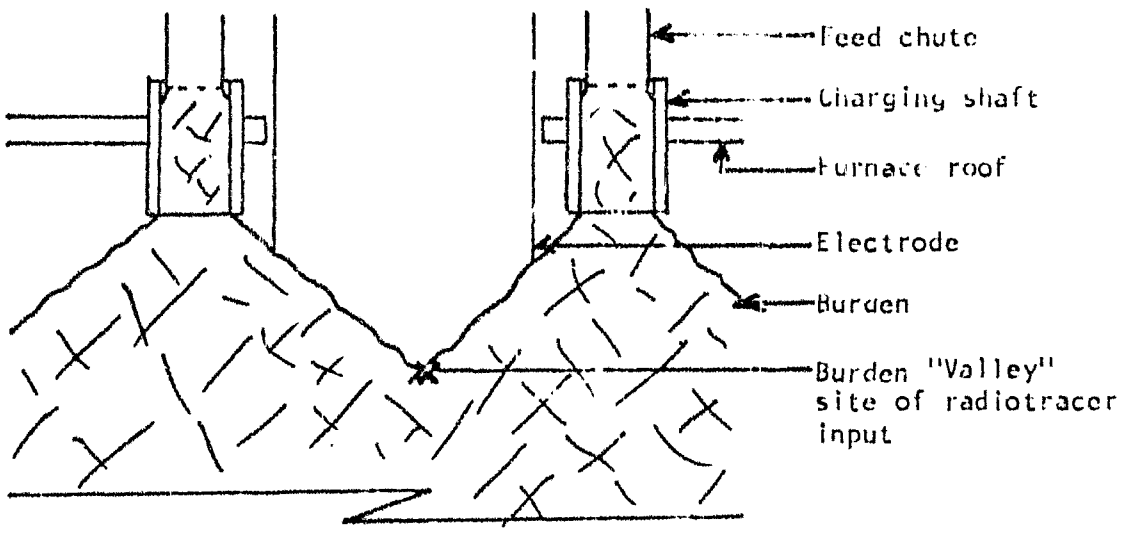

Figure 8. Schematic representation of a burden valley showing the site of radiotracer input

5.3. Monitoring of the furnace response to the radio-tracer input

During each experiment samples were taken of the furnace products for successive tappings. The initial slag and alloy samples were taken immediately before introduction of the radio-tracer. These samples were used to measure the "background" activity of the furnace products.

Samples were taken from the tapping launder using a sampling spoon. In the first four experiments three samples were taken at each tapping while in subsequent experiments four samples were taken at each tapping. The sampling was spread over the tapping interval so that an average composite sample could be obtained for each tapping. The number of samples taken per tapping was increased from three to four to obtain a larger and more representative composite sample.

In each experiment all the composite samples, including the "background" samples, were subjected to the same degree of crushing. In the initial experiments a single pass was made through a large jaw crusher with a maximum jaw aperture of 12,5 mm followed by a single pass through a small jaw crusher with a maximum jaw aperture of 8,5 mm. In subsequent experiments a single pass was made through a large jaw crusher with a maximum jaw aperture of 12,5 mm. The latter procedure was favoured because it simplified sample treatment.

After crushing, all the composite samples for a particular experiment were delivered to the South African Atomic Energy Board and the relative radioactivity of a

fixed mass of each composite sample was measured using an 8" (2o, 32 cm) NaI crystal detector. For each determination in a particular experiment it was necessary that the geometry of packing of each sample with respect to the NaI crystal be identical. This was achieved by subjecting each sample to the same crushing procedure, using a constant sample weight in each determination, and maintaining a constant packing density in each determination.

The relative radioactivity of each sample was expressed in terms of counts per unit time per unit mass. This was then corrected for "background" by subtracting the "background" sample counts from the value obtained for each sample other than the "background" sample. The furnace response was therefore obtained for each experiment in terms of counts per unit time per unit mass at each tap after radio-tracer input.

In some experiments a large time lapse was anticipated between the radio-tracer additions and the first appearance of radioactivity in the furnace products. Samples were not taken for the first few tappings after radio-tracer input to simplify the task of the furnace operators who were required to assist in the product sampling.

The duration of the sampling period following each radio-tracer input was determined by the nature of the experiment, and from experience gained from preceding experiments.

5.4. Data logging during each experiment

During each experiment the following data was recorded:-

(i) The time of radio-tracer input.

(ii) The site of radio-tracer input.

(iii) The time of the start and of the end of each tapping following radio-tracer input.

Using this information the time of each tapping after radio-tracer input was calculated and taken to be at the mid point of each tapping interval.

For each experiment the average values of the furnace parameters were calculated from the recorded operating data.

5.5. The experimental campaign

The experimental campaign of seventeen experiments consisted of three phases. These were:-

(i) Experiments on furnace M11 with 48 MVA transformers.

(ii) Experiments on furnace M10 with 48 MVA transformers.

(iii) Experiments on furnace M11 with 75 MVA transformers.

In all experiments the radio-tracer inputs were made into the active zone of rapid burden movement. Each of these phases will be described in turn

5.5.1. Experiments on furnace M11 with 48 MVA transformers

Six experiments were performed with a single radio-tracer input. In all these experiments other than the sixth, irradiated hematite ore was used as the radio-tracer. In the sixth experiment irradiated Hotazel ore was used as the radio-tracer.

In the fifth experiment the radio-tracer was introduced into a burden "valley". In the balance of the experiments the radio-tracer was introduced into the furnace through the charging shafts.

The sites of these radio-tracer inputs are superimposed on the plan view of the furnace sketched in Figure 9.

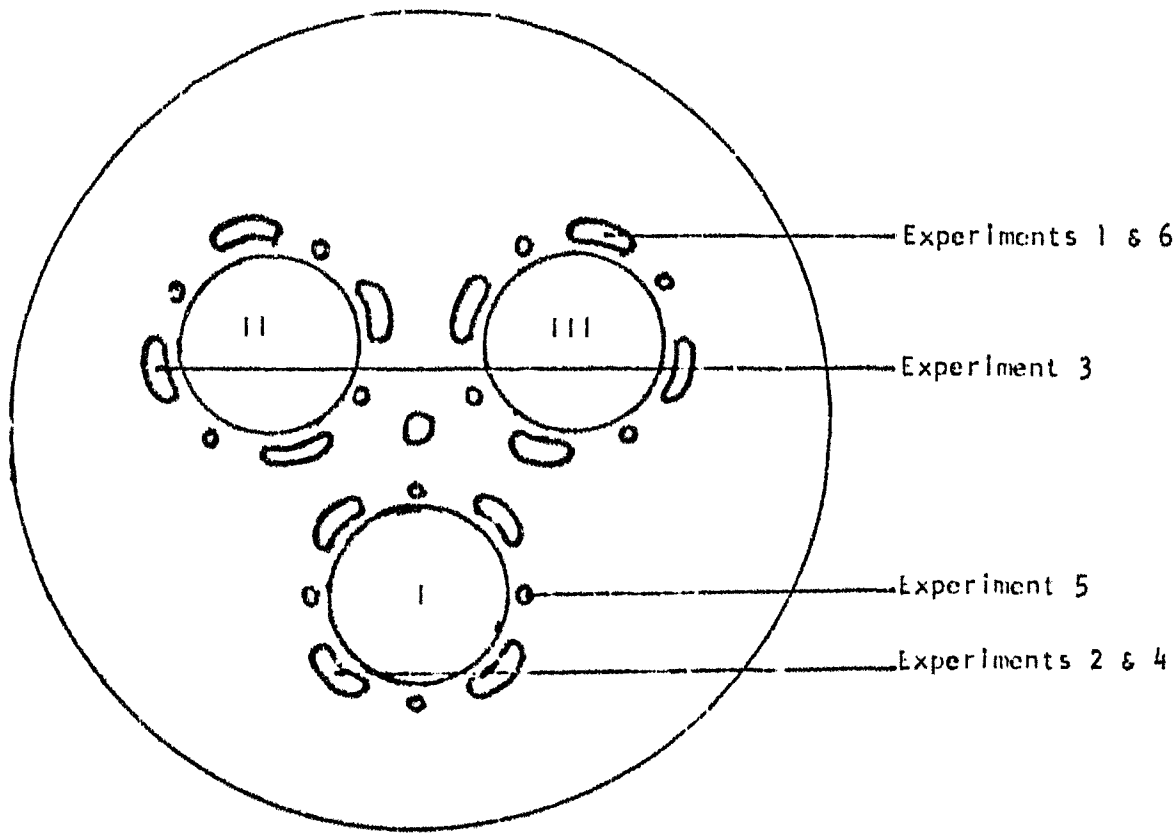

Figure 9. Sites of radiotracer inputs for the six experiments on furnace M11 with 48 MVA transformers

5.5.2. Experiments on furnace M10 with 48 MVA transformers

During this phase of the investigation five experiments were performed. These experiments were performed during the same period of time as the experiments on furnace M11.

All experiments other than the last were single input experiments in which irradiated hematite ore was introduced into a feed bunker.

The fifth and last experiment in this phase of the investigation was a multi-input experiment using Hotazel ore as radio-tracer. In this experiment twelve inputs of radio-tracer were made simultaneously to the twelve charging shafts feeding the three electrodes. In this experiment no input was made to the charging shaft feeding the furnace centre.

The sites of the charging shafts which were fed by the furnace bunkers receiving radio-tracer inputs are superimposed on the plan view of the furnace sketched in Figure 10.

5.5.3. Experiments on furnace M11 with 75 MVA transformers

During this phase of the investigation six experiments were performed.

In the first experiment irradiated hematite ore was introduced to the feed bunker feeding the central charging shaft, whilst in the sixth experiment an irradiated steel rod was used to make an input beneath electrode I.

Experiment 5. Radiotracer inputs to all charging shafts other than the central charging shaft

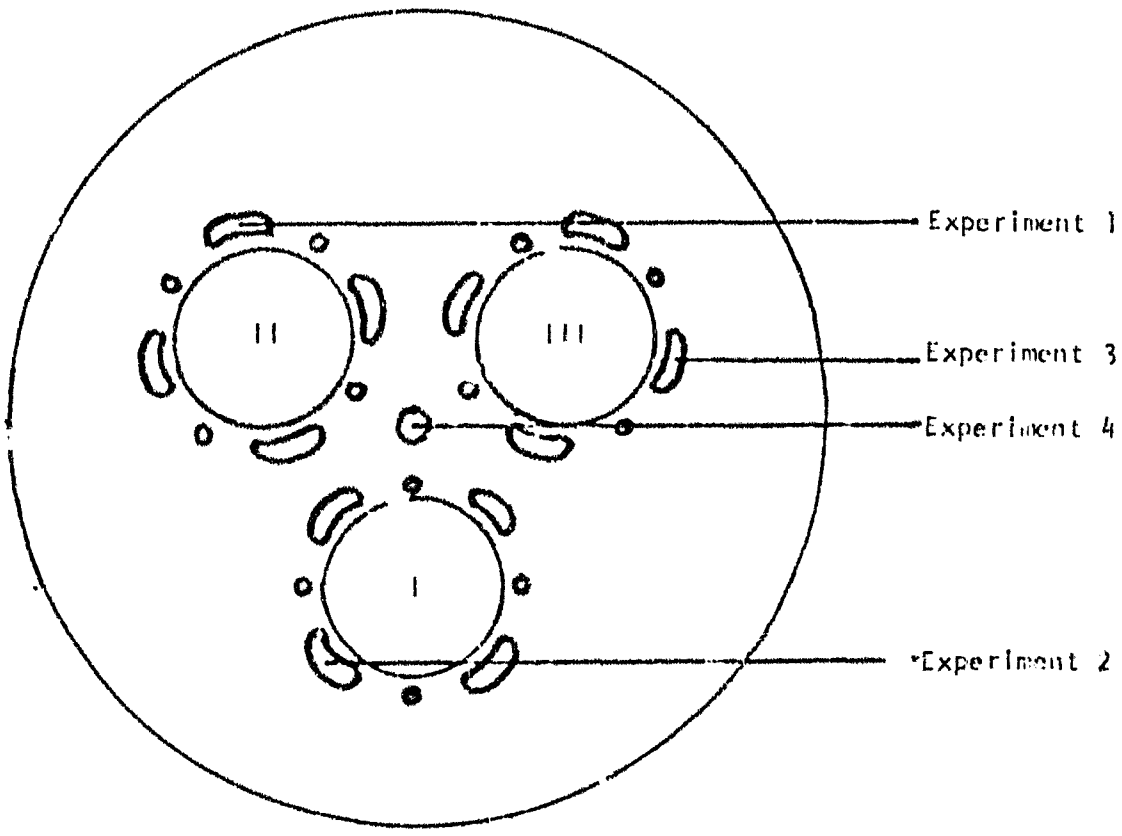

Figure 10. Sites of radiotracer inputs for the five experiments on furnace N10 with 48 MVA transformers

In the four multi-input experiments, inputs of irradiated Hotazel ore were made into the charging shafts. The sites of these inputs are shown on the furnace plan view sketched in Figure 11. The site of the input for the sixth experiment beneath electrode I is shown. Also shown is the central charging shaft into which the radio-tracer was added during the first experiment.

Experiment 2. Radiotracer inputs to all charging shafts other than the central charging shaft

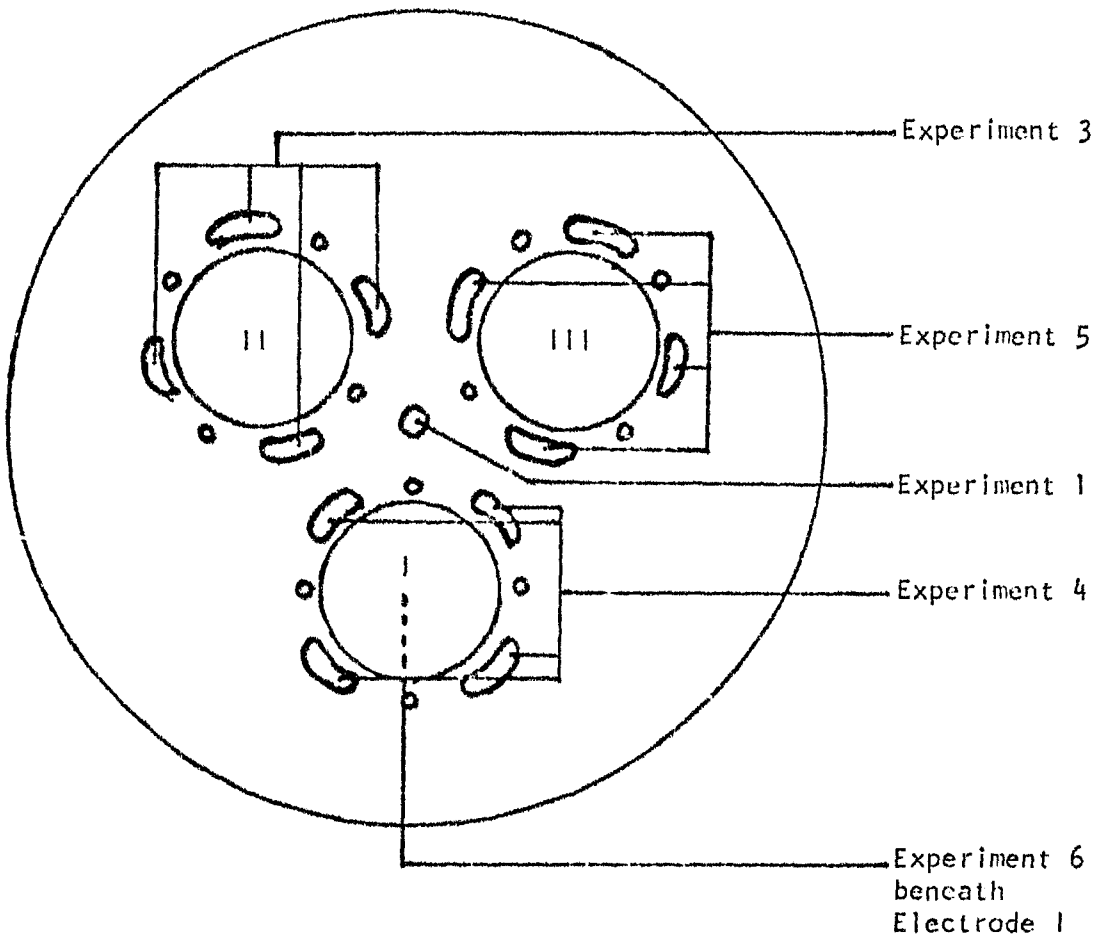

Figure 11. Sites of radiotracer inputs for the six experiments on furnace M11 with 75 MVA transformers

6. RESULTS

From each experiment the following results were obtained:-

(i) The slag or alloy phase furnace response expressed in terms of corrected counts per unit mass per unit time at each relevant tapping.

(ii) The time lapse after radio-tracer input for each tapping.

(iii) The average recorded values of the furnace operating parameters.

A plot of the counts as a function of the time lapse from radio-tracer input represents the residence time distribution for the furnace.

The residence time distributions of the alloy and slag phases for the six experiments on furnace M11 with 48 MVA transformers are tabulated in Tables 2 and 3 respectively.

Tables 4 and 5 represent the residence time distributions of the alloy and slag phases for the five experiments on furnace M10 with 48 MVA transformers.

The residence time distributions of the alloy and slag phases for the six experiments on furnace M11 with 75 MVA transformers are tabulated in Tables 6 and 7 respectively.

The average values of the furnace operating parameters for all three phases of the investigation are shown in Tables 8 to 11.

EXPERIMENT NUMBER											
1		2		3		4		5		6	
TIME Hours	COUNTS per 1 kg	TIME Hours	COUNTS per 1,5 kg	TIME Hours	COUNTS per 1 kg	TIME Hours	COUNTS per 1 kg	TIME Hours	COUNTS per 1 kg	TIME Hours	COUNTS per 1 kg
4,47	0	1,80	34	1,3	44	3.13	58	1,75	45	2,7	0
8,78	0	7,88	29	4,6	29	6,75	0	8,83	66	6,4	0
11,87	0	13,01	32	7,7	33	9,80	0	12,04	1 256	9,8	179
14,91	0	18,46	82	11,0	447	12,59	0	15,54	6 259	12,9	3 453
18,07	0	33,51	18 272	14,5	10 840	15,74	78	18,25	5 320	16,3	4 370
20,95	0	40,46	17 434	17,8	8 285	18,64	12 271	21,33	4 472	21,7	3 450
23,95	5 646	45,83	10 155	21,7	6 365	21,75	14 310	24,60	3 576	25,0	2 819
27,33	32 215	49,51	6 886	24,5	5 665	23,55	9 933	28,23	2 999	28,3	2 348
30,83	71 093	58,21	4 124	27,7	3 539	30,30	1 302	31,21	2 573	31,8	2 030
34,27	89 176	73,76	2 346	30,9	2 055	33,38	2 887	34,41	1 998	34,7	1 886
37,55	77 915	78,51	1 636	34,4	1 198	36,42	1 951	37,08	1 712	38,1	1 368
40,90	53 889	82,80	758	37,8	768	39,31	1 329	40,25	1 423	41,0	1 124
44,15	38 861	86,46	1 155	40,9	582	42,25	1 004	43,04	1 206	45,0	909
		89,51	1 010	44,1	675	45,46	682	47,00	979	48 3	691
		92,43	1 381	47,1	327	48,67	422	51,73	730	52,0	-
		95,71	719	49,7	210	51,88	286	55,04	499	55,5	450
				52,5	214	55,05	0	59,75	613		
						58,17	72	62,7.	382		

Table 2. Alloy phase residence time distributions for experiments on furnace Mil with 48 MVA transformers

EXPERIMENT NUMBER											
1		2		3		4		5		6	
TIME Hours	COUNTS per 0,6 kg	TIME Hours	COUNTS per 0,5 kg	TIME Hours	COUNTS per 0,5 kg	TIME Hours	COUNTS per 0,5 kg	TIME Hours	COUNTS per 0,5 kg	TIME Hours	COUNTS per 0,5 kg
4,47	0	1,26	0	4,0	35	2,05	72	7,29	0	1,6	0
7,87	0	6,93	23	7,0	27	5,75	38	10,83	248	5,7	0
11,08	0	11,46	0	10.0	123	9,00	7	14,51	341	8,9	0
14,25	0	16,13	0	13,3	296	11,84	0	17,50	476	12,1	117
17,38	0	32,13	0	16,7	322	14,92	0	20,12	256	14,7	150
20,33	0	37,38	395	20,7	98	17,63	0	23,46	133	20,9	190
23,38	0	43,80	115	24,0	31	20,75	438	27,62	149	24,3	9
26,55	867	48,76	0	26,5	0	23,42	566	30,46	38	27,1	0
29,75	3 953	57,01	0	30,0	0	29,88	0	33,75	2	31,0	0
33,18	3 298	65,13	0	33,4	0	32,46	22	36,12	0	33,8	0
36,38	3 822	76,13	0	36,5	0	35,50	0	38,91	0	37,2	0
40,50	2 185	81,96	0	40,0	0	38,21	0	42,41	0	40,5	64
43,52	1 815	85,93	0	43,4	0	41,59	0	44,79	0	43,7	0
		87,76	0	45,9	0	44,42	0	51,58	0	47,5	0
		91,88	0	49,0	0	47,75	0	54,96	0	50,2	-
		94,88	0	52,0	0	50,92	0	59,00	0	54,8	94
						54,05	0	62,50	0		

Table 3. Slag phase residence time distributions for experiments on furnace Mil with 48 MVA transformers

EXPERIMENT NUMBER									
1		2		3		4		5	
TIME Hours	COUNTS per 1 kg	TIME Hours	COUNTS per 1 kg	TIME Hours	COUNTS per 1 kg	TIME Hours	COUNTS per 1 kg	TIME Hours	COUNTS per 1 kg
13,0	2 878	8,42	33	6,30	0	20,3	8	1,00	0
16,3	8 421	11,54	0	9,29	11	23,8	47	4,00	0
19,6	7 082	14,46	39 855	12,63	709	27,7	39	7,21	0
22,8	5 668	17,38	6 728	15,88	6 590	31,3	8	10,29	234
25,6	4 580	20,42	3 265	18,92	6 948	34,9	28	13,58	443
29,0	3 710	23,67	2 294	23,17	5 226	38,3	0	16,91	2 085
32,4	2 891	27,25	1 967	26,17	4 461	41,3	0	20,2:	2 884
35,9	2 288	30,42	4 334	29,54	3 759	45,5	96	23,90	4 382
39,2	1 827	33,42	1 310	32,75	3 208	52,8	7	27,96	3 397
42,8	1 428	36,38	1 182	36,29	2 733	56,3	92	31,58	2 925
46,6	1 157	39,67	835	39,58	2 364	59,5	0	35,62	2 464
49,6	615	42,53	722	42,71	2 003	62,8	99	39,70	2 139
52,8	805	46,08	562	46,00	1 771	66,3	986	43,08	1 827
56,0	663	49,42	468	49,38	1 548	69,5	1 850	46,96	1 593
59,3	620	52,54	428	52,55	1 309	72,8	2 347	50,53	1 293
62,5	460	55,75	368	55,63	1 174	77,0	2 797	54,29	1 158
65,6	443	59,17	314	58,00	1 035	80,7	3 387	57,58	919
68,7	359	62,68	305	61,71	1 065	84,0	6 682	61,58	-
72,1	353	66,21	261	64,58	788	86,6	5 527	64,83	753
75.3	238	69,21	173	68,46	727	90,0	5 036		
78,9	323	72,46	189	71,50	697				
		75,46	180	74,83	595				

Table 4. Alloy phase residence time distributions for experiments on furnace M10 with 48 MVA transformers

EXPERIMENT NUMBER									
1		2		3		4		5	
TIME Hours	COUNTS per 0,5 kg	TIME Hours	COUNTS per 0,5 kg	TIME Hours	COUNTS per 0,5 kg	TIME Hours	COUNTS per 0,5 kg	TIME Hours	COUNTS per 0,5 kg
12,2	117	7,54	63	4,92	0	23,4	69	0,33	0
15,5	979	10,83	76	8,92	0	26,5	0	2,54	0
18,8	751	13,08	0	11,63	30	30,0	34	6,54	0
21,9	421	16,42	439	15,17	1 922	33,5	104	9,58	0
25,0	325	18,50	302	18,42	498	37,0	69	12,58	29
28,0	226	21,75	217	21,58	218	40,6	29	15,96	293
31,2	85	25,96	129	25,08	120	44,1	81	19,21	52
34,5	70	29,54	339	28,63	49	51,4	80	22,81	1 250
38,3	93	32,83	34	31,88	0	55,2	68	27,33	85
41,9	59	35,58	0	35,08	25	58,7	59	30,54	0
45,4	0	38,58	74	38,75	0	61,6	64	34,79	213
48,9	28	41,75	0	41,92	0	65,0	7	38,37	-
51,9	0	45,08	0	45,08	0	68,5	50	42,08	0
54,8	0	48,21	0	48,25	0	71,6	61	45,58	0
58,3	11	51,75	61	51,66	0	74,8	94	49,25	0
61,3	0	54,83	8	55,00	0	80,0	29	57,71	0
64,9	0	58,25	11	56,92	0	82,0	48	60,58	-
67,9	0	61,83	0	60,08	0	86,5	19	64,00	0
71,4	0	65,67	47	62,95	0	89,5	0		
74,6	0	68,08	34	70,21	0				
77,3	0	71,79	0	74,13	0				
		74,25	1						

Table 5. Slag phase residence time distributions for experiments on furnace M10 with 48 MVA transformers

EXPERIMENT NUMBER											
1		2		3		4		5		6	
TIME Hours	COUNTS per 1 kg	TIME Hours	COUNTS per 1 kg	TIME Hours	COUNTS per 1 kg	TIME Hours	COUNTS per 2 kg	TIME Hours	COUNTS per 2 kg	TIME Hours	COUNTS per 1,9 kg
18,13	7 123	1,21	0	2,50	0	1,67	-61	2,55	0	3,00	20 529
20,96	5 302	3,34	0	5,58	0	4,33	-31	5,55	0	5,91	14 785
23,59	4 346	6,92	0	8,96	0	6,97	-23	8,25	986	8,58	12 038
28,46	3 642	9,71	42	12,20	50	9,42	-17	10,71	1 460	11,29	9 675
31,05	3 090	12,46	34	15,66	286	11,95	47	13,63	1 708	13,41	7 804
33,59	2 685	15,67	213	18,79	614	14,79	261	17,00	3 883	16,83	6 614
36,21	2 303	18,71	292	22,25	3 634	17,67	3 604	20,46	3 372	19,96	4 922
39,05	1 990	22,80	417	25,21	5 148	20,35	5 291	24,33	2 972	23,08	3 537
41,67	1 625	26,05	476	28,62	5 833	23,71	4 378	27,71	2 901	26,29	2 262
44,09	1 421	28,84	478	32,21	4 204	26,63	3 257	30,00	2 481	29,12	1 698
46,59	1 238	31,62	551	35,83	3 107	30,08	3 563	32,71	1 934	32,57	1 296
49,30	1 057	34,05	543	39,33	2 962	32,67	2 719	35,67	1 556	35,54	988
52,00	825	36,67	493	42,84	2 437	35,25	1 852	39,04	1 207	39,08	770
54,92	697	39,55	431	47,85	2 290	38,50	1 473	42,13	1 033	41,62	590
57,67	561	41,92	324	49,58	1 684	41,41	1 218	45,30	810	45,13	401
60,67	499	45,88	343	53,32	2 016	44,21	1 020	48,30	670	47,87	296
63,36	439			57,83	2 222	47,41	788			50,58	261
65,95	428									53,21	199
68,13	355									56,71	134
70,84	274									58,87	85
73,13	223										
76,21	237										
78,50	159										
81,17	48										
83,71	80										
86,34	65										
88,84	75										
91,30	30										
93,30	53										
96,42	115										
99,25	74										
102,17	89										

Table 6. Alloy phase residence time distributions for experiments on furnace Mil with 75 MVA transformers

EXPERIMENT NUMBER									
1		2		3		4		5	
TIME minutes	COUNTS per 2.5 kg	TIME minutes	COUNTS per 2.5 kg	TIME minutes	COUNTS per 2.5 kg	TIME minutes	COUNTS per 2.5 kg	TIME minutes	COUNTS per 2.5 kg
17,55	1 045	2,38	63	1,67	0	2,75	1	2,54	0
20,42	142	5,46	85	4,75	0	5,33	-56	4,71	23
22,67	13	9,21	139	8,24	49	8,21	-176	8,58	127
27,67	0	11,71	100	11,33	50	11,00	-82	12,05	215
30,17	-	14,21	129	14,50	72	13,88	-49	13,96	154
32,71	0	17,38	0	17,66	407	16,04	21	16,13	245
35,53	0	20,50	167	21,12	805	17,00	33	18,45	-
38,21	0	24,71	196	24,33	1 527	19,83	85	22,62	135
40,92	0	27,71	69	27,50	365	22,96	181	26,62	244
43,30	0	30,71	93	31,37	578	25,96	62	29,33	71
45,96	0	33,30	36	35,00	746	28,25	128	32,05	49
48,67	0	36,00	52	38,51	217	32,08	80	35,25	0
53,96	0	38,52	79	41,87	0	34,88	68	38,13	0
56,50	26	41,21	109	45,16	90	36,83	88	41,67	0
59,34	95	45,71	0	49,21	27	40,75	55	44,13	0
62,84	10			52,54	0	43,25	19	47,25	0
65,34	19			57,04	0	46,29	-1		
67,34	0								
70,17	-								
72,17	0								
75,17	0								
77,50	0								
80,42	0								
83,05	0								
85,42	0								
88,10	0								
90,30	0								
93,30	0								
95,46	0								
98,25	0								
101,17	0								

Table 7. Slag phase residence time distributions for experiments on furnace Mil with 75 MVA transformers

EXPERIMENT NUMBER	FURNACE LOAD MW	TRANSFORMER PRIMARY CONNECTION	TRANSFORMER SECONDARY TAP	PRIMARY LINE CURRENT A			ELECTRODE CURRENT KA			PRIMARY LINE VOLTAGE kV
				1	2	3	I	II	III	
EXPERIMENTS ON FURNACE M11 WITH 48 MVA TRANSFORMERS										
1	25	Delta	22	910	979	853	101	103	96	32,4
2	18	Star	14	605	653	616	85	87	75	32,2
3	26	Delta	22	839	880	840	101	96	90	32,4
4	26	Delta	22	871	913	867	103	99	93	32,4
5	26	Delta	22	852	907	845	101	99	94	32,5
6	26	Delta	22	854	921	850	100	100	92	32,3
EXPERIMENTS ON FURNACE M10 WITH 48 MVA TRANSFORMERS										
1	26	Delta	22	857	893	837	98	98	93	32,3
2	25	Delta	22	866	903	850	99	100	94	32,2
3	26	Delta	22	858	897	862	98	99	97	32,7
4	20	Delta	20	785	828	800	93	94	93	32,9
5	22,6	Delta	21	877	885	871	101,0	99,6	99,9	33,6
EXPERIMENTS ON FURNACE M11 WITH 75 MVA TRANSFORMERS										
1	32,8	Delta	24	1 258	1 324	1 345	121,2	121,2	122,3	32,9
2	33,6	Delta	25	1 281	1 372	1 384	123,4	124,1	124,0	32,8
3	24,9	Delta	21	1 092	1 137	1 142	116,5	115,1	115,9	32,5
4	30,5	Delta	24	1 197	1 279	1 292	119,6	119,8	119,6	32,9
5	29,2	Delta	23	1 172	1 256	1 258	117,5	117,6	117,5	32,8
6	31,4	Delta	24	1 252	1 331	1 349	122,1	122,2	120,8	32,7

Table 8. Average electrical furnace parameters recorded during experimentation

EXPERIMENT NUMBER	ENERGY CONSUMPTION PER TAPPING CYCLE MW.h	ALLOY MASS PER TAPPING t	SLAG TO ALLOY MASS RATIO	RAW MATERIAL FEEDRATE t/h	TIME BETWEEN TAPPINGS h		DURATION OF TAPPING h		DOWNTIME h
					ALLOY	SLAG	ALLOY	SLAG	
EXPERIMENTS ON FURNACE M11 WITH 48 MVA TRANSFORMERS									
1	81	24,72	0,93	25,84	3,3	3,3	-	-	0
2	81	25,15	1,15	14,69	6,3	6,2	-	-	6,08
3	78	24,97	1,00	27,33	3,2	3,2	0,30	0,65	0
4	73	25,83	0,98	26,80	3,2	3,3	0,27	0,62	3,17
5	82	23,44	1,16	25,95	3,5	3,5	0,34	0,52	2,00
6	85	26,71	1,03	28,82	3,5	3,5	0,43	0,50	0
EXPERIMENTS ON FURNACE M10 WITH 48 MVA TRANSFORMERS									
1	81	25,34	0,86	27,85	3,3	3,3	0,42	0,70	0
2	77	23,42	0,96	27,19	3,2	3,2	0,40	0,58	0
3	80	23,74	1,05	29,95	3,3	3,3	0,51	0,73	0
4	77	23,63	0,92	22,17	3,7	3,7	0,39	0,44	2,10
5	81	-	0,72	26,80	3,55	3,54	0,64	0,55	0
EXPERIMENTS ON FURNACE M11 WITH 75 MVA TRANSFORMERS									
1	87	-	0,48	32,43	2,70	2,79	0,55	0,57	1,92
2	97	34,10	0,86	32,66	2,98	3,10	0,51	0,55	1,00
3	85	32,64	0,49	24,03	3,46	3,44	0,61	0,63	1,17
4	84	28,17	0,86	33,48	2,86	2,84	-	-	1,02
5	87	24,73	0,87	30,24	3,03	3,01	0,68	0,61	0,83
6	92	30,43	0,99	34,12	2,94	-	0,69	-	0,92

Table 9. Average non-electrical furnace paramcters recorded during experimentation

EXPERIMENT NUMBER	ALLOY ANALYSIS (MASS %)					SLAG ANALYSIS (MASS %)					
	Mn	Fe	Si	P	S	MnO	SiO_2	CaO	MgO	Al_2O_3	FeO
EXPERIMENTS ON FURNACE M11 WITH 48 MVA TRANSFORMERS											
1	78,5	13,6	0,14	0,083	0,009	20,0	33,6	29,7	7,87	4,20	0,16
2	74,9	17,2	0,07	0,088	0,008	27,4	29,5	25,7	7,32	4,63	0,25
3	76,8	15,3	0,14	0,083	0,009	22,4	33,9	28,2	7,65	4,75	0,18
4	78,2	13,8	0,17	0,086	0,008	24,7	37,8	28,4	7,55	4,56	0,18
5	76,4	15,7	0,10	0,079	0,011	24,5	32,0	28,5	7,79	4,21	0,23
6	76,5	15,3	0,12	0,081	0,011	23,9	31,6	28,2	7,82	4,40	0,13
EXPERIMENTS ON FURNACE M10 WITH 48 MVA TRANSFORMERS											
1	78,5	13,6	0,14	0,083	0,009	22,6	32,9	28,6	7,70	4,67	0,18
2	78,0	14,0	0,15	0,084	0,009	25,6	32,4	27,4	7,49	4,47	0,22
3	76,4	15,6	0,11	0,081	0,010	24,8	31,9	28,1	7,53	4,10	0,19
4	77,8	14,3	0,12	0,074	0,010	24,6	31,4	27,6	7,85	4,37	0,19
5	75,2	16,9	0,12	0,078	0,016	27,6	30,3	29,6	7,25	4,05	0,24
EXPERIMENTS ON FURNACE M11 WITH 75 MVA TRANSFORMERS											
1	76,6	15,4	0,14	0,077	0,014	24,0	31,5	31,5	7,66	4,14	0,20
2	77,7	14,4	0,13	0,090	0,020	25,2	31,5	30,0	6,86	3,95	0,34
3	78,3	13,7	0,34	0,079	0,016	16,0	35,1	32,7	8,09	4,34	0,23
4	76,9	15,0	0,31	0,090	0,012	21,7	33,9	30,6	7,70	4,16	0,33
5	77,3	14,6	0,21	0,098	0,013	21,6	34,8	30,7	7,43	4,20	0,24
6	76,7	15,4	0,15	0,078	0,009	25,5	32,5	27,9	7,50	4,11	0,18

Table 10. Average product analysis recorded during experimentation

EXPERIMENT NUMBER	% OF THEORETICAL CARBON REQUIREMENT IN THE FEED
EXPERIMENTS ON FURNACE M11 WITH 48 MVA TRANSFORMERS	
1	94,6
2	100,3
3	96,0
4	100,0
5	96,7
6	105,5
EXPERIMENTS ON FURNACE M10 WITH 48 MVA TRANSFORMERS	
1	104,2
2	103,4
3	95,1
4	97,2
5	123,2
EXPERIMENTS ON FURNACE M11 WITH 75 MVA TRANSFORMERS	
1	100,6
2	101,8
3	99,9
4	103,6
5	99,4
6	98,0

Table 11. Average percentage of the theoretical carbon requirement in the furnace feed recorded during experimentation

The values for the per cent of the theoretical carbon requirement in the furnace feed given in Table 11 were calculated as follows:-

For each experiment the mass per cent of iron, manganese and carbon were calculated from the raw material analysis and the relative proportions of the charge components in the burden mix. Based on the following assumptions the theoretical carbon requirement in mass per cent was calculated.

(i) All the Fe was present as Fe_2O_3.

(ii) The Fe_2O_3 was reduced by the reaction,
$Fe_2O_3 + C = 2Fe + 3CO$.

(iii) All the Mn was in the form MnO prior to any consumption of carbon by the Mn oxides.

(iv) All the MnO was reduced by the reaction,
$7MnO + 10C = Mn_7C_3 + 7CO$.

From these assumptions the theoretical carbon requirement for complete reduction in mass per cent was,

$$\% \text{ Fe}/3{,}33 + \% \text{ Mn}/3{,}21.$$

Hence the per cent of theoretical carbon requirement in the furnace feed was given by

$$\frac{\% \text{ C}}{\frac{\% \text{ Fe}}{3{,}33} + \frac{\% \text{ Mn}}{3{,}21}} \times 100$$

7. ANALYSIS OF RESULTS

7.1. Introduction

Results obtained for the slag phase were not analysed because it was very doubtful that these results were reproducible. This was because of the low signal-to-noise ratios in the measured responses and alloy entrapment within the slag.

When the stimulus is a radio-tracer input to the furnace feed, the response signal is the radioactivity level in the discharge due to this stimulus. The response noise is the radioactivity level in the furnace discharge due to natural or "background" radioactivity. In response measurement both signal and noise are recorded. To obtain the response signal the response noise is measured prior to stimulus of the furnace, and this noise is subtracted from the total response measured after stimulus.

In general the response noise is subject to random fluctuations, but, provided the response signal is sufficiently large, the influence of the noise fluctuations is damped out. If the response signal-to-noise ratio is small, noise fluctuations are important and the results are not significant.

For one slag phase result the response peak signal-to-noise ratio was 1,28. In the balance of results for this phase the peak signal-to-noise ratios were less than 0,70. Hence these results were not significant.

Visual examination of slag samples taken during the experimental campaign revealed that alloy beads were entrapped in the slag, and that the amount of alloy entrapment in the slag varied from tapping to tapping. It may be shown for slags and alloys of typical compositions that in mixtures containing a little over one mass per cent alloy, the slag and alloy introduce equal amounts of iron into the mixture. Consequently the extent and variation of alloy entrapment in the slag strongly influenced the forms of the slag phase responses obtained by altering the amounts of Fe^{59} present in the slag samples monitored. Hence these results had no significance.

The alloy phase result for experiment 2 on furnace M11 with 75 MVA transformers had a peak signal-to-noise ratio of 0,22 and so was not analysed. For the balance of the alloy phase results the peak signal-to-noise ratios varied from a minimum of 1,48 to a maximum of 64,5.

Many of the residence time distributions for the alloy phase were truncated and single parameters to describe the residence time distributions could not be calculated.

At each furnace tapping the response signal was expressed in counts per unit time per unit mass. From one tapping to the next the amount of material tapped varied, influencing the amount of radio-tracer discharged at each tapping. To obtain a relative counts value for the radio-activity level of the total furnace discharge at each tapping the counts recorded were multiplied by the relative mass tapped at each tapping. The relative

mass tapped was calculated as the ratio of the mass tapped during the particular tapping to the maximum mass tapped at a single tapping during the experiment. A plot of the corrected counts as a function of time lapse after radio-tracer input gave the true residence time distribution for each experiment. These corrected results were analysed.

7.2. Correlations between the average operating parameters recorded during the experimentation

To facilitate the comparison of residence time distribution data with furnace operating data, simple correlations between operating parameters were considered.

The ranges of operating conditions prevailing during experimentation on furnace M11 with 48 MVA transformers, and on furnace M10 with 48 MVA transformers, were small in each case, and hence the evaluation of correlations was difficult.

In the evaluation of correlations, the following sets of data were considered:-

(i) The data recorded for the experiments on furnace M11 with 48 MVA transformers.

(ii) The data recorded for the experiments on furnace M10 with 48 MVA transformers.

(iii) The data recorded for the experiments on furnace M11 with 75 MVA transformers.

(iv) The data recorded for all the experiments on furnace M11.

The most important operating parameter is the furnace load which is the energy input to the furnace.

Consequently correlations between the furnace load as dependent variable, and the following independent variables were considered:-

(i) The primary line voltage.

(ii) The sum of the squared electrode currents.

(iii) The energy consumption per alloy tapping cycle.

(iv) The time lapse between alloy tappings.

(v) The mass percentage MnO in the slag.

(vi) The furnace feedrate.

(vii) The mass percentage Mn in the alloy.

(viii) The alloy production rate.

(ix) The slag to alloy mass ratio.

(x) The mass ratio : MnO/Mn.

Other correlations considered were as follows:-

(i) The mass percentage Mn in the alloy as dependent variable and the mass percentage MnO in the slag as independent variable.

(ii) The furnace feedrate as dependent variable and the mass ratio : MnO/Mn as independent variable.

(iii) The percentage of the theoretical carbon requirement in the feed as dependent variable and the following as independent variables:-

(a) The mass percentage MnO in the slag.

(b) The mass ratio MnO/Mn.

(iv) The alloy production rate as dependent variable and the furnace feedrate as independent variable.

(i) The primary line voltage.

(ii) The sum of the squared electrode currents.

(iii) The energy consumption per alloy tapping cycle.

(iv) The time lapse between alloy tappings.

(v) The mass percentage MnO in the slag.

(vi) The furnace feedrate.

(vii) The mass percentage Mn in the alloy.

(viii) The alloy production rate.

(ix) The slag to alloy mass ratio.

(x) The mass ratio : MnO/Mn.

Other correlations considered were as follows:-

(i) The mass percentage Mn in the alloy as dependent variable and the mass percentage MnO in the slag as independent variable.

(ii) The furnace feedrate as dependent variable and the mass ratio : MnO/Mn as independent variable.

(iii) The percentage of the theoretical carbon requirement in the feed as dependent variable and the following as independent variables:-

(a) The mass percentage MnO in the slag.

(b) The mass ratio MnO/Mn.

(iv) The alloy production rate as dependent variable and the furnace feedrate as independent variable.

(v) The ratio: furnace load to furnace feedrate as dependent variable and the mass ratio: MnO to Mn as independent variable.

Linear correlations were obtained using standard linear regression analysis.[71] These correlations were tested as follows:-

(i) By use of the Students' t-distribution at the 99 per cent confidence level to assess whether a correlation existed.[71]

(ii) By use of the coefficient of determination to assess the value of the correlation.[71] The closer this coefficient is to unity the better the correlation. Only correlations with coefficients of determination of greater than 0,89 were considered.

Non-linear correlations were obtained using the standard Law and Bailey non-linear regression technique with a convergence test.[72] These correlations were tested by use of the information per observation point. The larger this value the better the correlation. Only correlations with values for the information per observation point of greater than 1×10^6 were used.

The three linear correlations obtained involved the furnace load as dependent variable (y). For the experiments on furnace M11 with 48 MVA transformers the correlation obtained with time lapse between alloy tappings as independent variable (x) was:-

$$y = -2,597x + 34,45$$

For the experiments on furnace M11 with 75 MVA transformers two correlations were obtained. The correlation obtained

with the sum of the squared electrode circuits as dependent variable (x) was:-

$$y = 1,386x - 29,51$$

For the mass per cent MnO in the slag as independent variable (x) the correlation was:-

$$y = 0,8363x + 11,72$$

For all the experiments on furnace M11 a non-linear correlation was obtained with furnace load as dependant variable (y) and furnace feedrate as independent variable (x). This correlation was:-

$$y = 0,0107x^2 + 0,2302x + 12,3604$$

7.3. Single parameter description of residence time distributions

A computer program, shown in Appendix A, was used to calculate the parameters described in Section 3.2 for some of the residence time distributions. This analysis was restricted to results where there was no truncation at the start of the distribution, and where the ratio of the final experimental value to the peak experimental value was less than 0,01.

As the distributions analysed were discrete rather than continuous, integrals were replaced by summations in the analysis.

The mean residence time $\bar{t}a$ was calculated as,

$$\bar{t}a = \frac{\sum_{i=m}^{N} C_i \, t_i \, \Delta t_i}{\sum_{i=m}^{N} C_i \, \Delta t_i}$$

where, C_i = counts at i*th* tapping,

$\Delta t_m = (t_{m+1} - t_m)/2$,

$\Delta t_N = (t_N - t_{N-1})/2$,

and $\Delta t_i = (t_{i+1} - t_{i-1})/2$, $m<i<N$.

The m*th* tapping was the first tapping at which the corrected counts were greater than zero. The N*th* tapping was the last tapping at which the response was measured.

The normalized distribution in terms of units of mean residence time, θ, was calculated from,

$$C_i' = \frac{C_i}{\sum_{i=m}^{N} C_i \, \Delta\theta_i}$$

where $\theta_i = t_i/\bar{t}a$

and $\Delta\theta_i = \Delta t_i/\bar{t}a$

A plot of C_i' as a function of θ_i gave the C-curve, $C(\theta)$.

The F-curve, $F(\theta)$, was obtained by calculation from,

$$F_i = \sum_{k=m}^{i} C_k' \, \Delta\theta_k$$

and plotting F_i as a function of θ_i.

Moments of the C-curve about the origin and mean were calculated using the following equations:-

$$M_k' = \sum_{i=m}^{N} \theta_i^k \, C_i' \, \Delta\theta_i \qquad k = 1,2 \ldots\ldots 5,$$

and

$$M_k = \sum_{i=m}^{N} (\theta_i - 1)^k \, C_i' \, \Delta\theta_i \qquad k = 1,2 \ldots\ldots 5.$$

where, M_k' = k*th* moment about the origin

M_k = k*th* moment about the mean.

All these calculations were performed using a single computer program. The mean, and variance in terms of units of mean residence time, for the results analysed are shown in Table 12. The C and F-curves are shown in Figures 12 to 17. The computer program is given in Appendix A.

EXPERIMENT NUMBER	FURNACE NUMBER AND RATING	MEAN $\bar{t}a$	VARIANCE σ^2
4	M11, 48 MVA	25,46	0,0914
2	M10, 48 MVA	20,15	0,2930
6	M11, 75 MVA	13,76	0,5354

Table 12. Single parameters to describe residence time distribution

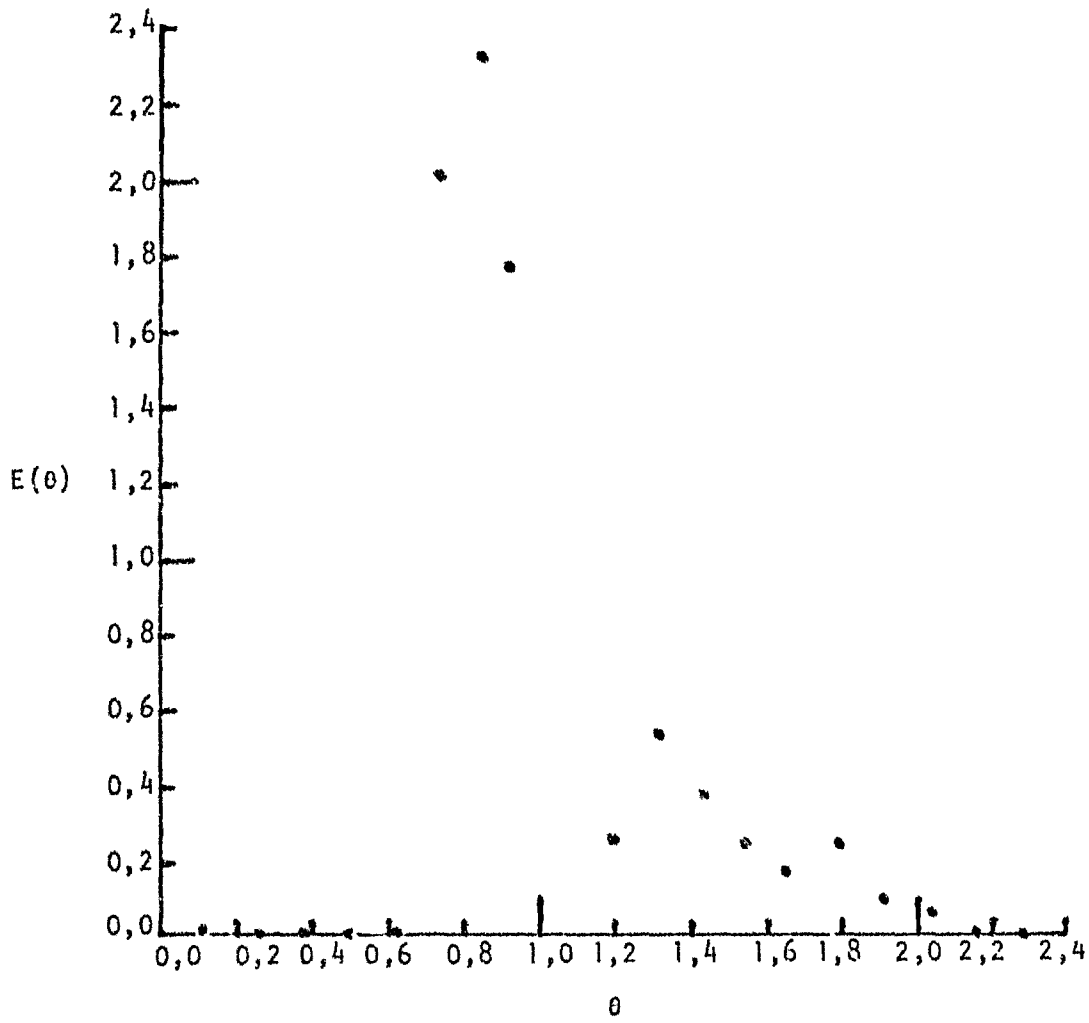

Figure 12. C-curve for experiment 4 on furnace M11 with 48 MVA transformers

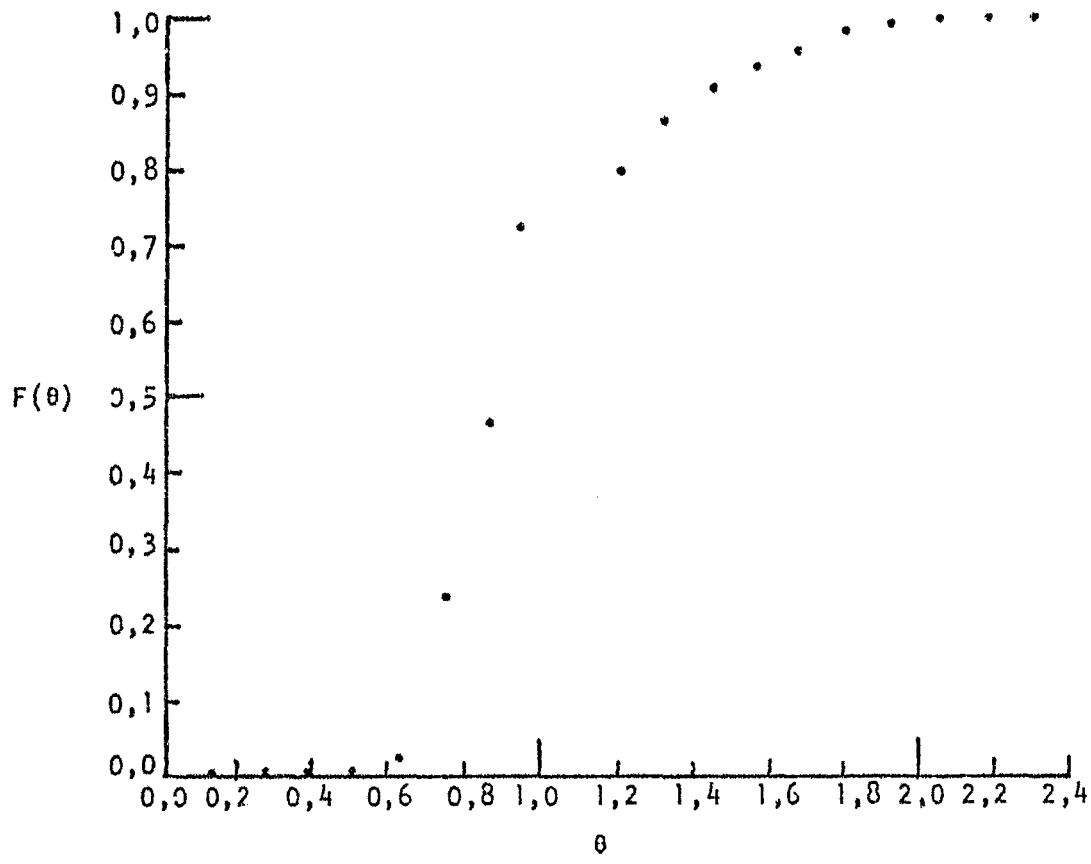

Figure 13. F-curve for experiment 4 on furnace M11 with 48 MVA transformers

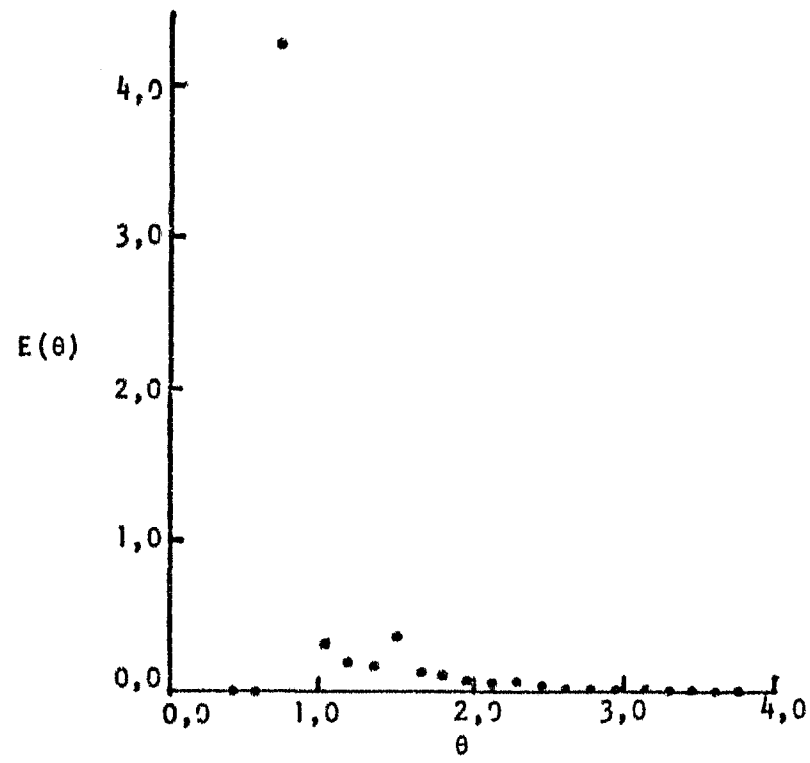

Figure 14. C-curve for experiment 2 on furnace M10 with 48 MVA transformers

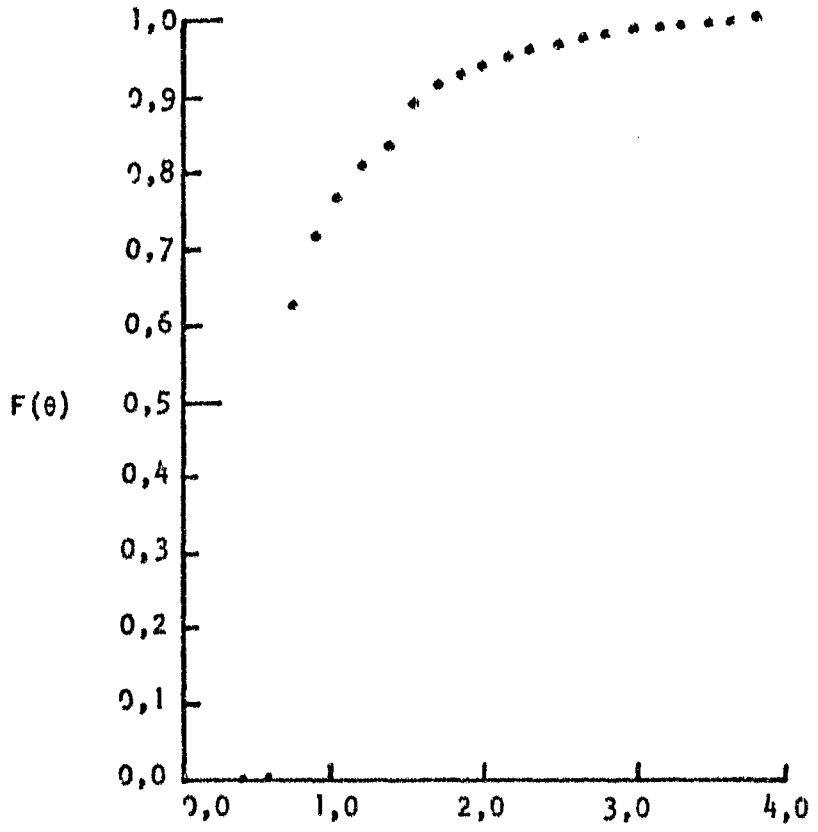

Figure 15. F-curve for experiment 2 on furnace M10 with 48 MVA transformers

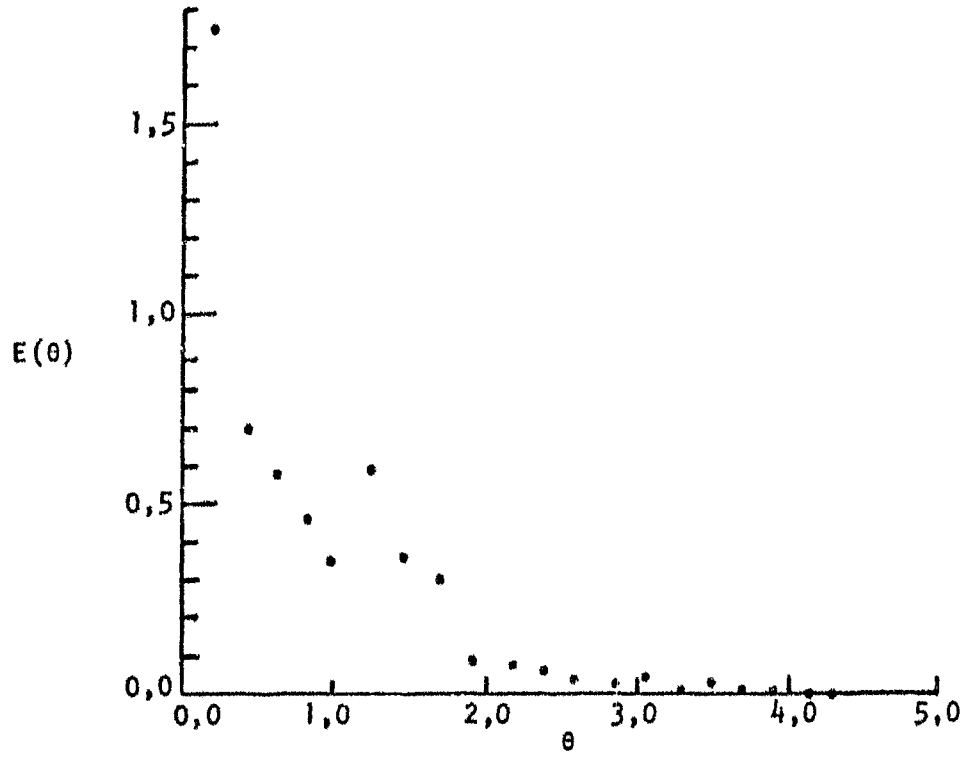

Figure 16. C-curve for experiment 6 on furnace M11 with 75 MVA transformers

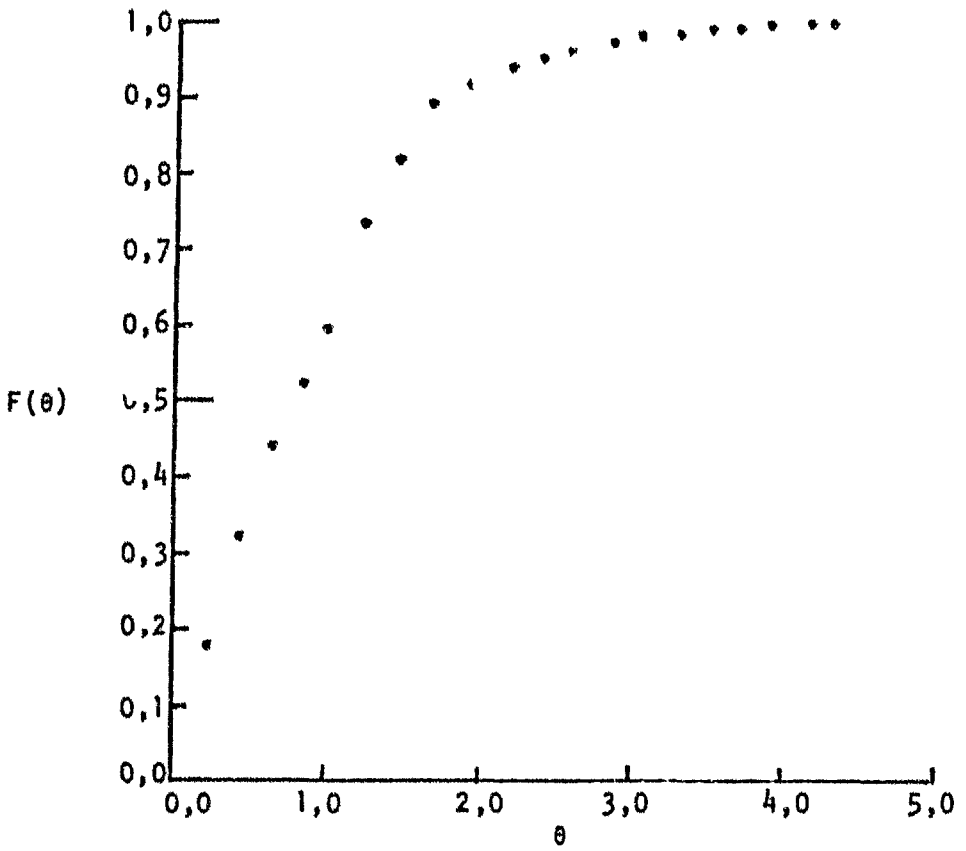

Figure 17. F-curve for experiment 6 on furnace M11 with 75 MVA transformers

7.4. Description of residence time distributions by means of a theoretical model

The equations developed in Section 4.4 were used to describe the measured residence time distributions. The optimum values of the model parameters in these equations were obtained for each result by applying the standard Law and Bailey non-linear regression technique with a convergence test using a computer.[72]

The computer program developed consisted of a combination of available library subprograms and user written subprograms. Variations of the basic computer program were developed to deal with the following conditions:-

(i) Single input experiments.

(ii) Multi-input experiments.

(iii) Single input experiments where the initial portion of the distribution was truncated.

Due to regression problems, it was found that optimum values of the model parameters were not always obtained with different initial guesses of the parameter values. This was considered to be due to the following reasons:-

(i) The extremely non-linear nature of the experimental results.

(ii) The generation of numbers beyond the dimensional limits of the computer.

Consequently an additional variation of the basic computer program permitted regression on each of an unlimited number of sets of initial values.

A full description of the development and final configuration of the computer program is given in Appendix B.

For single input experiments the equations used to describe the residence time distributions obtained were equations (18) and (19) (refer Section 4.4). These are reproduced below:-

$$C_1 = \frac{V_i C_o \bar{t}}{2\ V_{inv}\ (t_o + t_1)} \left(\text{erf} \left(\frac{t_1}{2\sqrt{Dt}} - \frac{1}{2\sqrt{D}} \right) - \text{erf} \left(- \frac{1}{2\sqrt{D}} \right) \right) \qquad (18)$$

$$C_i = \frac{V_i C_o \bar{t}}{2\ V_{inv}\ (t_i - t_{i-1})} \left(\text{erf} \left(\frac{t_i}{2\sqrt{Dt}} - \frac{1}{2\sqrt{D}} \right) - \text{erf} \left(\frac{t_{i-1}}{2\sqrt{Dt}} - \frac{1}{2\sqrt{D}} \right) \right) + C_{i-1} \left(1 - \frac{V_{i-1}}{V_{inv}} \right) \qquad (19)$$

$i = 2, \ldots . N.$

The four model parameters here were Co, $\bar{t}$, D and Vinv. By means of the computer program the optimum values of Co, $\bar{t}$, D and Vinv and the theoretically computed residence time distribution were obtained. For some experiments the residence time distributions were truncated at the start of the distribution and the missing values were predicted by the computer program.

For multi-input experiments it was assumed that each input was subject to the same degree of dispersion in the dispersed plug flow region. In addition it was assumed that the maximum number of different $\bar{t}$s in the dispersed plug flow region was four. These assumptions were made to limit the number of parameters to be optimized in the regression analysis.

For these experiments the maximum number of parameters to be optimized was seven. The equations used to describe these residence time distributions were equations (20) and (21) (refer Section 4.4) which are reproduced below:-

$$C_1 = \sum_{k=1}^{m} C_1,k \quad m \leq 4 \tag{20}$$

$$C_i = \sum_{k=1}^{m} C_i,k \quad i = 2, \ldots N. \text{ and } m \leq 4 \tag{21}$$

The values of C_1,k and C_i,k were given by equations (20) and (21) using the relevant values of $\bar{t}k$. By means of the computer program the optimum values of Co, D, Vinv, $\bar{t}_1, \ldots \bar{t}_m$ and m were obtained together with the theoretically computed residence time distribution.

In one experiment (experiment 6 on furnace M11 with 75 MVA transformers) a single input of radio-tracer was made beneath the electrode tips. For this experiment a simplified equation was used to describe the residence time distribution obtained. Here it was assumed that the radio-tracer was introduced directly to the C.S.T.R. For an initial amount of radio-tracer Co introduced at time t = o the concentration at the first tapping after input was,

$$C_1 = \frac{Co}{Vinv} \tag{22}$$

For subsequent tappings

$$C_i = C_{i-1}\left(1 - \frac{V_{i-1}}{Vinv}\right) \quad i = 2, \ldots N \tag{23}$$

The computer program based on equations (22) and (23) was used to obtain the optimum values of Co and Vinv and the theoretically computed residence time distribution.

7.4.1. Experiments on furnace M11 with 48 MVA transformers

The values obtained for the parameters for these results are given in Table 13. Experimental and theoretically computed residence time distributions are given in Figures 18 to 23.

7.4.2. Experiments on furnace M10 with 48 MVA transformers

The values obtained for the parameters for these results are given in Table 14. Experimental and theoretically computed residence time distributions are given in Figures 24 to 28.

7.4.3. Experiments on furnace M11 with 75 MVA transformers

The experimental result for experiment 2 during this phase of investigation was not analysed. The values obtained for the parameters for these results are tabulated in Table 15. The experimental and theoretically computed residence time distributions are given in Figures 29 to 33.

Experiment Number	Co	$\bar{t}$ Hours	D	Vinv m^3	Sum of Squares
1	48251,4	29,799	0,00682	12,494	$8,380\times10^{6}$
2	25221,8	28,484	0,00923	9,972	$2,304\times10^{6}$
3	6711,4	11,941	0,00099	15,545	$2,522\times10^{6}$
4	3811,2	18,414	0.00120	8,280	$4,442\times10^{6}$
5	6964,3	13,381	0,00584	21,048	$1,241\times10^{6}$
6	4232,2	13,356	0,01021	19,393	$1,922\times10^{6}$

Table 13. Model parameters for experiments on M11 with 48 MVA transformers

Experiment Number	Co	$\bar{t}$ Hours	D	Vinv m^3	Sum of Squares
1	8293,7	13,808	0,01002	20,478	$1,822\times10^{6}$
2	5763,3	13,080	0,00173	4,476	$6,857\times10^{5}$
3	7530,0	15,109	0,00100	23,967	$1,095\times10^{6}$
4	$1,998\times10^{15}$	72,186	0,00181	$6,724\times10^{14}$	$1,601\times10^{6}$
5	25 [illegible]	19,908	0,00959	16,038	$1,670\times10^{6}$

Table 14. [illegible]arameters for experiments on M10 with 48 MVA transformers

[illegible]	[illegible]	[illegible]	[illegible]	[illegible]
[illegible]	[illegible]	[illegible]	[illegible]	[illegible]
[illegible]	[illegible]	[illegible]	[illegible]	[illegible]
[illegible]	[illegible]	[illegible]	[illegible]	[illegible]
[illegible]	[illegible]	[illegible]	[illegible]	[illegible]
[illegible]	[illegible]	[illegible]	[illegible]	[illegible]

[illegible]

Experiment Number	Co	$\bar{t}$ Hours	D	Vinv m^3	Sum of Squares
1	5116,6	15,906	0,01248	26,909	$3,740\times10^6$
3	4547,4	22,347	0,00994	34,132	$2,059\times10^6$
4	2751,2	18,846	0,01159	15,283	$1,026\times10^6$
5	5923,3	16,275	0,00910	22,037	$3,556\times10^6$
6	268489	-	-	15,408	$3,010\times10^7$

Table 15. Model parameters for experiments on M11 with 75 MVA transformers

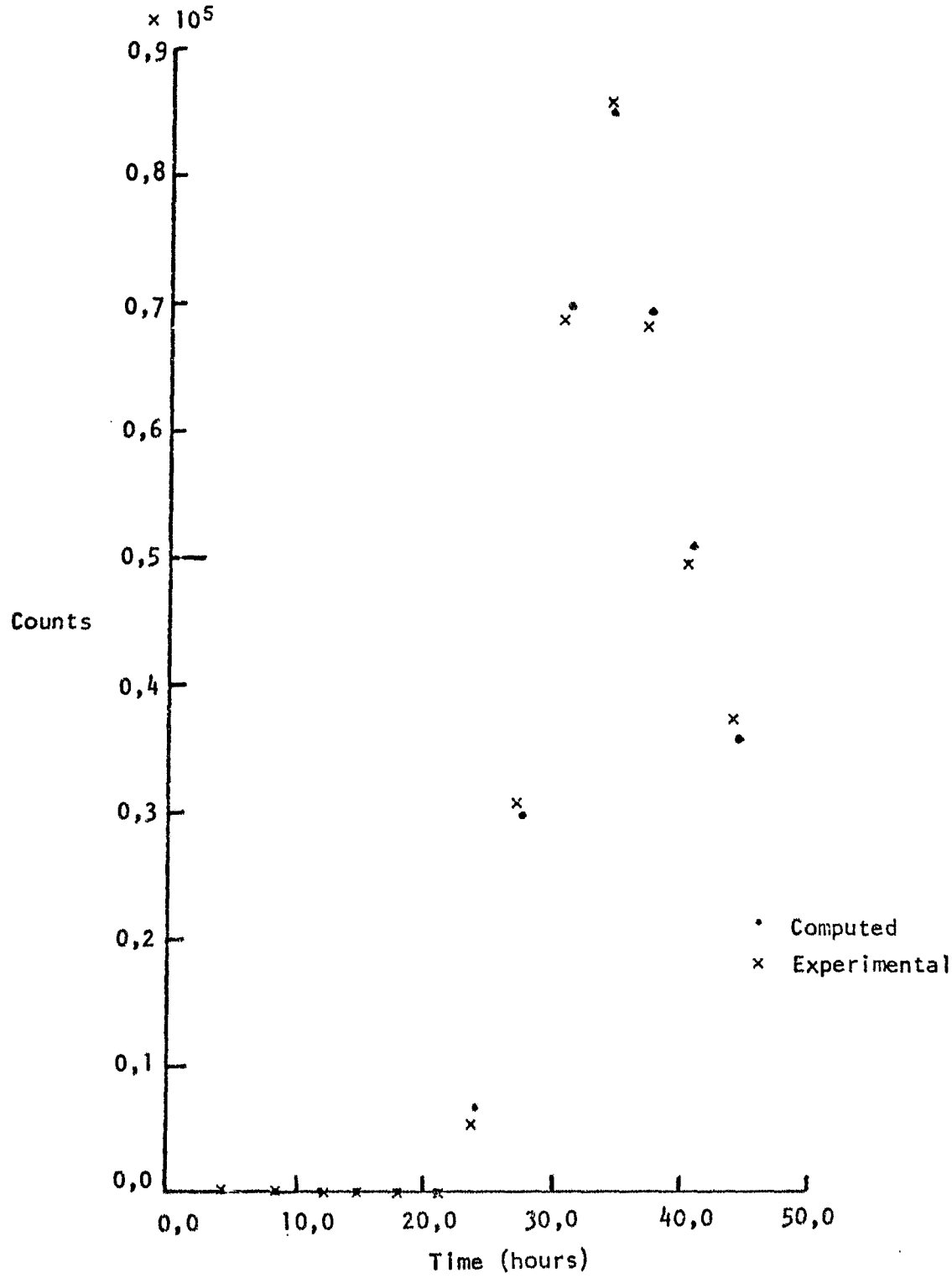

Figure 18. Experimental and computed residence time distribution for experiment 1 on furnace M11 with 48 MVA transformers

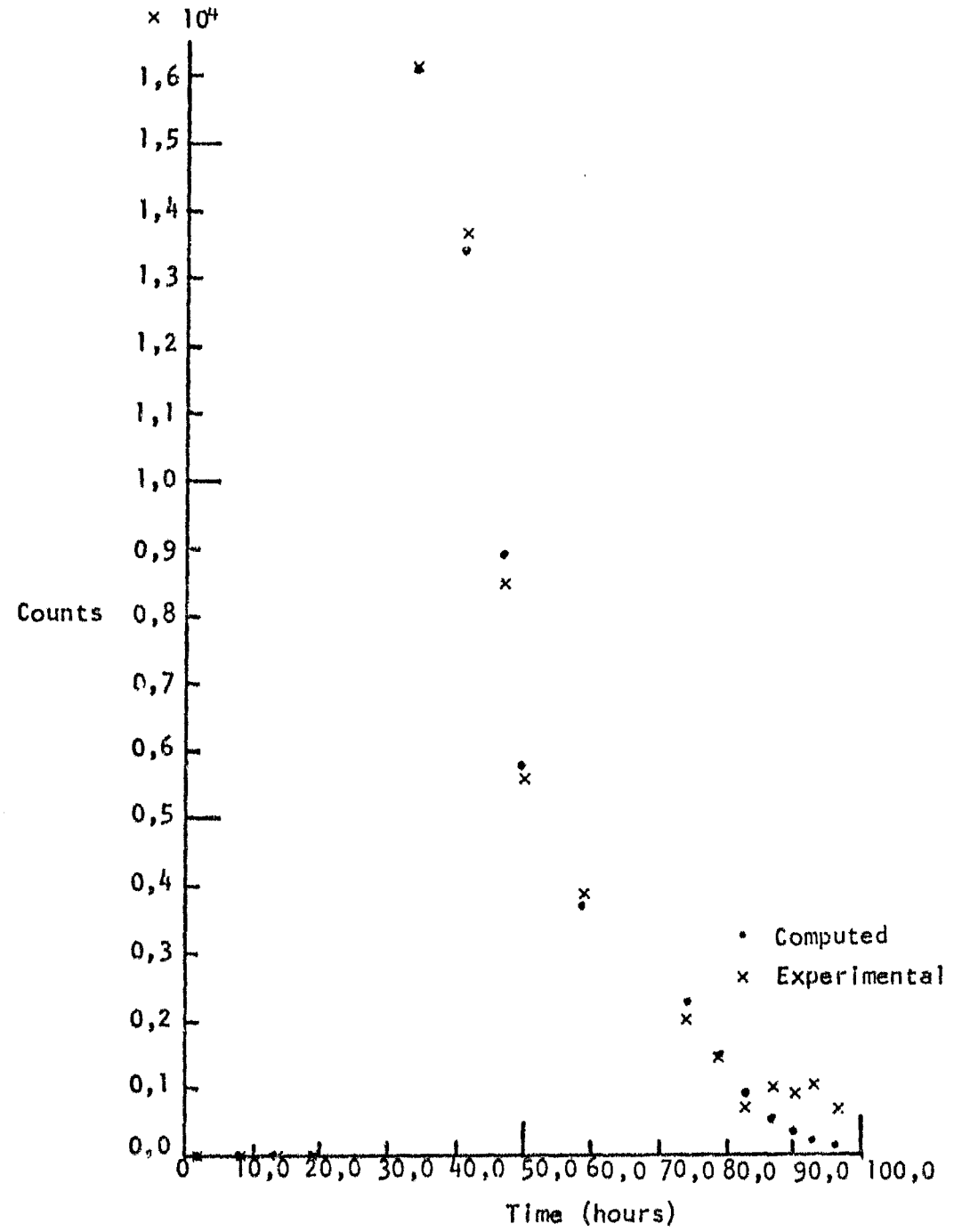

Figure 19. Experimental and computed residence time distribution for experiment 2 on furnace M11 with 48 MVA transformers

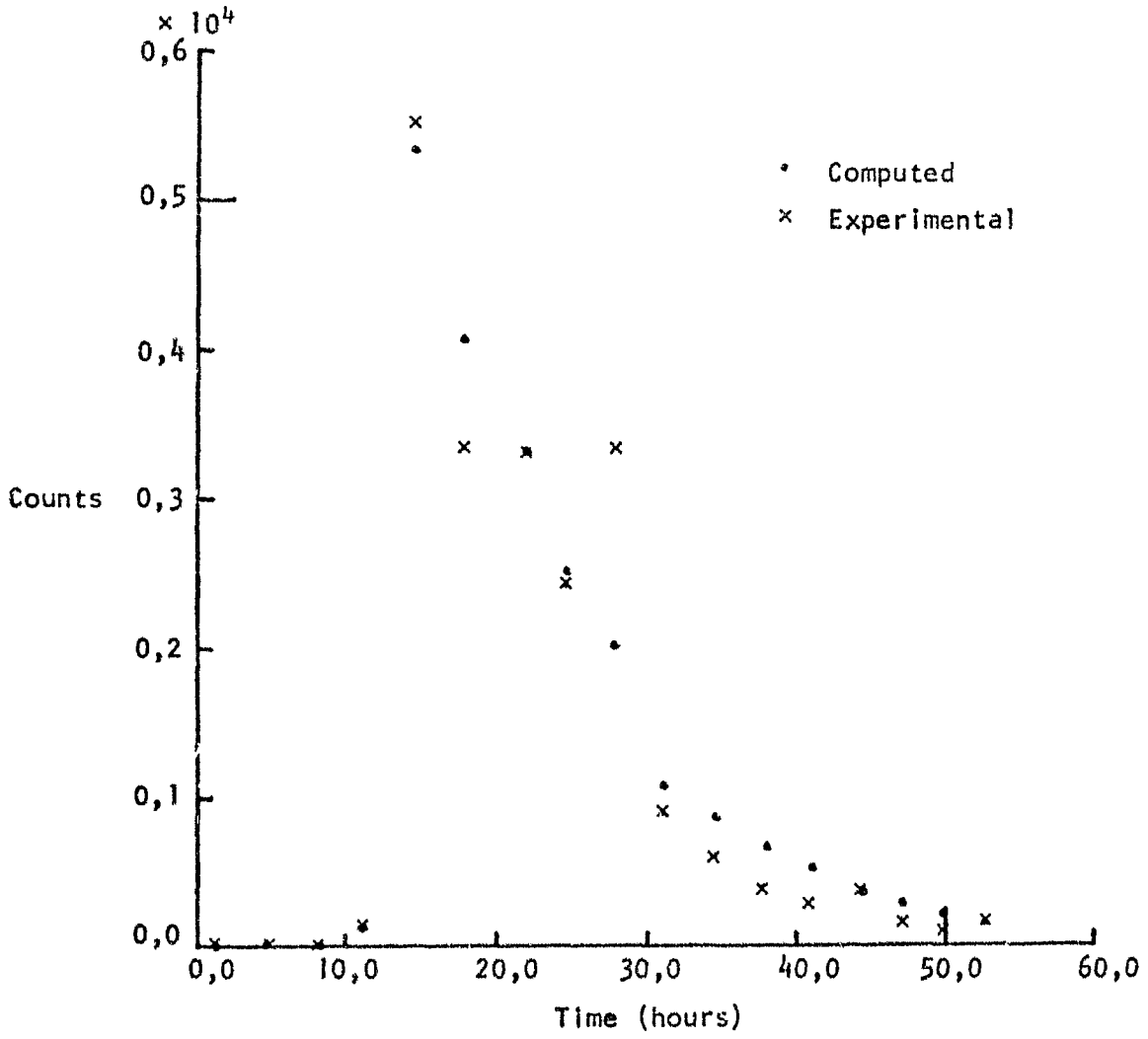

Figure 20. Experimental and computed residence time distribution for experiment 3 on furnace M11 with 48 MVA transformer

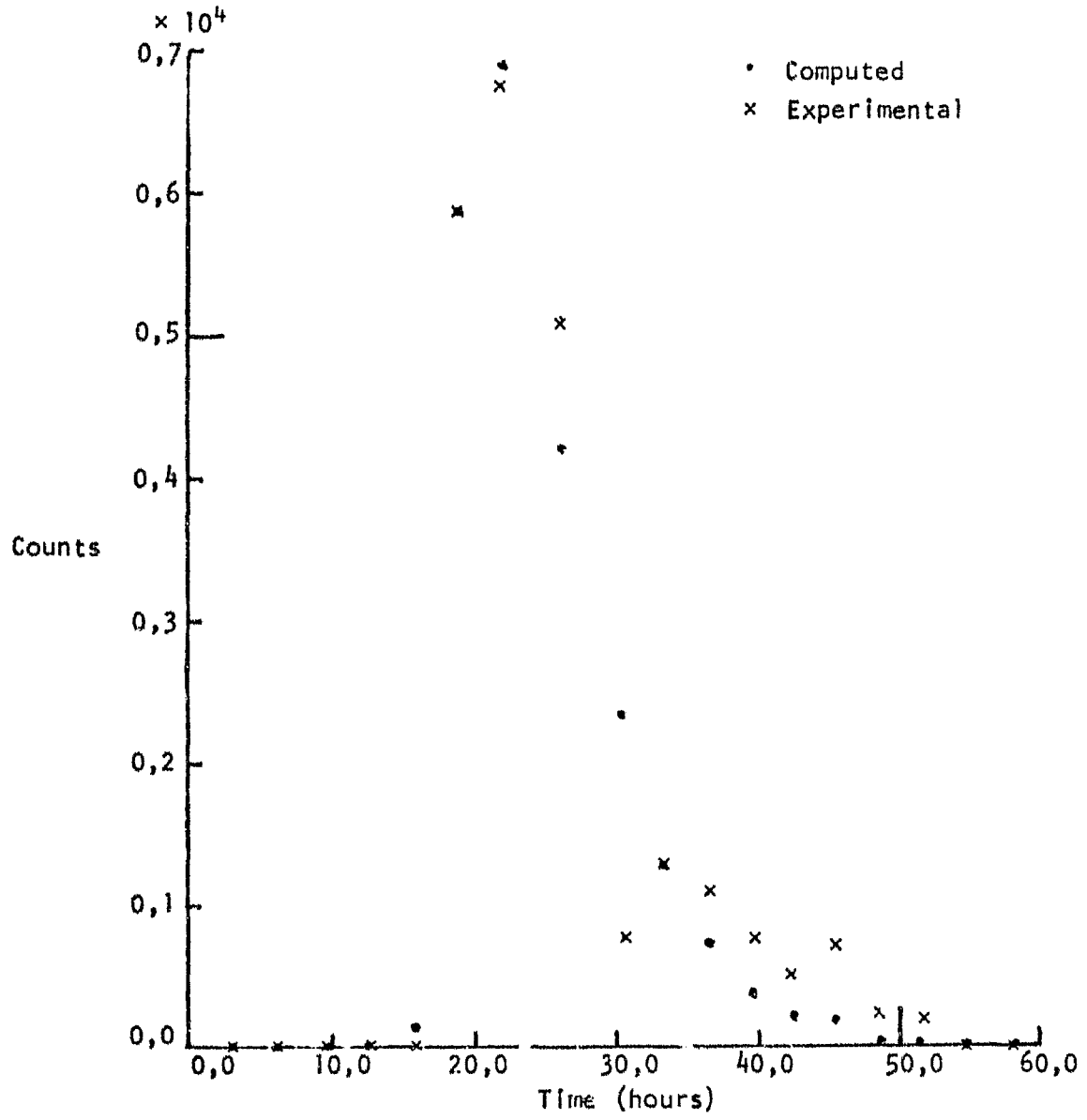

Figure 21. Experimental and computed residence time distribution for experiment 4 on furnace M11 with 48 MVA transformers

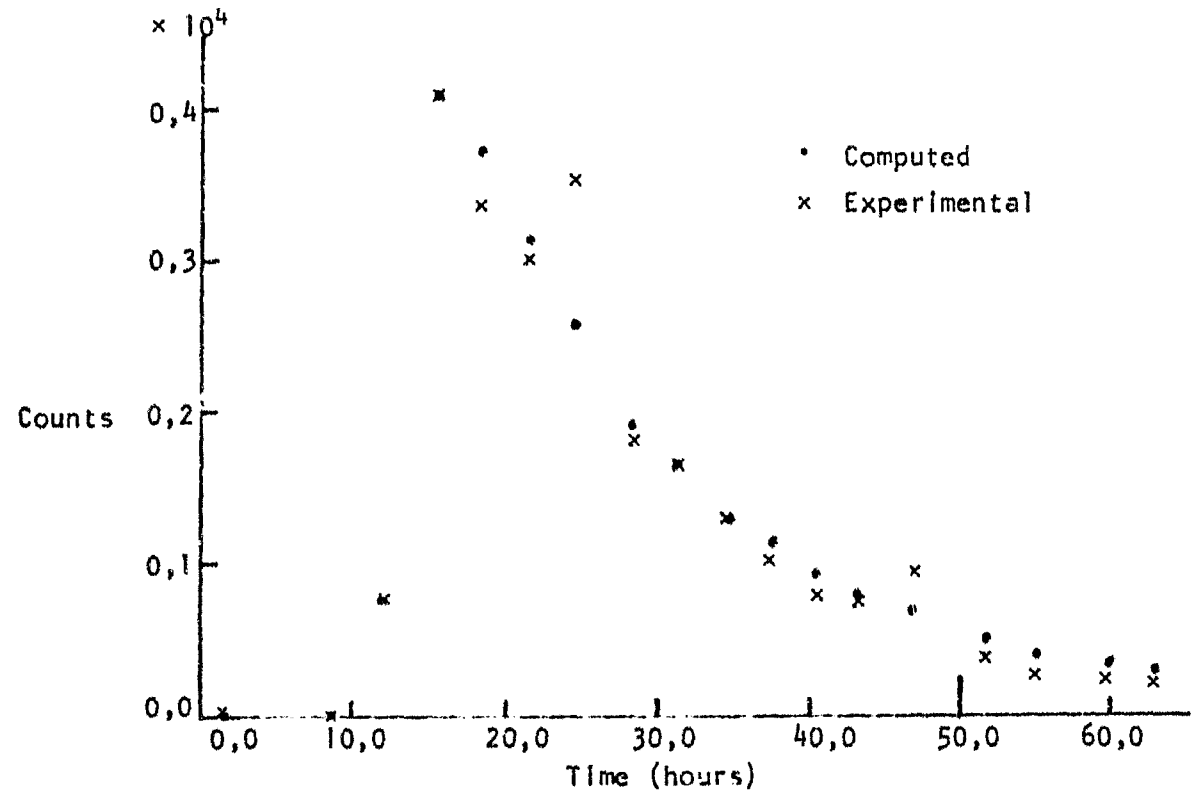

Figure 22. Experimental and computed residence time distribution for experiment 5 on furnace M11 with 48 MVA transformers

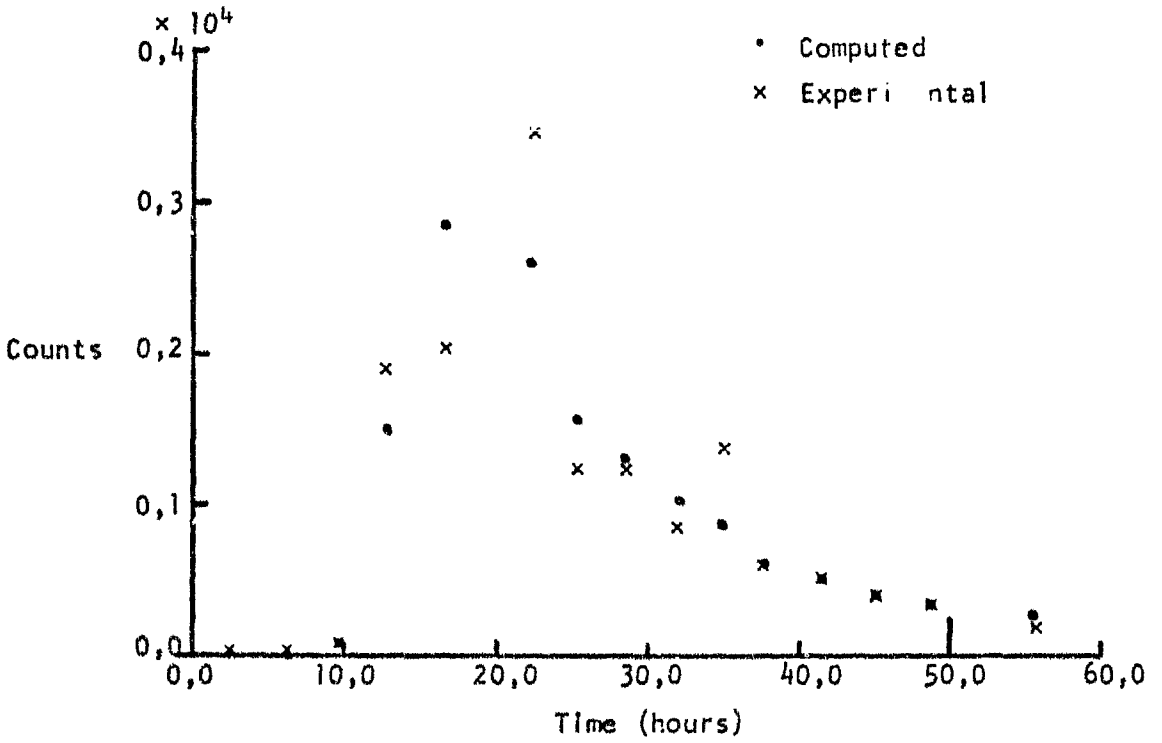

Figure 23. Experimental and computed residence time distributions for experiment 6 on furnace M11 with 48 MVA transformers

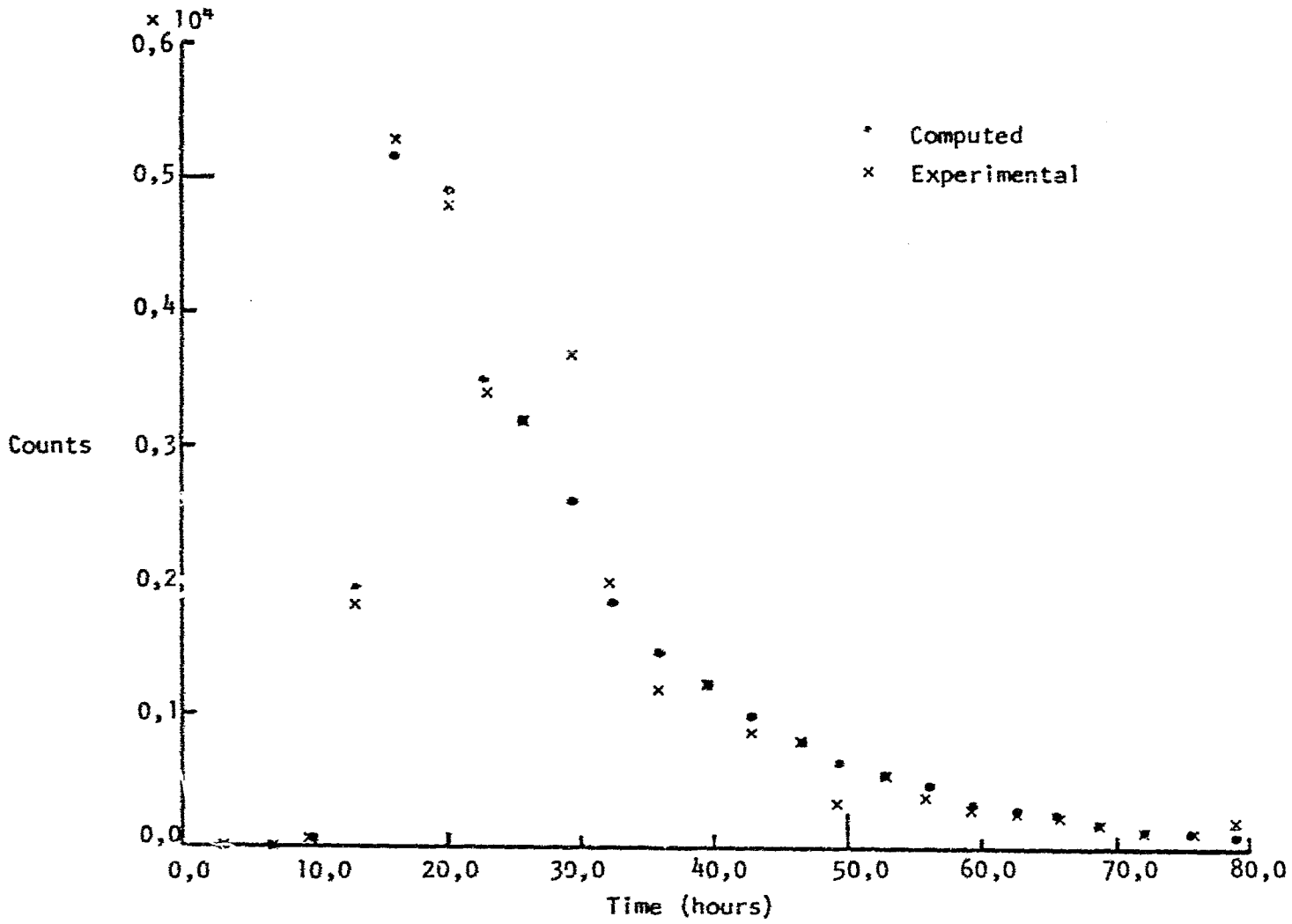

Figure 24. Experimental and computed residence time distributions for experiment 1 on furnace M10 with 48 MVA transformers

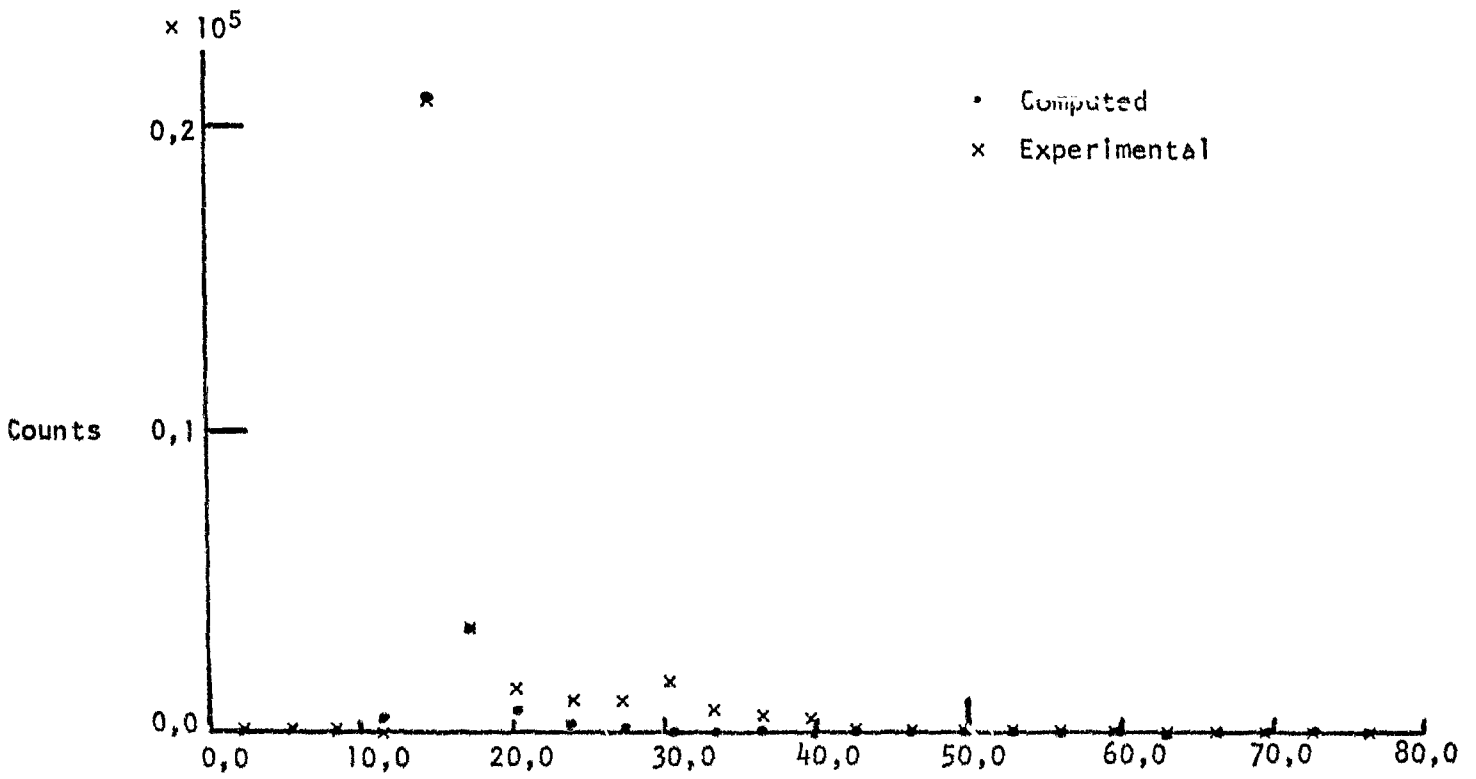

Figure 25. Experimental and computed residence time distribution for experiment 2 on furnace M10 with 48 MVA transformers

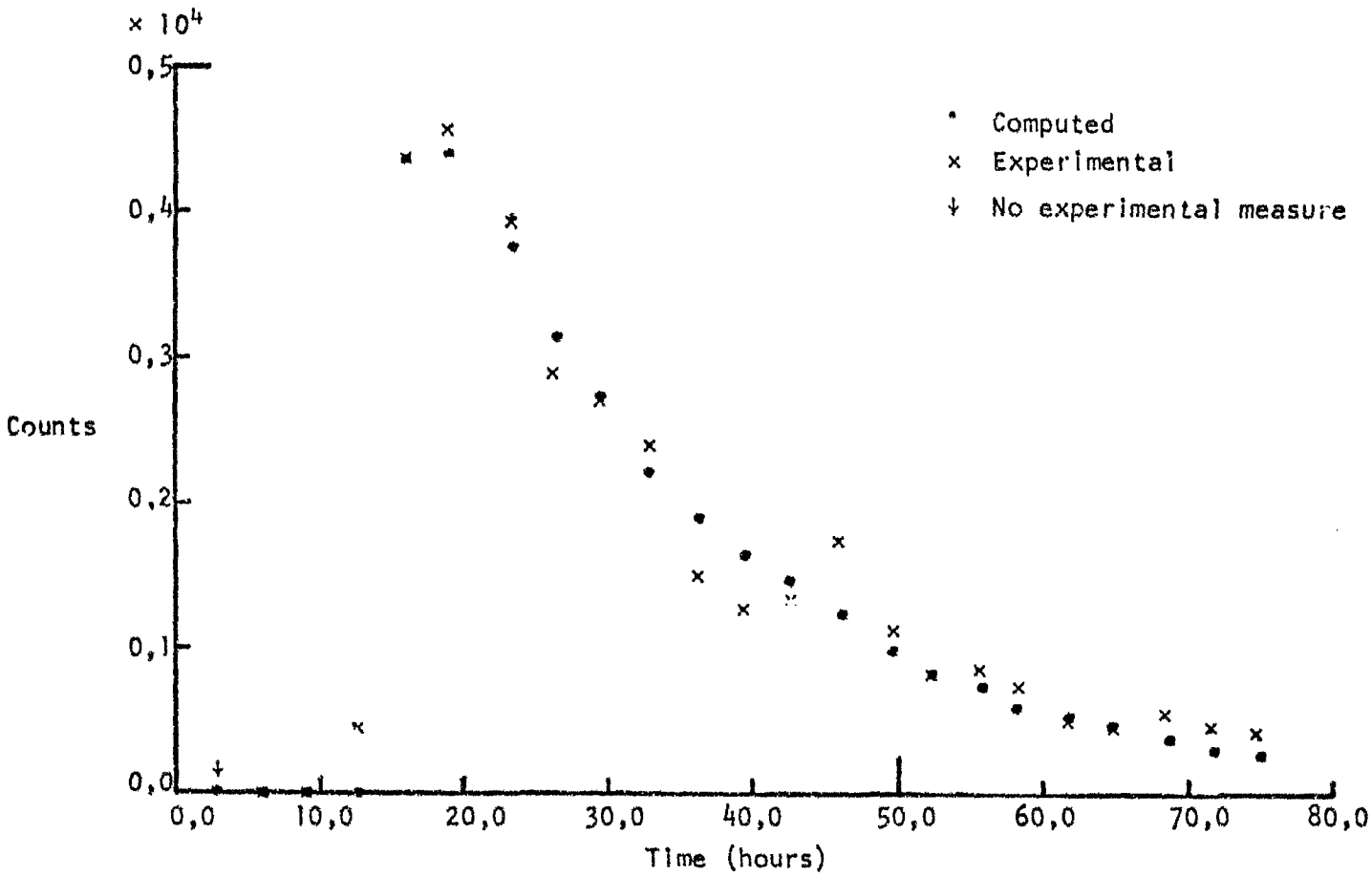

Figure 26. Experimental and computed residence time distribution for experiment 3 on furnace M10 with 48 MVA transformers

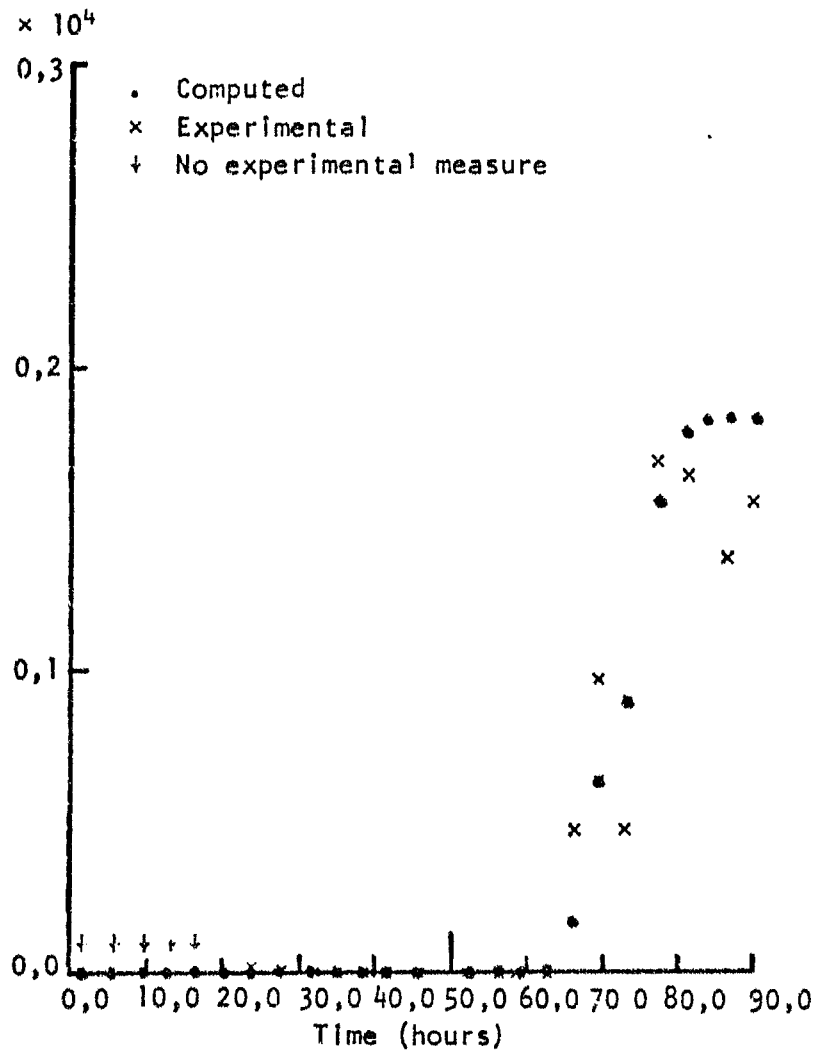

Figure 27. Experimental and computed residence time distributions for experiment 4 on furnace M10 with 48 MVA transformers

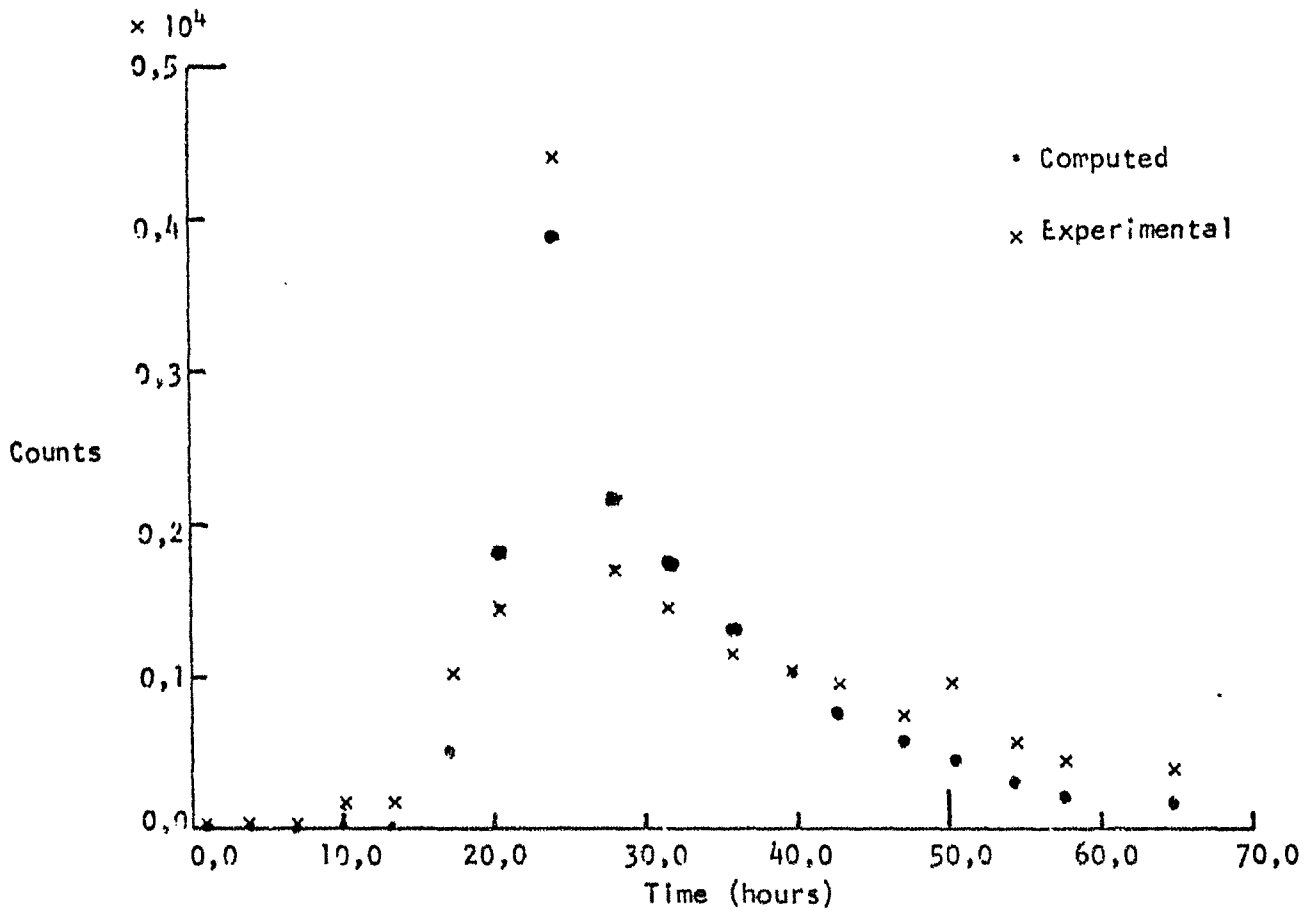

Figure 28. Experimental and computed residence time distribution for experiment 5 on furnace M10 with 48 MVA transformers

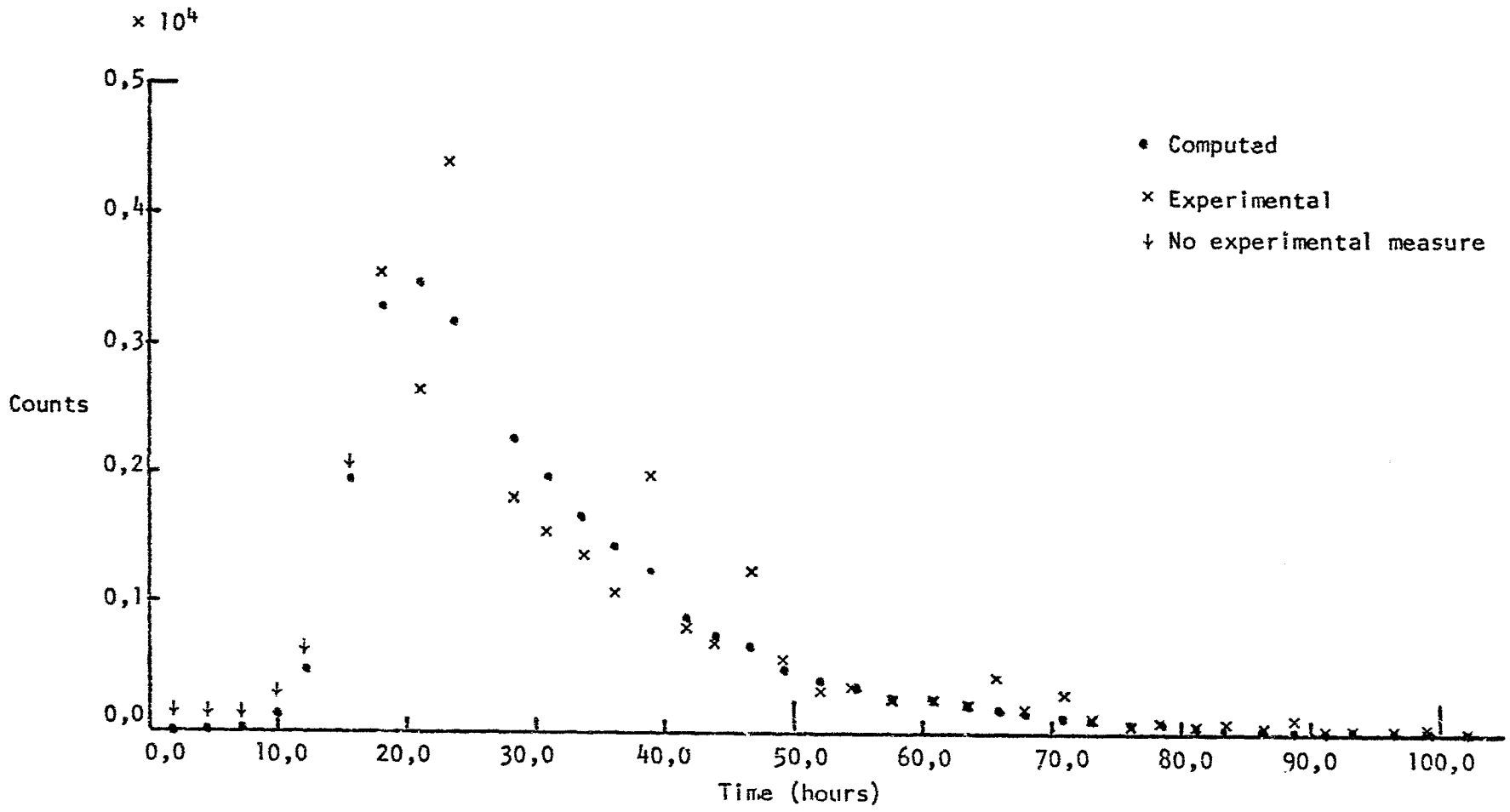

Figure 29. Experimental and computed residence time distribution for experiment 1 on furnace M11 with 75 MVA transformers

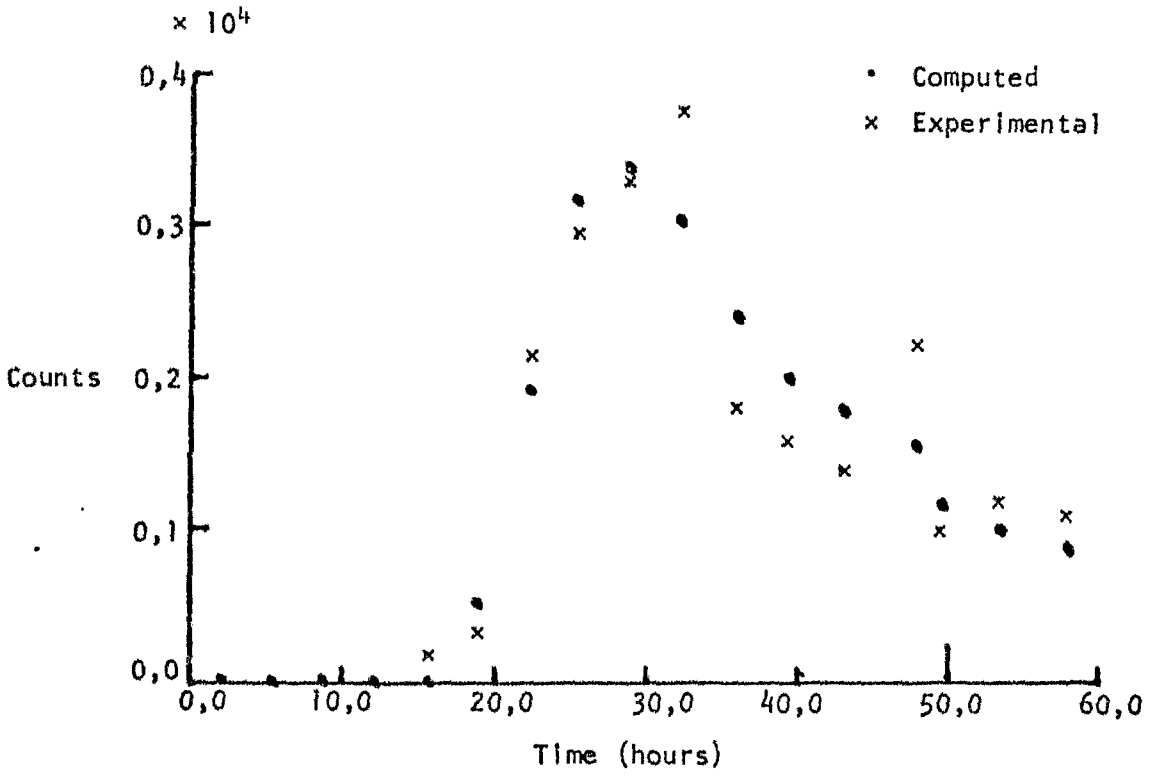

Figure 30. Experimental and computed residence time distribution for experiment 3 on furnace M11 with 75 MVA transformers

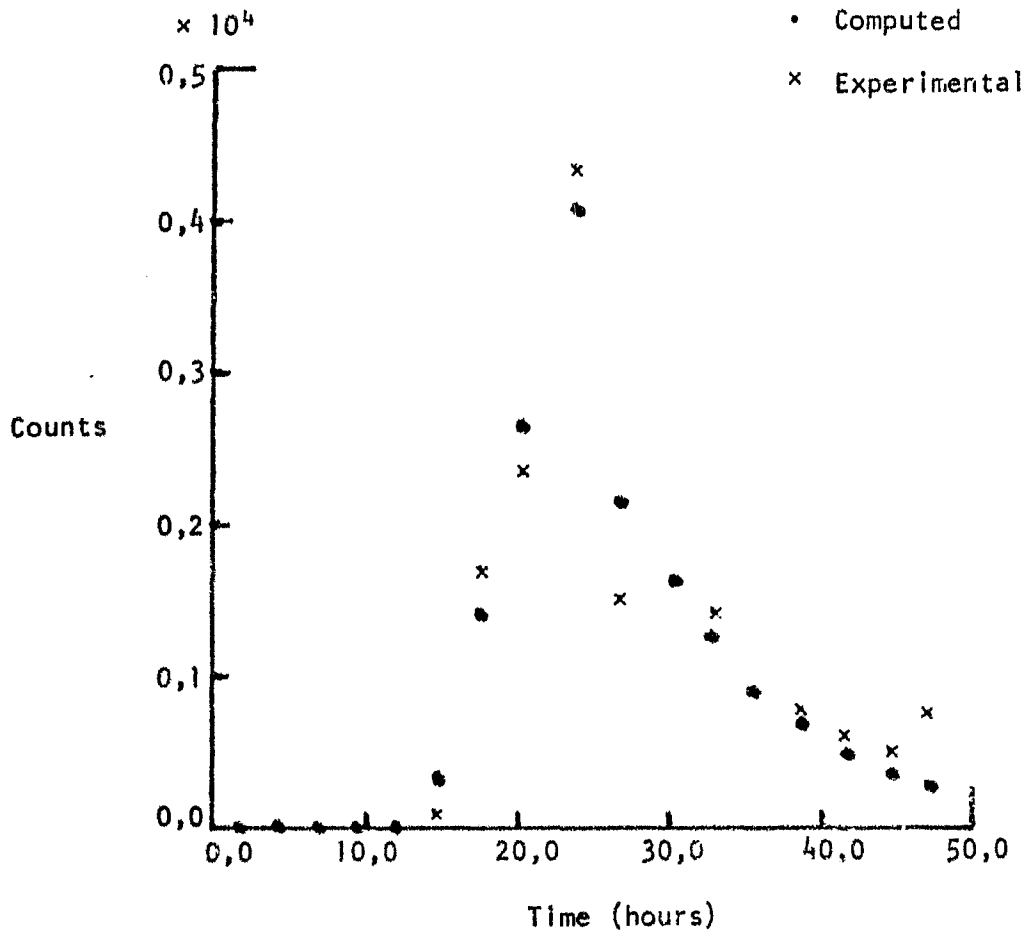

Figure 31. Experimental and computed residence time distribution for experiment 4 on furnace M11 with 75 MVA transformers

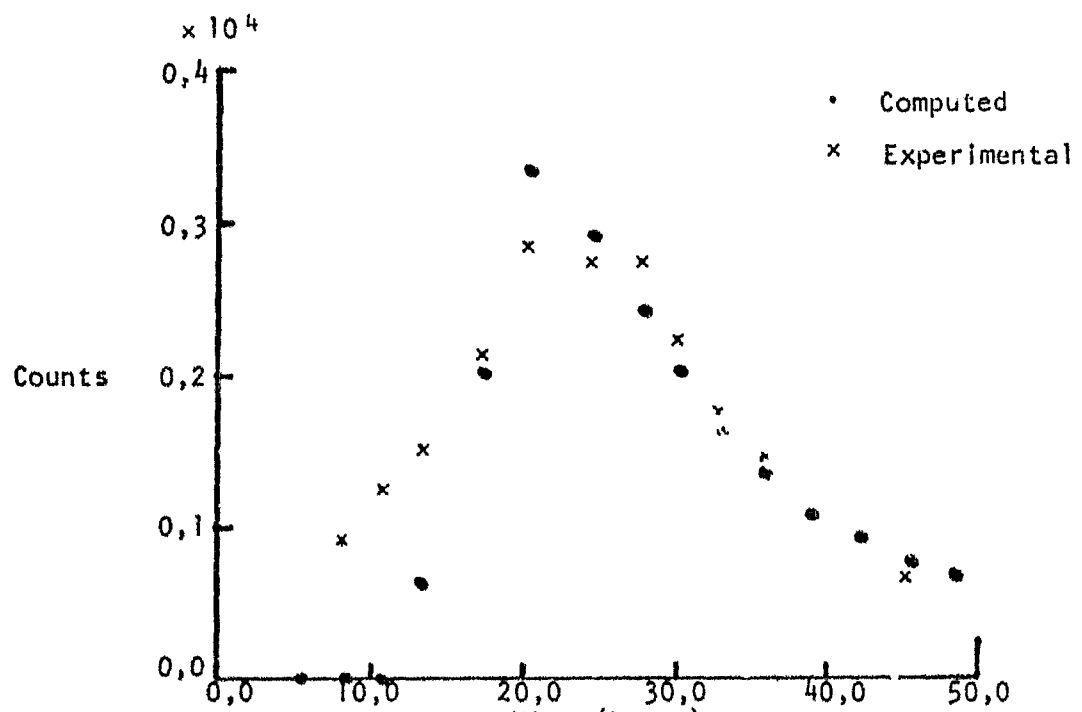

Figure 32. Experimental and computed residence time distribution for experiment 5 on furnace M11 with 75 MVA transformers

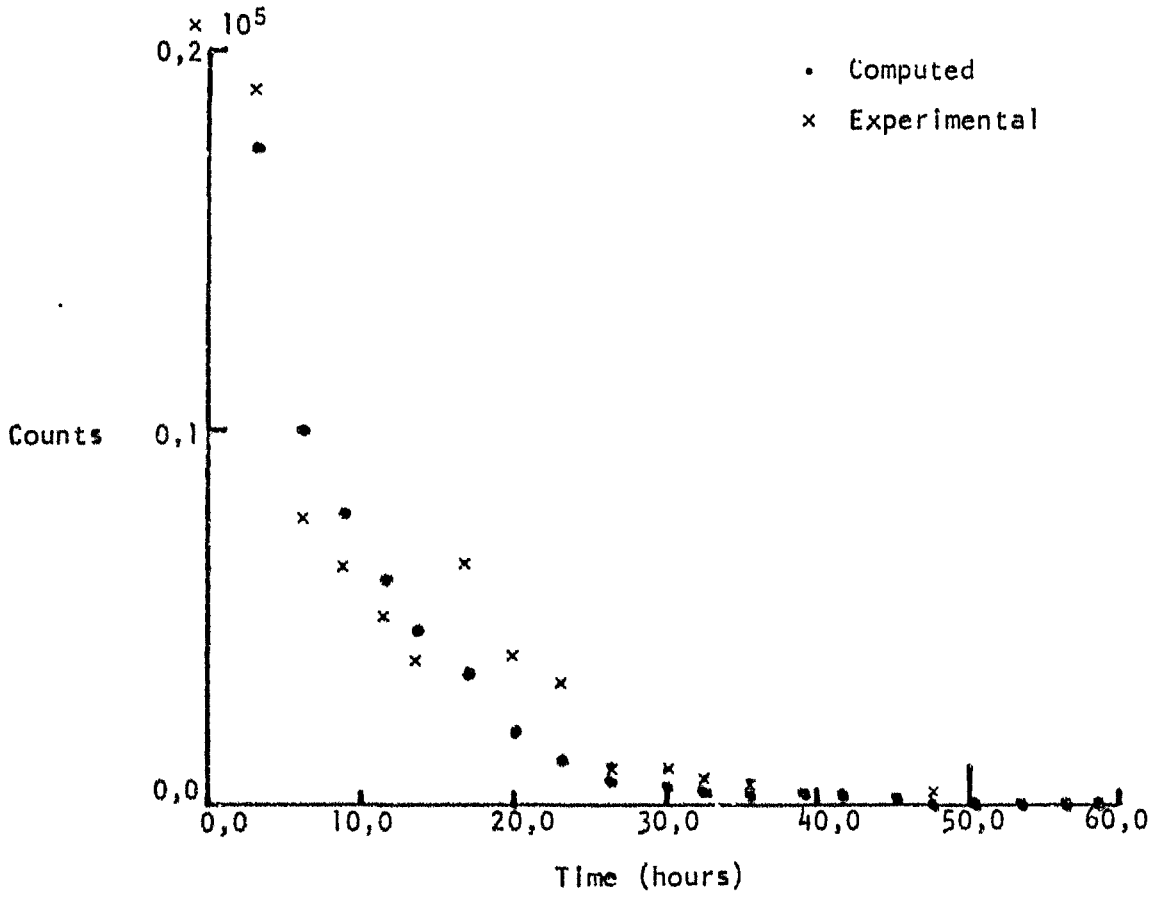

Figure 33. Experimental and computed residence time distribution for experiment 6 on furnace M11 with 75 MVA transformers

7.5. Correlations between model parameters and average furnace operating parameters

The model parameters $\bar{t}$ and Vinv were considered in this analysis.

Correlations were assessed graphically. Analysis was restricted to linear correlations except in cases where obvious non-linear correlations existed.

Correlations between both $\bar{t}$ and Vinv and the following average furnace operating parameters were considered:-

(i) The furnace load.

(ii) The furnace feedrate.

(iii) The alloy discharge rate.

(iv) The time lapse between alloy tappings.

(v) The primary line voltage.

(vi) The sum of the squared electrode currents.

(vii) The mass ratio : MnO/Mn.

Correlation between $\bar{t}$ and Vinv was also considered. For each correlation the same sets of data used in Section 7.2 were considered.

No correlations were found to exist for the above comparisons on a graphical basis. Hence no correlations were evaluated by regression analysis.

8. DISCUSSION

8.1. Introduction

Time and experimental costs limited the number of experiments in this investigation. To reduce experimental costs and the duration of the experimental campaign two furnaces were investigated simultaneously. Thus it was not possible to perform a full-scale investigation of either of the two furnaces. The investigation served primarily to establish techniques for the measurement and analysis of residence time distributions.

Many experiments were performed with different numbers and sites of radio-tracer inputs. Where necessary several of the same experiments were performed to perfect the particular experimental technique. Sites of radio-tracer inputs were selected so as to ensure that the inputs entered the active zone surrounding the electrodes.

The three points of radio-tracer input were beneath the electrode tips, at the stockline level and in the furnace bunkers. Both single and multi-input experiments were performed and a different technique was used to introduce the radio-tracer at each point. Single input experiments permitted investigation of selected furnace zones while multi-input experiments permitted investigation of overall burden descent through the furnace.

The lack of sufficient experimental data prevented any statistically significant quantitative analysis of

the mechanism and rate of burden descent through the furnaces. However sufficient data was accumulated to permit qualitative analysis of burden descent through the furnace. On the basis of the information obtained it seems possible to design future experiments to obtain conclusive information about burden descent through these furnaces.

8.2. The experimental procedure

The experimental procedures developed to measure residence time distributions for submerged-arc furnaces were based on the stimulus-response technique using radio-tracer inputs as stimuli. Provided suitable radioactive sources were available, both slag and alloy phase residence time distributions could be measured.

The radioisotope, Fe^{59}, proved to be a suitable radio-active source for alloy phase residence time distribution measurements. In initial experiments hematite ore was irradiated to produce Fe^{59} and this was used as the radio-tracer material. This represented a compromise between the use of a radio-tracer which closely resembled the process feed material and a radio-tracer which could be easily produced and safely handled. The South African Atomic Energy Board subsequently developed a technique whereby Fe^{59} could be safely produced by irradiation of Hotazel manganese ore. This permitted the use of actual process feed material as radio-tracer in later experiments. The use of irradiated Hotazel manganese ore as radio-tracer represented an improvement in the experimental technique.

The radioisotope, Fe^{59}, was an unsuitable radioactive source for slag phase residence time distribution measurements for two reasons. Due to the low concentration of FeO in these slags, highly radioactive radio-tracer inputs were required for production of sufficient Fe^{59} in the slag as FeO to permit reliable response measurement. Alloy entrapment within the slag resulted in random introduction of relatively large quantities of Fe^{59} into

the slag and the resultant "noise" made the results obtained unreliable. Although the former problem could have been eliminated by the use of highly radioactive radio-tracers, their use would have compounded the influence of alloy entrapment in the slag. The selection and use of a suitable source of radioactivity for slag phase residence time distribution measurements was beyond the scope of the investigation.

The experimental procedure in this investigation could have been improved by use of direct on-line response measurement. Unfortunately at the time of investigation portable detectors were insufficiently sensitive for direct on-line response measurement under the conditions which existed on these furnaces. Direct on-line response measurement is more accurate, simplifies response measurement, and eliminates truncation problems.

Had a portable detector been available during the investigation, truncation of the residence time distributions would have been avoided. A portable detector would have been used to determine from samples taken, when to start, and when to stop, sampling of the alloy discharge from the furnace for response measurement.

8,3. Correlations between average furnace operating parameters

The large number of variables influencing furnace operation between and during experiments made it extremely difficult to obtain correlations between average furnace operating parameters. This task was made more difficult by the fact that many of these variables, such as burden resistivity, and the reactivity of burden components, could not be monitored. Consequently very few simple correlations were obtained. All correlations obtained had furnace load, P, as dependent variable.

For experiments on furnace M11 with 75 MVA transformers two correlations were obtained. The following type of correlation was obtained with electrode current, I:-

$$P = k \sum_{i=1}^{3} I_i^2 - \ell$$

where k and ℓ are constants.

For the furnace,

$$P = R_1 I_1^2 + R_2 I_2^2 + R_3 I_3^2$$

where R = resistance.

Provided $k = R_1 = R_2 = R_3$, $\quad P = k \sum_{i=1}^{3} I_i^2$

This equation has the same form as the correlation obtained. The following form of correlation was obtained with the mass per cent MnO in the slag, %MnO:-

$$P = k\ \%MnO + \ell$$

where k and ℓ are constants.

This correlation could not be explained by simple considerations and had to be attributed to the influence

of reducing conditions in the furnace.

For experiments on furnace M11 with 48 MVA transformers, a correlation with time lapse between alloy tappings, t, of the following form was obtained:-

$$P = -kt + \ell$$

where k and ℓ are constants.

This correlation expressed the fact that, as furnace load increases, the time lapse between alloy tappings may be decreased due to the faster smelting rate.

For all experiments on furnace M11 the following form of correlation was obtained with furnace feedrate, t/h:-

$$P = k_1 (t/h)^2 + k_2 (t/h) + \ell$$

where k_1, k_2 and ℓ are constants.

This correlation was an expression of the fact that there is a maximum rate at which burden can be smelted for this furnace.

As the primary object of establishing correlations between furnace operating parameters was to assist in comparing this data to residence time distribution data, more complex correlations were not considered.

8.4. Single parameter description of residence time distributions

Due to truncation problems, single parameters were calculated for only three single-input experiments. These were experiment 4 on furnace M11 with 48 MVA transformers, experiment 2 on furnace M10 with 48 MVA transformers and experiment 6 on furnace M11 with 75 MVA transformers. Sites of radio-tracer input for these experiments were a charging shaft, a feed bunker, and beneath an electrode tip respectively. The single parameters calculated for the residence time distributions included the mean residence time, $\bar{t}a$, and the variance in units of mean residence time, σ^2. Each of these will be discussed in turn.

8.4.1. The mean residence time, $\bar{t}a$

Provided burden descent through the active zone of the furnace is uniform a comparison between $\bar{t}a$, measured by means of a single radio-tracer input, and the nominal mean residence time, $\bar{t}n$, will show that there is a stagnant region in the furnace in that $\bar{t}n$ will be greater than $\bar{t}a$. Where burden descent through the active zone is non-uniform this comparison is only valid if $\bar{t}a$ is measured by means of many simultaneous radio-tracer inputs to all portions of the feed to the active zone.

In this analysis it was assumed that burden descent through the active zone was uniform and that comparison of $\bar{t}a$ and $\bar{t}n$ would show whether stagnancy did exist within the furnace volume. (The basis for this assumption is discussed in Section 8.5.3).

For each result analysed, $\bar{t}n$ was calculated from,

$$\bar{t}n = \frac{M}{m}$$

where M = mass capacity of the furnace
m = mass feed rate to the furnace.

For each experiment m was known. The mass capacity of the furnaces up to the stockline was calculated to be 1 015 tonnes. This calculation is given in Appendix C. Due to the large number of assumptions made in calculation of M, it was not possible to estimate the error in the value of 1 015 tonnes, and this could only be considered to give an order of magnitude value. Consequently the values calculated for $\bar{t}n$ could only be considered to be order of magnitude values. The values of $\bar{t}a$ and $\bar{t}n$ are given in Table 16.

Comparison of these values showed that in each case $\bar{t}a$ was smaller than $\bar{t}n$.

Experiment Number	Mean residence time	
	Measured, $\bar{t}a$	Theoretical, $\bar{t}n$
4 (M11 - 48 MVA)	25,46 hours	37,9 hours
2 (M10 - 48 MVA)	20,15 hours	37,3 hours
6 (M11 - 75 MVA)	13,76 hours	29,7 hours

Table 16. Measured and theoretically calculated mean residence times

For experiment 6 (furnace M11 - 75 MVA) this was partly because $\bar{t}n$ had been calculated for up to the stockline while $\bar{t}a$ had been measured from beneath an electrode tip.

For the remaining two experiments the larger values for $\bar{t}n$ compared to $\bar{t}a$ confirm the existence of a stagnant or inactive zone within the furnace volume.

8.4.2. The variance, σ^2

This parameter measured the extent of the deviation from either of perfectly mixed flow or plug flow. For perfectly mixed flow $\sigma^2 = 1$ whilst for plug flow $\sigma^2 = 0$.

The relatively small value of 0,0914 obtained for σ^2 in experiment 4 (furnace M11 - 48 MVA) showed that flow of the radio-tracer input through the furnace in this experiment was substantially plug flow in character. For experiment 1 (furnace M10 - 48 MVA) and experiment 6 (furnace M11 - 75 MVA) the increase in the values of σ^2 of 0,2930 and 0,5354 respectively showed that the flow of the radio-tracer inputs through the furnace for these experiments was tending more and more towards perfectly mixed flow. In experiment 6 the radio-tracer was introduced directly into the C.S.T.R. region and hence σ^2 should be very close to unity.

The smaller value obtained for σ^2 was probably due to truncation of the tail of the residence time distribution rather than due to deviation from perfectly mixed flow.

Consideration of the parameter σ^2 showed that the residence time distributions measured could not be described by either of the idealized flow patterns.

8.5. Description of residence time distributions by means of a theoretical model

8.5.1. Introduction

Examination of Figures 18 to 33 showed that the experimentally measured residence time distributions closely conformed to the theoretically computed residence time distributions. This indicated that the actual flow structure in the furnaces had many of the specific features included in the theoretical model. This was particularly well illustrated by experiment 6 on furnace M11 with 75 MVA transformers. In this experiment the radio-tracer was directly introduced into the furnace zone represented in the model by a C.S.T.R. The theoretically computed residence time distribution for this experiment closely conformed to the experimentally measured residence time distribution. This indicated that the zone beneath the electrode tips was correctly described by a C.S.T.R. Consequently it was assumed that the zone above the electrode tips was correctly described by the dispersed plug flow region.

Although an alternative composite model was developed to account for flow through the furnaces it was not possible to use this model to predict the residence time distribution. This was due to the limited time available for the investigation. However consideration of the physical structure of the furnace indicated that the alternative model probably did not as closely resemble the actual flow mechanism in the furnace as did the model used in this investigation. During the experimental campaign four groups of three samples each were taken at one of the alloy tappings. The variation in the relative

activity between these four groups of samples was very slight and of a random nature. This indicated that the alloy pool was well-mixed and accurately described by the C.S.T.R. model used in the analysis of the results.

8.5.2. Sensitivity of model parameters to regression analysis

The dispersion number D was probably insensitive to regression analysis due to the low precision and limited extent of the experimental data. This difficulty showed up as a computer precision problem resulting in generation of numbers beyond the dimensional limits of the computer. In the analysis two initial values of D, namely 0,001 and 0,01 were considered for each result.

When initial values of D = 0,01 were used the computer program did regress on D and in most cases the final values obtained for D were less than 0,01. In general the solutions obtained for each value of D were independent of the initial values of the other model parameters. However in isolated cases very poor solutions were obtained with an initial value of D = 0,001. Due to the problem, solutions obtained with the initial value D = 0,01 were generally better than those obtained with the initial value D = 0,001.

When reasonable solutions were obtained for both initial values of D the final values obtained for the parameters $\bar{t}$ and Vinv differed by about 10 per cent. Since the computed residence time distributions closely reproduced the experimentally measured results, it was concluded that the problem in regression on D did not

adversely affect the analysis. However it was not possible to attach any significance to the value of D other than to conclude that the degree of dispersion in the dispersed plug flow region was small.

During regression analysis of residence time distributions truncated immediately beyond the peak, unacceptably high final values of Vinv were obtained. This did not reflect a failing in the model. The information concerning the perfectly mixed region of the furnace is contained in the exponential decay portion of the curve. When that portion of the curve is missing no information concerning Vinv is obtained. This is shown by unacceptably high values of Vinv. Provided a sufficient portion of the decay portion of the residence time distribution was measured this problem did not occur and values obtained for Vinv were considered to be meaningful.

8.5.3. Analysis of model parameters

Only the model parameters $\bar{t}$ and Vinv were considered in this analysis. As the model parameter Co was a linear scale factor representing the initial concentration it was not considered important and so was not analysed.

It was not possible to perform statistical, quantitative, analysis due to the limited number of experiments performed and the large number of variables subject to change during experimentation. Graphical correlations between $\bar{t}$ and Vinv were considered but no simple correlations were obtained.

Qualitative analysis of the values of $\bar{t}$ and Vinv was performed. This analysis involved the use of theoretical considerations to explain the values obtained for the parameters under the particular conditions of operation at each experiment.

8.5.4. Effect of position of radio-tracer input on mean residence times

All radio-tracer inputs were made to the active zone of the furnace. At the stockline level this active zone is in the form of a "clover leaf" (refer Figure 1) surrounding the electrodes and the burden descends rapidly in this region. The balance of the furnace volume is effectively stagnant and little smelting is carried out in this volume. Since only a limited number of experiments could be performed, inputs of radio-tracer were restricted to the active zone to obtain the maximum amount of information about the region in which smelting took place.

In the model of flow through the furnace two flow regions are considered. In the upper region of the furnace, the burden is predominantly solid and dispersed plug flow occurs. In the region beneath the electrode tips the burden is molten and mixed flow occurs in the slag and alloy layers. It is important to consider the influence of the position of radio-tracer input on the values of the mean residence times obtained from the model for these two regions of flow.

The mean residence time within the C.S.T.R. region of the furnace, $\bar{t}$inv, may be calculated from the furnace inventory volume, Vinv, as follows:-

$$\bar{t}_{inv} = \frac{Minv}{m}$$

where Minv = inventory mass of alloy
m = alloy mass discharge rate.

For each experiment m was calculated from the average alloy mass tapped per alloy tapping and the average time lapse between each alloy tapping (refer Table 9). Minv was calculated from the alloy inventory volume, Vinv, and the extrapolated alloy density at the tapping temperature taken to be 6,65 tonnes/m^3.[73]

Each of the flow regions in the furnace will be considered in turn.

8.5.4.1. The dispersed plug flow region of the furnace

In the dispersed plug flow region, the mean residence times for inputs of radio-tracer to the inactive zone will be significantly larger than the mean residence times for inputs of radio-tracer to the active furnace zone. In this investigation this marked variation in the values of mean residence times was not observed since all inputs of radio-tracer were made to the active zone of the furnace.

Provided the input of radio-tracer is made to the active zone, the radial position of this input relative to the electrode, and the position of the electrode relative to the alloy tapping hole should not significantly influence the mean residence time within the dispersed plug flow region of the furnace. This assumes relatively homogeneous flow within the dispersed plug flow region of the active zone.

Inputs of radio-tracer to the dispersed plug flow region of the active zone were made at two levels. These two levels were the stockline level (i.e., charging shafts and "burden valley") and the level of the furnace bunker. For inputs at the stockline level mean residence times should be smaller than for inputs at the level of the furnace bunkers.

Analysis of the multi-input experiments confirmed that burden descent is relatively uniform around a particular electrode. The experiments were number 3, 4, and 5 on furnace M11 with 75 MVA transformers. In each of these multi-input experiments, four radio-tracer inputs were equally disposed around one particular electrode. Analysis of each of these experiments showed that the descent of the burden around each electrode was relatively uniform and that the mean residence times for the four inputs in each experiment were best described by a single value.

Tables 17 and 18 give the values for the mean residence time and relative position of radio-tracer input for inputs at stockline level and to the furnace bunkers respectively. Three input positions are considered relative to the alloy tapping hole. For both furnaces electrode I is the closest electrode to the alloy tapping hole. The central charging shaft is the next closest input position to the alloy tapping hole for both furnaces. For both furnaces electrodes II and III are considered to be equidistant from the alloy tapping hole and are positions of input most remote from the tapping hole.

Tables 17 and 18 respectively provide no statistical

POSITION OF INPUT	EXPERIMENT NUMBER	FURNACE	RAW MATERIAL FEEDRATE t/h	FURNACE LOAD MW	$\bar{t}$ HOURS	$\bar{t}_{inv}$ HOURS
CLOSEST TO ALLOY TAPPING HOLE						
Electrode I†	6	M11 (75 MVA)	34,12	31,4	-	9,9
Electrode I	2	M11 (48 MVA)	14,69	18	28,5	16,7
Electrode I	4	M11 (48 MVA)	26,80	26	18,4	6,8
Electrode I	5	M11 (48 MVA)	25,95	26	13,4	20,9
Electrode I*	4	M11 (75 MVA)	33,48	30,5	18,8	10,3
FARTHEST FROM ALLOY TAPPING HOLE						
Electrode II	3	M11 (48 MVA)	27,33	26	11,9	13,2
Electrode II*	3	M11 (75 MVA)	24,03	24,9	22,3	24,0
Electrode III*	5	M11 (75 MVA)	30,24	29,2	16,3	17,9
Electrode III	1	M11 (48 MVA)	25,84	25	29,8	11,1
Electrode III	6	M11 (48 MVA)	28,82	26	13,4	16,9
All electrodes**	5	M10 (48 MVA)	26,80	22,6	19,9	-

† Input directly to C.S.T.R. beneath electrode tip.

* Four inputs.

** Twelve inputs.

Table 17. Values for the mean residence times in the dispersed plug flow region ($\bar{t}$) and the C.S.T.R. region ($\bar{t}_{inv}$) of the furnaces for inputs at stockline level and beneath the electrode tips to the active furnace zone.

POSITION OF INPUT	EXPERIMENT NUMBER	FURNACE	RAW MATERIAL FEEDRATE t/h	FURNACE LOAD MW	$\bar{t}$ HOURS	$\bar{t}_{inv}$ HOURS
CLOSEST TO ALLOY TAPPING HOLE						
Closest : Electrode I	2	M10 (48 MVA)	27,19	25	13,1	4,1
Central Charging	4	M10 (48 MVA)	22,17	20	72,2	-
Shaft	1	M11 (75 MVA)	32,43	32,8	15,9	-
FARTHEST FROM ALLOY TAPPING HOLE						
Farthest Electrode III	3	M10 (48 MVA)	29,95	26	15,1	22,2
Electrode II	1	M10 (48 MVA)	27,85	26	13,8	17,8

Table 18. Values for the mean residence times in the dispersed plug flow region ($\bar{t}$) and the C.S.T.R. region ($\bar{t}_{inv}$) of the furnaces for inputs to the furnace bunkers feeding the active furnace zone.

evidence that the position of radio-tracer input relative to the alloy tapping hole influences the value of $\bar{t}$. In one multi-input experiment, experiment 5 on furnace M10 with 48 MVA transformers, 12 radio-tracer inputs were equally disposed around the electrodes (four inputs per electrode). Analysis of this experiment showed that burden descent within the active zone was quite uniform and that the mean residence times of these inputs were best described by a single value. Consequently it may be concluded that values obtained for $\bar{t}$ during the experimental campaign were determined by the conditions of operation and not the position of radio-tracer input relative to the alloy tapping hole.

Comparison of the values for $\bar{t}$ given in Tables 17 and 18 did not show that values obtained for inputs to the furnace bunkers were larger than inputs at stockline level. On the basis of this comparison the average values obtained for inputs to the furnace bunkers were smaller than for inputs at stockline level. This contradictory result could only be attributed to the over-riding influence of furnace operation conditions on the values of $\bar{t}$. Since all experiments in Table 17 except one, were performed on furnace M11 and all experiments in Table 18 except one, were performed on furnace M10, this contradictory result also illustrated that comparisons between two different furnaces are not valid. In calculating the average values of $\bar{t}$ for these two types of experiments the value of $\bar{t}$ = 72,2 hours obtained for experiment 4 on furnace M10 with 48 MVA transformers was not considered. This was because it is believed that this unusually high value was due to temporary stoppage of the radio-tracer input in the feed chute feeding from the furnace bunker to the charging shaft.

In analysis of the influence of operating conditions on the values obtained for $\bar{t}$, the influence of the level of radio-tracer input was eliminated by considering each type of experiment independently.

8.5.4.2. The C.S.T.R. region of the furnace

It is possible that either one continuous alloy pool exists beneath the electrode tips, or the alloy pool is divided into several discrete pools. However observations of variations in the positions of the electrodes immediately after alloy tappings indicate that the alloy pool is usually continuous.

If one alloy pool exists in the hearth region of the furnace and this pool can be represented by a C.S.T.R., the position of radio-tracer input, irrespective of whether this is to the active or the inactive furnace zone, has no influence on $\bar{t}_{inv}$. Analysis of experimental results has confirmed that it is valid to represent the alloy pool by a C.S.T.R. Comparison of the values for $\bar{t}_{inv}$ in Tables 17 and 18 provides no statistical evidence that the positions of radio-tracer input influence the values of $\bar{t}_{inv}$. Consequently variations in values obtained for $\bar{t}_{inv}$ during the experimental campaign must be attributed to the influence of furnace operating conditions.

For abnormal furnace operating condition the continuous alloy pool in the furnace hearth may be broken down into several alloy pools. This could well occur when an electrode breaks and operation is continued with a very short electrode stubb. Under these circumstances $\bar{t}_{inv}$

would depend on the position of radio-tracer input. Since essentially normal operating conditions prevailed during most runs of the experimental campaign no apparent influence of the position of radio-tracer input on the value of $\bar{t}_{inv}$ was observed.

8.5.5. Influence of operating conditions on mean residence time in dispersed plug flow region

The significance of the model parameter $\bar{t}$ is that it provides an estimate of the time spent by a burden element in the region above the electrode tips where the burden is predominantly solid. There are several factors which may influence the value of $\bar{t}$ within the dispersed plug flow region of the active zone.

The mass throughput of the furnace is one of these factors. The raw material feedrate to the furnace is a measure of mass throughput. The mass throughput to the furnace may be changed by a change in either, or both, the horizontal, cross-sectional area of the active zone, or the rate of burden descent through the furnace. In general thi hange is achieved by a change in the heat input to the furnace or by a change in the distribution of heat through the furnace.

From Westly's principle of heat distribution, heat is available for pre-heating the burden and heat is available for reduction.[57, 59] (Refer Section 4.1). The relative amounts of heat available for these processes are determined by the heat distribution factor K. The smaller the value of K the more heat available for reduction and the less heat available for pre-heating the

burden. There is an optimum value of K for smooth furnace operation and significant deviation from this value results in erratic furnace operation.

Reduction occurs primarily in the vicinity of the electrode tips, so that as the amount of heat available for reduction changes, the build-up of accretions on the furnace wall may be influenced. This occurs if the change in heat available for reduction changes the configuration of the isothermal surfaces emanating from the electrode tips. A change in the build-up of accretions on the furnace wall will result in a change in the horizontal, cross-sectional dimensions of the active zones since these accretions give rise to the active zone.

Alternatively a change in heat available for reduction may influence the rate of burden descent through the active zone. Either, or both of these changes will occur with a change in heat available for reduction and both of these changes will result in a change in mass throughput of the furnace.

When these changes have opposing influences on mass throughput (e.g., increase in rate of burden descent and decrease in the horizonal, cross-sectional dimensions of the active zone), the predominant change will determine the change in mass throughput of the furnace. The value of $\bar{t}$ will only change with a change in mass throughput of the furnace, if this change is determined by a change in the rate of burden descent through the furnace. This statement implies that a change in heat available for reduction does not influence the vertical length of the dispersed plug flow region of the active zone. For the purpose of the analysis this was assumed to be the case.

Consequently in the analysis of the values obtained for $\bar{t}$, changes in $\bar{t}$ between experiments were compared on the basis of changes in the feedrate of the raw materials between the same experiments. On the basis of this comparison and the above discussion the mechanism whereby mass throughput of the furnace changed from experiment to experiment was determined.

The heat available for reduction will change if either the total heat input to the furnace is changed and/or the value of K is changed. Since only small deviations of K from its optimum value may be tolerated for stable furnace operation the heat available for reduction is usually changed by altering the total heat input to the furnace. A measure of the total heat input to the furnace is the furnace load.

Consequently in the analysis, changes in raw material feed rate were compared to changes in furnace load. Where corresponding changes were observed to occur, it was concluded that a change in mass throughput of the furnace was a consequence of a change in the heat available for reduction arising from a change in total heat input to the furnace. Where changes observed did not correspond it was concluded that a change in mass throughput was a result of a change in K or was due to the influence of factors other than heat available for reduction.

The value of $\bar{t}$ within the dispersed plug flow region of the active zone is dependent on the depth of electrode penetration and probably also on the rate of alloy discharge from the furnace. The influence of these factors was ignored in the analysis.

The influence of the level of radio-tracer input above the furnace hearth was taken into account by comparing experiments in which the radio-tracer inputs were made at the same vertical level above the furnace hearth.

On the basis of these considerations the values obtained for $\bar{t}$ were analysed. It must be emphasized that this analysis hinged on the assumption that the mass throughput of the furnace was determined by the total heat input to the furnace, and, the distribution of this heat through the furnace. This assumption, together with the concepts developed to describe how heat influenced the mass throughput of the furnace, may not be true.

However their use did make it possible to attempt to reconcile the changes observed in operating conditions with changes in the mean residence time, $\bar{t}$. Assessment of the validity of this treatment was beyond the scope of the investigation. As before, due to the lack of a sufficient number of experiments of each type, it was difficult to determine whether trends observed were a consequence of the mechanism of burden descent, or, were due to experimental or operational variations which were not taken into account. Consequently this analysis served primarily to illustrate how these concepts could be applied in the analysis of a sufficiently large number of experiments of the same type.

8.5.5.1. Radio-tracer inputs to charging shafts

The values for the raw material feedrate, the mean residence time, and the furnace load for these experiments are given in Table 19 in order of decreasing raw material feedrate. Examination of these values showed that three groups could be identified as shown in the table.

For group A, raw material feedrate and furnace load were high, and mean residence time was small. With the exception of experiment 4, furnace M11 (48 MVA), as the raw material feedrate decreased, the mean residence time became smaller and the furnace load either decreased or remained constant. This indicated the following:-

(i) Decreased material throughput was due to a decrease in the cross-sectional dimension of the active zone.

(ii) Although the decrease in active zone dimension was accompanied by an increase in rate of burden descent, this increase was insufficient to prevent a decrease in material throughput.

(iii) Where a decrease in furnace load occurred, these changes were largely due to a decrease in the total heat input to the furnace. Where furnace load remained constant, these changes were due to a change in heat distribution through the furnace.

(iv) For experiment 4, furnace M11 (48 MVA) the decreased material throughput was due to a decrease in both cross-sectional dimension of the active zone, and rate of burden descent. The rate of burden descent for this experiment was lower than for all other experiments in this group except for experiment 4, furnace M11 (75 MVA).

GROUP	FURNACE	EXPERIMENT NUMBER	RAW MATERIAL FEEDRATE t/h	MEAN RESIDENCE TIME HOURS	FURNACE LOAD MW
A	M11 (75 MVA)	4	33,48	18,8	30,5
	M11 (75 MVA)	5	30,24	16,3	29,2
	M11 (48 MVA)	6	28,82	13,4	26
	M11 (48 MVA)	3	27,33	11,9	26
	M11 (48 MVA)	4	26,80	18,4	26
B	M10 (48 MVA)	5	26,80	19,9	22,6
	M11 (48 MVA)	5	25,95	13,4	26
C	M11 (48 MVA)	1	25,84	29,8	25
	M11 (75 MVA)	3	24,03	22,3	24,9
	M11 (48 MVA)	2	14,69	28,5	18

Table 19. Values for relevant operating parameters and mean residence time in order of decreasing raw material feedrate for experiments with radio-tracer inputs to charging shafts

The experiments in group B were isolated since they were intermediate between groups A and C. Furthermore the result for experiment 5, furnace M10 (48 MVA), appeared anomalous in that although the furnace load was low, the raw material feedrate was relatively high. In addition the mean residence time was large indicating a low rate of burden descent. This illustrated the fact that results for the two furnaces, M10 and M11, could not be compared due to inherent differences in operation of the furnaces. These differences probably arose due to different techniques of commissioning the furnaces and because M10 was much older than M11. For the other experiment in this group, experiment 5, furnace M11 (48 MVA), comparison with group A experiments revealed:-

(i) This experiment was very similar to experiment 6, furnace M11 (48 MVA), in that the mean residence time and furnace load for these experiments were the same.

(ii) The lower material throughput for experiment 5, furnace M11 (48 MVA), in comparison to experiment 6, furnace M11 (48 MVA), was due to a decrease in the cross-sectional active zone dimension as a consequence of a change in heat distribution through the furnace. In experiment 5, furnace M11 (48 MVA) the radio-tracer was introduced at a lower level into the "burden valley". This may partially explain obtaining the same value of $\bar{t}$ as in experiment 6, furnace M11 (48 MVA).

For group C, raw material feedrate and furnace load were low, and mean residence time was large. For these experiments the following was observed:-

(i) Decreased material throughput was due to a decrease in cross-sectional dimension of the active zone arising as a consequence of decreased total heat input.

(ii) Between experiments 1, furnace M11 (48 MVA), and 3, furnace M11 (75 MVA), and between experiments 1, furnace M11 (48 MVA), and 2, furnace M11 (48 MVA), decrease in active zone dimension was accompanied by an increase in rate of burden descent. This was particularly pronounced between experiment 1, furnace M11 (48 MVA), and experiment 3, furnace M11 (75 MVA). However the increased rate of burden descent was insufficient to neutralize the influence of the decrease in the size of the active zone. Between experiment 3, furnace M11 (75 MVA), and experiment 2, furnace M11 (48 MVA) the rate of burden descent decreased, contributing to the decrease in mass throughput of the furnace.

Comparing group C experiments to the balance of these experiments other than experiment 5, furnace M10 (48 MVA), showed:-

(i) Decreased material throughput was accompanied by a decrease in rate of burden descent.

(ii) Decreased rate of burden descent was a consequence of a decrease in total heat input to the furnace.

8.5.5.2. Radio-tracer inputs to furnace bunkers

The values for the raw material feedrate, the furnace load, and the mean residence time for these experiments are given in Table 20.

FURNACE	EXPERIMENT NUMBER	RAW MATERIAL FEEDRATE t/h	MEAN RESIDENCE TIME HOURS	FURNACE LOAD MW
M11 (75 MVA)	1	32,43	15,9	32,8
M10 (48 MVA)	3	29,95	15,1	26
M10 (48 MVA)	1	27,85	13,8	26
M10 (48 MVA)	2	27,19	13,1	25
M10 (48 MVA)	4	22,17	72,2	20

Table 20. Values for relevant operating parameters and mean residence time in order of decreasing raw material feedrate for experiments with radio-tracer inputs to feed bunkers

Consider the experiments 1, 2 and 3 on furnace M10 (48 MVA). Here the decreased material throughput for the experiments was due to a decrease in the cross-sectional dimension of the active zone. Between experiment 2 and the remaining experiments the decrease in active zone size was due to a decrease in total heat input. Between experiments 1 and 3 this was due to a change in heat distribution through the furnace. In each case the change in active zone size was accompanied by an increase in rate of burden descent, but this influence was negated by the decrease in the size of the active zone.

Comparison of these three experiments with experiment 4 on furnace M10 (48 MVA) showed that the decreased material throughput for this experiment was a consequence of a decrease in rate of burden descent due to a decrease in total heat input to the furnace. The unusually large value of $\bar{t}$ for experiment 4, furnace M10 (48 MVA), was

probably partly due to hold-up of the radio-tracer input within the feed chute.

Experiment 1, furnace M11 (75 MVA), was not compared to the other experiment of this type as it was the only experiment on furnace M11.

It must be emphasized that the conclusions made with regard to the influence of furnace operation on $\bar{t}$ are not based on any factual evidence. The above treatment represents an opinion as to how conditions of operation of the furnace could have caused the observed variation in $\bar{t}$.

8.5.6. The alloy inventory volume in the furnace hearth and the mean residence time in the C.S.T.R. region of the furnace

The model parameter Vinv provided an estimate of the alloy volume within the furnace which behaved as a C.S.T.R. for each experiment. The mean residence time in the C.S.T.R. region of the furnace, $\bar{t}inv$, was calculated from Vinv and the average alloy discharge rate for each experiment.

The values of these parameters are given in Tables 21 and 22 respectively. Comparisons between the two furnaces were not considered due to the inherent differences in their behaviour caused by differences in age and the commissioning procedure of the furnaces.

Examination of Table 21 and 22 showed that the values of $\bar{t}inv$ and Vinv for experiment 4 on furnace M11 with 48 MVA transformers and experiment 2 on furnace M10 with 48 MVA transformers were substantially smaller than the values

GROUP	EXPERIMENT NUMBER	FURNACE	FURNACE LOAD MW	RAW MATERIAL FEEDRATE t/h	ALLOY DISCHARGE RATE t/tapping	RATIO:- ALLOY DISCHARGE / RAW FEED	Vinv	$\bar{t}$inv
A	2	M11 (48 MVA)	18	14,69	25,15	1,71	10,0	16,7
	3	M11 (75 MVA)	24,9	24,03	32,64	1,48	34,1	24,0
B	1	M11 (48 MVA)	25	25,84	24,72	0,96	12,5	11,1
	3	M11 (48 MVA)	26	27,33	24,97	0,91	15,5	13,2
	4	M11 (48 MVA)	26	26,80	25,83	0,96	8,3	6,8
	5	M11 (48 MVA)	26	25,95	23,44	0,90	21,0	20,9
	6	M11 (48 MVA)	26	28,62	26,71	0,89	19,4	16,9
C	4	M11 (75 MVA)	30,5	33,48	28,17	0,84	15,3	10,3
	5	M11 (75 MVA)	29,2	30,24	24,73	0,82	22,0	17,9
	6	M11 (75 MVA)	31,4	34,12	30,43	0,89	15,4	9,9
	1	M11 (75 MVA)	32,8	32,43	-	-	26,9	-

Teble 21. Values of the model parameters Vinv and $\bar{t}$inv and relevant operating parameters for experiments on furnace M11

EXPERIMENT NUMBER	FURNACE	FURNACE LOAD MW	RAW MATERIAL FEEDRATE t/h	ALLOY DISCHARGE RATE t/tapping	RATIO:- ALLOY DISCHARGE / RAW FEED	Vinv	$\bar{t}$inv
1	M10 (48 MVA)	26	27,85	25,34	0,91	20,5	17,8
2	M10 (48 MVA)	25	27,19	23,42	0,86	4,5	4,1
3	M10 (48 MVA)	26	29,95	23,74	0,79	24,0	22,2
5	M10 (48 MVA)	22,6	26,80	-	-	16,0	-

Table .2. Values of the model parameters Vinv and $\bar{t}$inv and relevant operating parameters for experiments on furnace M10

obtained for the remainder of experiments on the furnaces. This could have been because the alloy bath consisted of several discrete pools during these experiments. For the balance of experiments on both furnaces it was assumed that one continuous pool existed in the furnace hearth.

Theoretically there are several operational factors which will influence the alloy inventory volume within the furnace.

The alloy inventory volume will be influenced by the relative amount of heat dissipated from the electrode tips. If the amount of heat dissipated is increased the formation of accretion on the furnace walls and the hearth floor is decreased and the size of the alloy pool is increased.

The relative values of the raw material feedrate and alloy discharge rate will also influence the volume of the continuous alloy pool. As the rate of alloy discharge is increased relative to the raw material feedrate the volume of the alloy pool is decreased.

The experiments on furnace M11 were classified into three groups on the basis of similar furnace loads, raw material feedrates, alloy discharge rates and ratios of alloy discharge rate to raw material feedrate.

Comparison of the values obtained for Vinv and $\bar{t}$inv for experiments within each group and between each group failed to reveal any of the expected trends outlined above.

Values for Vinv for experiments 3, 4, 5 and 6 on furnace M11 with 48 MVA transformers were discussed on a

similar basis to the analysis used to explain changes observed in $\bar{t}$, the mean residence time in the dispersed plug flow region of the furnace. In analysis of the changes observed in $\bar{t}$ for these experiments it was assumed that the heat dissipated from the electrode tips, and hence the active zone cross-sectional dimensions, decreased from experiment 6 to 3 to 4 to 5. It would therefore be expected that the values obtained for Vinv for these experiments should decrease in a corresponding fashion. The values obtained for Vinv for experiments 6, 3, 4 and 5 respectively were 19,4 m^3, 15,5 m^3, 8,3 m^3 and 21,0 m^3. The value of 21,0 m^3 obtained for experiment 5 did not show the expected trend. The very small value of 8,3 m^3 for experiment 4 was probably due to a breakdown of the alloy bath into several pools.

Examination of the values of $\bar{t}inv$ and Vinv for experiments on furnace M10, given in Table 22 also failed to reveal any of the expected trends.

3.5.7. The overall mean residence time in the furnace, $\bar{t}fce$

The overall mean residence time in the furnace, $\bar{t}fce$ was obtained from the sum of $\bar{t}inv$ and $\bar{t}$. Values for $\bar{t}fce$ for experiments on furnace M11 and M10 are given in Tables 23 and 24 respectively. Also given in these tables are the theoretically calculated overall nominal mean residence times, $\bar{t}n$. The values for $\bar{t}n$ were calculated from the mass capacity of the furnace (refer Appendix B) and the raw material feedrate.

With the exception of experiment 4 on furnace M11 with 48 MVA transformers and experiment 2 on furnace M10 with 48 MVA transformers comparison of $\bar{t}fce$ and $\bar{t}n$ for experiments on both

EXPERIMENT NUMBER	FURNACE	$\bar{t}$	$\bar{t}inv$	$\bar{t}fce$	$\bar{t}n$	FURNACE LOAD MW
1	M11 (75 MVA)	15,9	-	-	31,3	32,8
6	M11 (75 MVA)	-	9,9	-	29,7	31,4
4	M11 (75 MVA)	18,8	10,3	29,1	30,3	30,5
5	M11 (75 MVA)	16,3	17,9	34,2	33,6	29,2
3	M11 (48 MVA)	11,9	13,2	25,1	37,2	26
4	M11 (48 MVA)	18,4	6,8	25,2	37,9	26
6	M11 (48 MVA)	13,4	16,9	30,3	35,3	26
5	M11 (48 MVA)	13,4	20,9	34,3	39,1	26
1	M11 (48 MVA)	29,8	11,1	40,9	39,3	25
3	M11 (75 MVA)	22,?	24,0	46,3	42,3	24,9
2	M11 (48 MVA)	28,5	16,7	45,2	69,1	18

Table 23. Values of the predicted overall mean residence time from the model, $\bar{t}fce$, and the theoretically calculated overall nominal mean residence time, $\bar{t}n$, for experiments on furnace M11.

EXPERIMENT NUMBER	FURNACE	$\bar{t}$	$\bar{t}inv$	$\bar{t}fce$	$\bar{t}n$	FURNACE LOAD MW
1	M10 (48 MVA)	13,8	17,8	31,6	36,4	26
3	M10 (48 MVA)	15,1	22,2	37,3	33,9	26
2	M10 (48 MVA)	13,1	4,1	17,2	37,3	25
5	M10 (48 MVA)	19,9	-	-	37,9	22,6
4	M10 (48 MVA)	72,2	-	-	45,9	20

Table 24. Values of the predicted overall mean residence time from the model, $\bar{t}fce$, and the theoretically calculated overall nominal mean residence time, $\bar{t}n$ for experiments on furnace M10.

furnaces showed that $\bar{t}n$ was larger than $\bar{t}fce$. This was to be expected since in the calculation of $\bar{t}n$ the existence of stagnancy was not taken into account. The order of magnitude values for $\bar{t}fce$ and $\bar{t}n$ were similar indicating that the calculated mass capacity of the furnace was a realistic figure.

For experiments on furnace M10 it was expected that the difference between $\bar{t}fce$ and $\bar{t}n$ would be smaller than for experiments on furnace M11. In the experiments on furnace M10, $\bar{t}fce$ represented the overall mean residence time from the feed bunkers. In the experiments on furnace M11 and in the calculation of $\bar{t}n$ for all experiments, $\bar{t}fce$ and $\bar{t}n$ respectively represented the overall mean residence time from the stockline level. Consequently for experiments on furnace M10 an additional volume was considered in the estimation of $\bar{t}fce$ and hence the values of $\bar{t}fce$ were increased. The average differences between $\bar{t}fce$ and $\bar{t}n$ for experiments on furnace M11 and M10 confirmed this. (Values for experiment 4, furnace M11 - 48 MVA, and experiment 2, furnace M10 - 48 MVA, were not considered).

Observation of the values of $\bar{t}fce$ and the furnace load for experiments on furnace M11 indicated that, as expected, $\bar{t}fce$ increased with decreasing furnace load.

8.5.8. Significance of analysis of the model parameters

The lack of primary experimental data made it impossible to carry out a statistical analysis of the model parameters. Consequently an attempt was made to explain any observed trends using a few theoretical concepts. The validity of these explanations could not be determined.

The aim of the discussion of the model parameters has therefore been to outline fundamental concepts which may be applied in extensive investigations using radio-tracers on the mechanism of burden movement through submerged-arc furnaces. Sufficient experimental data must be accumulated to permit quantitative statistical analysis of the results. Once sufficient data are available, a critical assessment will be possible of the value of the comments on the influence on burden movement of factors such as heat distribution and raw material feedrate.

8.6. Future Work

The logical extension of the radio-tracer study is:-

(i) Extensive measurement of alloy and slag phase residence time distributions for a particular furnace, or several furnaces, using the experimental technique developed. A long term investigation is required so as to accumulate sufficient data to permit statistical analysis of the residence time distributions obtained from the various types of experiments, under the wide range of operating conditions which prevail on these furnaces. Slag phase residence time distribution measurement will require selection of a suitable radio-tracer.

(ii) Extensive measurement of the residence time distributions for the various carbonaceous reducing agents used on these furnaces. An experimental technique would have to be developed for measurement of these residence time distributions. Another theoretical model would also have to be developed to compute these experimentally determined residence time distributions. The flow behaviour of

carbonaceous reducing agents of the burden is not the same as that of the slag and alloy forming components of the burden due to the formation of a coke bed and evolution of gaseous products.

(iii) Use of the theoretical model developed in this investigation to compute the experimentally determined residence time distributions. By statistical analysis of model parameters and furnace operating parameters it may be possible to determine the influence of conditions of operation on burden movement through submerged-arc furnaces. This analysis may show whether the concepts developed for qualitative analysis of model parameters were valid.

(iv) Development and use of alternative composite models to determine whether the conclusions regarding flow patterns based on the model used in this investigation were unique.

The ultimate objective of this type of investigation is to clearly define the mechanism of burden movement through the submerged-arc furnace and to determine the influence of operating conditions on burden movement through the furnace. Provided this can be achieved the efficiency of the furnace as a production unit may be optimized.

If the isothermal surfaces within the furnace can be delineated by means of temperature measurements using probes, a krowledge of the mechanism and rate of burden movement through the furnace provides the means of determining the time rate of change of environmental conditions experienced by burden elements descending

through the furnace. This information together with experimentally determined kinetic data for reactions occurring in the furnace may be used to obtain valuable insight into the processes occurring within the furnace. By delineating the isothermal surfaces within the furnace it may be possible to measure the size of the active zone.

9. CONCLUSION

An experimental technique based on the stimulus-response technique using a radio-tracer input as the stimulus was successfully developed to measure residence time distributions of the alloy phase for two industrial submerged-arc furnaces producing high-carbon ferro-manganese. The response was the level of radio-activity due to the radio-isotope Fe^{59}.

Due to the limited time available for the investigation, insufficient experiments were performed to permit a statistical analysis of the results. The problem of insufficient data was accentuated by truncation of many of the experimental residence time distributions.

These truncation problems permitted single parameter analysis of only three of the seventeen experimental residence time distributions. Comparison of experimentally measured mean residence times and calculated mean residence times for these three experiments verified the existence of stagnant zones within the furnace volume. The variance for these three residence time distributions showed that burden movement through the furnace could not be described by either of the two idealized patterns of flow-plug flow and mixed flow.

Using observations of the mode of burden movement through the furnace, a qualitative picture of the inner structure of the submerged-arc furnace, and by examination of the form of the experimentally measured residence time distributions, a composite model was developed to describe the mechanism of burden movement through the furnace. This composite model consisted of a dispersed plug flow region

in the upper regions of the furnace feeding a constantly stirred tank reactor beneath the electrode tips. Non-linear regression analysis of the equations developed from the composite model permitted selection of optimum values of model parameters to give the computed residence time distribution. For each residence time distribution the computed result closely approximated the experimentally measured result for realistic values of the model parameters and hence it was concluded that the composite model was a valid representation of burden movemert through the furnace.

The most important model parameters were the mean residence time in the dispersed plug flow region, $\bar{t}$, and the alloy inventory volume in the constantly stirred tank reactor, Vinv. No correlations were found to exist between these two parameters and the furnace operating parameters. This was probably due to insufficient experimental data.

The mean residence time in the C.S.T.R. region of the furnace, $\bar{t}inv$, was calculated from Vinv. The values of Vinv, $\bar{t}inv$ and $\bar{t}$ were analysed qualitatively by considering the influence of positions of radio-tracer inputs. Although no conclusive trends emerged from this analysis, it was hypothesized that provided the radio-tracer inputs were made to the active zone of the furnace, the only significant influence on $\bar{t}$ would be the influence on $\bar{t}$ of the level of radio-tracer input above the alloy tapping hole.

An attempt was made to explain the changes in the values of $\bar{t}$, Vinv and $\bar{t}inv$ between experiments in terms of changes in total heat input to the furnace, heat

distribution through the furnace, raw material feed rate and alloy discharge rate. Although this analysis did not provide any statistically significant information, this was probably due to the lack of sufficient results and the complex influence of many variables on the mechanism of burden movement.

The overall mean residence time of the furnace, $\bar{t}fce$, was obtained for each experiment by summation of $\bar{t}$ and $\bar{t}inv$. Comparison of $\bar{t}fce$ and $\bar{t}n$, the overall nominal mean residence time of the furnace showed that in general $\bar{t}fce$ was smaller than $\bar{t}n$. This confirmed that a portion of the total furnace volume was stagnant.

A major contribution of this investigation was the development of techniques for the measurement and analysis of residence time distributions. An extensive investigation must be undertaken in the future to prove or disprove the concept of the mechanism of burden movement.

APPENDIX A. Computer program for single parameter evaluation of residence time distribution.

```
GJD      ACCT 37  DEPT OF METALLURGY                    FILE   GJD5                    WED  2/4/76 (76-154)        TIME 17.53.58
L.0001  REAL T(35),F(35),S(35),SS(35),DT(35),TT(35),CTT(35),EM(35),D(35),W(35),RR(35),AA(35),AR(35)
L.0002  REAL XR(35),TP(35),VC(35),DL(35),RA(35),G(35)
L.0003  READ(5,1)N,M
L.0004  DO 2 IA=1,N
L.0005 2 READ(5,1)I(IA),F(IA)
L.0006 1 FORMAT(2Y)
L.0007  DO 2000 IZ=1,N
L.0008  READ(5,2000) AM(IZ)
L.0009 2000 FORMAT(Y)
L.0010  III=1
L.0011  GO TO 5000
L.0012 5000 JJJ=III+1
L.0013  III=JJJ
L.0014  IF(III.EQ.2) GO TO 5007
L.0015  IF(III.EQ.3) GO TO 5002
L.0016  IF(III.EQ.4) GO TO 5003
L.0017  IF(III.EQ.5) GO TO 5004
L.0018 5007 WRITE(6,5008)
L.0019  GO TO 5001
L.0020 5002 VEK=AM(1)
L.0021  WRITE(6,5006)
L.0022  DO 2001 IY=2,N
L.0023  SEK=AM(IY)-VEK
L.0024  IF(SEK.GT.0.) GO TO 2002
L.0025  GO TO 2001
L.0026 2002 VEK=AM(IY)
L.0027  GO TO 2001
L.0028 2001 CONTINUE
L.0029  DO 2003 IX=1,N
L.0030 2003 F(IX)=F(IX)*AM(IX)/VEK
L.0031  GO TO 5001
L.0032 5003 WRITE(6,5027)
L.0033  VVV1=F(1)
L.0034  DO 5009 KKK=2,N
L.0035  VVV2=F(KKK)-VVV1
L.0036  IF(VVV2.GT.0.) GO TO 5010
L.0037  GO TO 5009
L.0038 5010 VVV1=F(KKK)
L.0039  GO TO 5009
L.0040 5009 CONTINUE
L.0041  LLL=0
L.0042  GO TO 5011
L.0043 5011 LLL=LLL+1
L.0044  LLL=LLL
L.0045  IF(VVV1.EQ.F(LLL)) GO TO 5012
L.0046  GO TO 5011
L.0047 5013 IF(LLL.EQ.N) GO TO 5014
L.0048  GO TO 5011
L.0049 5014 WRITE(6,5015)
L.0050  STOP
L.0051 5015 FORMAT(///,T4,'ERROR IN PEAK DET.')
L.0052 5012 WRITE(6,5016) LLL
L.0053 5016 FORMAT(///,T4,'PEAK VALUE AT ',Y)
L.0054  GO TO 5017
```

```
L.0055 5017 NNN=LLL
L.0056  GO TO 5018
L.0057 5018 IIJ=NNN+1
L.0058  NNN=IIJ
L.0059  VVV3=F(NNN)/VVV1
L.0060  IF(VVV3.LT.0.190) GO TO 5019
L.0061  IF(NNN.EQ.N) GO TO 5020
L.0062  GO TO 5018
L.0063 5019 WRITE(6,5021)
L.0064 5021 FORMAT(//,T4,'RATIO 0.19C')
L.0065  N=NNN
L.0066  GO TO 5001
L.0067 5020 IIK=LLL
L.0068  GO TO 5022
L.0069 5022 IIL=IIK+1
L.0070  IIK=IIL
L.0071  VVV4=F(IIK)/VVV1
L.0072  IF(VVV4.LT.0.600) GO TO 5023
L.0073  IF(IIK.EQ.N) GO TO 5024
L.0074  GO TO 5022
L.0075 5023 WRITE(6,5025)
L.0076 5025 FORMAT(//,T4,'RATIO 0.60C')
L.0077  N=IIK
L.0078  GO TO 5001
L.0079 5024 WRITE(6,5026)
L.0080 5026 FORMAT(//,T4,'TERMINATE-RATIO>0.600')
L.0081  GO TO 5004
L.0082 5008 FORMAT(///,T4,'STRAIGHT CALC.')
L.0083 5006 FORMAT(///,T4,'MASS CONSIDERED')
L.0084 5027 FORMAT(///,T4,'TRUNCATED CALC.')
L.0085 5001 NA=N-1
L.0086  MM=M+3
L.0087  DO 3 IB=1,MM
L.0088  S(IB)=0.000000
L.0089 3 SS(IB)=0.000000
L.0090  DT(1)=(T(2)-T(1))/2
L.0091  DT(N)=(T(N)-T(NA))/2
L.0092  DO 4 IC=2,NA
L.0093 4 DT(IC)=(T(IC+1)-T(IC-1))/2
L.0094  DO 5 ID=1,N
L.0095  SA=F(ID)*DT(ID)
L.0096  SB=F(ID)*DT(ID)*T(ID)
L.0097  A=SA+S(1)
L.0098  B=SB+S(2)
L.0099  S(1)=A
L.0100 5 S(2)=B
L.0101  R=S(2)/S(1)
L.0102  DO 6 IE=1,N
L.0103 6 TT(IE)=T(IE)/R
L.0104  DTT(1)=(TT(2)-TT(1))/2
L.0105  DTT(N)=(TT(N)-TT(NA))/2
L.0106  DO 7 IF=2,NA
L.0107 7 DTT(IF)=(TT(IF+1)-TT(IF-1))/2
L.0108  DO 8 IG=1,N
L.0109  SC=F(IG)*DTT(IG)
L.0110  C=SC+S(3)
L.0111 8 S(3)=C
L.0112  DO 9 IH=1,N
L.0113 9 FN(IH)=F(IH)/S(3)
```

```
L.0114  WRITE(6,10)R
L.0115 10 FORMAT(T4,'MEAN RESIDENCE VALUE=',Y)
L.0116  WRITE(6,100)S(1),S(3)
L.0117 100 FORMAT(/,T4,'AREA=',Y,2X,'UN-NORM-REC. AREA=',Y)
L.0118  WRITE(6,11)
L.0119 11 FORMAT(//,T6,'X-VALU',5X,'COUNTS',5X,'MODI-X',5X,'C-VALU',5X,'F-VALU',5X,'INTVAL')
L.0120  Z=TT(1)
L.0121 ZZ=0.000000
L.0122  DO 12 II=1,N
L.0123  D(II)=FN(II)*DTT(II)+ZZ
L.0124  ZZ=D(II)
L.0125  V(II)=Z+DTT(II)
L.0126  Z=V(II)
L.0127 12 WRITE(6,13)T(II),F(II),TT(II),FN(II),C(II),V(II)
L.0128 13 FORMAT(3X,F9.2,1X,F10.2,1X,F10.6,1X,F10.6,1X,F10.7,1X,F10.6)
L.0129  WRITE(6,101)
L.0130 101 FORMAT(//,T4,'MONO',5X,'MEMMORN',5X,'MCMEAN')
L.0131  DO 14 IJ=1,N
L.0132  AA(1)=TT(IJ)*FN(IJ)*DTT(IJ)
L.0133  RP(1)=AA(1)+SS(1)
L.0134 14 SS(1)=RP(1)
L.0135  DO 15 IK=1,N
L.0136  DO 16 IL=1,N
L.0137  AA(IK+1)=(TT(IL)**(IK+1))*FN(IL)*DTT(IL)
L.0138  AB(IK)=(TT(IL)-RP(1))**IK)*FN(IL)*DTT(IL)
L.0139  RP(IK+1)=AA(IK+1)+S(IK+3)
L.0140  S(IK+3)=RP(IK+1)
L.0141  RR(IK)=AB(IK)+SS(IK+1)
L.0142 16 SS(IK+1)=RR(IK)
L.0143 15 WRITE(6,17)IK,RP(IK),RR(IK)
L.0144 17 FORMAT(T6,I1,4X,F10.6,1X,F10.6)
L.0145  SP=0.000000
L.0146  K=0
L.0147  VB=TT(1)
L.0148  GO TO 18
L.0149 18 KA=K+1
L.0150  H=DTT(KA)*D(KA)
L.0151  H=H+SP
L.0152  SP=HU
L.0153  VA=VB+DTT(KA)
L.0154  VB=VA
L.0155 K=KA
L.0156  GO TO 19
L.0157 19 IF(VB.LT.1.000000)GO TO 18
L.0158  WRITE(6,20)SP,VB
L.0159 20 FORMAT(//,T4,'HOLDBACK=',F10.7,10X,'TIME=',F10.7)
L.0160  WRITE(6,21)
L.0161  WRITE(6,1000)
L.0162 1000 FORMAT(//,T4,'PERFECT M',1X,'TIME VAL.')
L.0163 21 FORMAT(//,T4,'SEGREGATION')
L.0164  DO 22 IM=1,N
L.0165  IP(IM)=-TT(IM)
L.0166  VC(IM)=1.000000-EXP(IP(IM))
L.0167 22 WRITE(6,33)VC(IM),TT(IM)
L.0168  SQ=0.000000
L.0169  L=0
L.0170  WRITE(6,1001)
L.0171 1001 FORMAT(//,T10,'VAL DIFF.',5X,'AREA')
L.0172  GO TO 23
```

```
L.0173 23 LA=L+1
L.0174  L=LA
L.0175  AR=(DTT(LA)*D(LA))-(DTT(LA)*VC(LA))
L.0176  IF(LA.EQ.N)GO TO 24
L.0177  AS=AR+SQ
L.0178  SQ=AS
L.0179  D1(LA)=D(LA)-VC(LA)
L.0180  WRITE(6,25)D1(LA),SQ
L.0181 25 FORMAT(T30,Y,5X,Y)
L.0182  RA(LA)=ABS(D1(LA))
L.0183  IF(RA(LA).LT.0.010000)GO TO 26
L.0184  GO TO 23
L.0185 24 WRITE(6,27)
L.0186 27 FORMAT(T4,'SEG. TERM. AFTER N STEPS')
L.0187  GO TO 28
L.0188 26 WRITE(6,29)SQ
L.0189 29 FORMAT(T4,'SEGREGATION=',Y)
L.0190  GO TO 28
L.0191 28 WRITE(6,30)
L.0192 30 FORMAT(//,T4,'INTENSITY FN.')
L.0193  WRITE(6,31)
L.0194 31 FORMAT(T4,'INTENT',5X,'TIME')
L.0195  DO 32 IN=1,N
L.0196  QUK=1.000000-D(IN)
L.0197  IF(QUK.EQ.0.) GO TO 3333
L.0198  GO TO 3331
L.0199 3331 G(IN)=FN(IN)/QUK
L.0200  WRITE(6,33) G(IN),TT(IN)
L.0201  GO TO 32
L.0202 3333 WRITE(6,3335) TT(IN)
L.0203 3335 FORMAT(T2,'INFINITE',3X,F10.7)
L.0204  GO TO 32
L.0205 32 CONTINUE
L.0206 33 FORMAT(T2,F10.6,1X,F10.7)
L.0207  IF(TT(N).LE.2.000000)GO TO 34
L.0208  BC=0.000000
L.0209  DO 36 ID=1,N
L.0210  IF(TT(ID).GT.2.000000)GO TO 36
L.0211  BA=FN(ID)*TT(ID)*DTT(ID)
L.0212  BP=FN(ID)*DTT(ID)
L.0213  BB=BA+BC
L.0214  BPP=BP+SS(MM)
L.0215  BC=BB
L.0216  SS(MM)=BPP
L.0217 36 CONTINUE
L.0218  BZ=BC/SS(MM)
L.0219  BD=1.000000-BZ
L.0220  WRITE(6,37)BD
L.0221 37 FORMAT(//,T4,'DEADWATER FRAC.=',F10.7)
L.0222  GO TO 38
L.0223 34 WRITE(6,35)FN(N)
L.0224 35 FORMAT(//,T4,'ZERO DEADSPACE,C-CURVE=',F10.7)
L.0225  GO TO 38
L.0226 38 J=0
L.0227  GO TO 39
L.0228 39 JA=J+1
L.0229  J=JA
L.0230  IF(FN(JA).GT.0.001000)GO TO 40
L.0231  GO TO 39
```

```
L.0232 40 WRITE(6,41)TT(JA),FN(JA)
L.0233 41 FORMAT(//,T4,'PLUG FLOW FRAC.=',F10.7,10X,'C-CURVE=',F10.6)
L.0234  GO TO 5000
L.0235 5004 STOP
```

APPENDIX B. Computer optimization of parameters in equations to describe residence time distributions

The standard Law and Bailey non-linear regression technique[72] with a convergence test was used to obtain the optimum model parameters. A subroutine subprogram to perform the non-linear regression analysis, known as LBREG, was available. This subprogram formed the basis of the computer program used. To perform the non-linear regression analysis using LBREG two further subprograms were required. These were:-

(i) A subroutine for the solution of a set of simultaneous equations. Subprogram CQCRT was available for this purpose.

(ii) A subroutine to compute the sum of squares and coefficient matrix. Subprogram SOFSQ was written for this purpose. On completion of the regression analysis SOFSQ was required to print out the predicted values of the function being analysed. The subroutine ANSWER was written for this purpose.

The calling of LBREG, and the input of data was achieved through the main program, MAIN. One additional subroutine, required by SOFSQ, was to calculate the error function. Subroutine ERRINT was available for this purpose.

The total non-linear regression program configuration is illustrated in Figure B1.

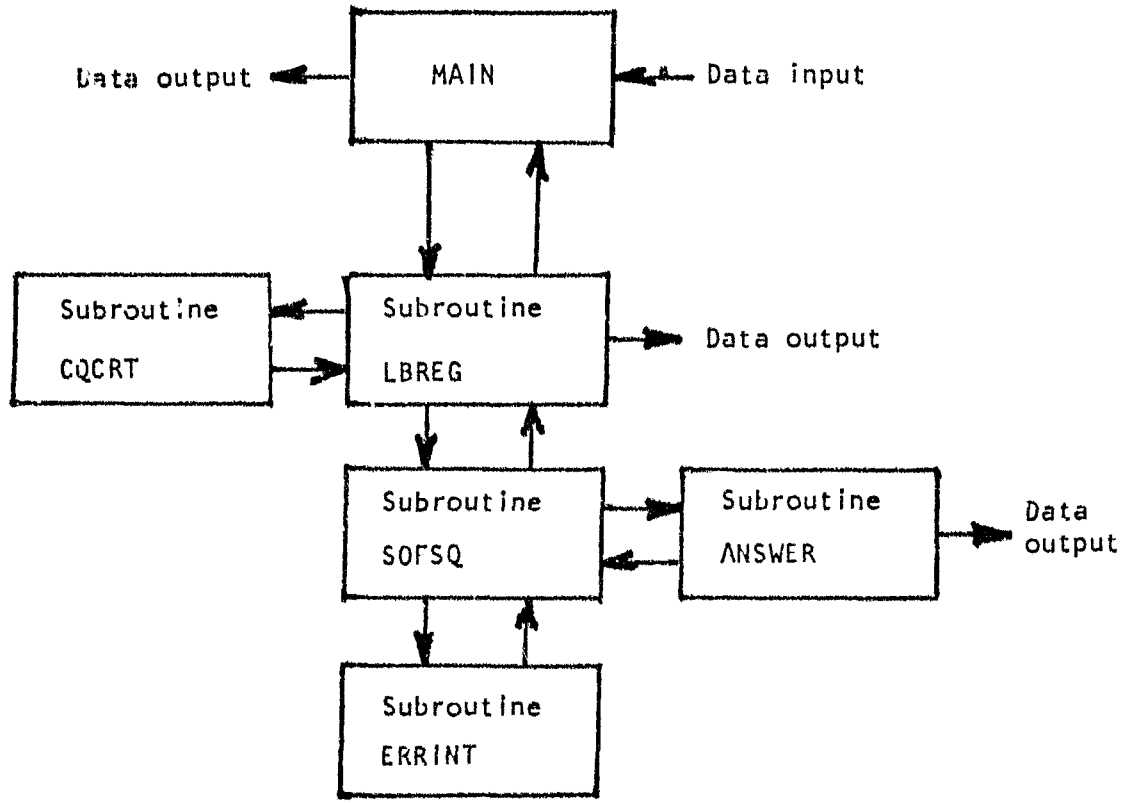

Figure B1. Total non-linear regression program configuration

B.1. Subroutine SOFSQ

To fit a function $y_i = f(b_1, b_2 \ldots x_i)$, where $b_1, b_2 \ldots$ are the parameters, for I pairs of values (Y_i, x_i), the sum of squares SA is given by,

$$SA = \sum_{i=1}^{I} (Y_i - y_i)^2$$

The coefficient matrix C has a typical term Cm,n where

$$Cm,n = \sum_{i=1}^{I} \frac{\partial y_i}{\partial b_m} \cdot \frac{\partial y_i}{\partial b_n}$$

This matrix has one more column than the number of rows. This column is given by:-

$$C_m = \sum_{i=1}^{I} (Y_i - y_i) \cdot \frac{\partial y_i}{\partial b_m}$$

SOFSQ was developed to calculate:-

(i) y_i at each experimental point.

(ii) $Y_i - y_i$ at each experimental point.

(iii) $\frac{\partial y_i}{\partial b_m}$ at each experimental point for each parameter b_m.

(iv) The sum of squares, SA.

(v) The coefficient matrix, C.

B.1.1. Single input experiments

The equations used to describe the residence time distributions measured were:-

$$C_1 = \frac{V_1 Co\bar{t}}{2\ Vinv\ (t_1+t_o)}\left\{erf\left(\frac{t_1}{2\sqrt{D\bar{t}}} - \frac{1}{2\sqrt{D}}\right) - erf\left(-\frac{1}{2\sqrt{D}}\right)\right\} \qquad (B1)$$

$$C_i = \frac{V_i Co\bar{t}}{2\ Vinv\ (t_i-t_{i-1})}\left\{erf\left(\frac{t_i}{2\sqrt{D\bar{t}}} - \frac{1}{2\sqrt{D}}\right) - erf\left(\frac{t_{i-1}}{2\sqrt{D\bar{t}}} - \frac{1}{2\sqrt{D}}\right)\right\} + C_{i-1}\left(1 - \frac{V_{i-1}}{Vinv}\right) \quad i = 2, \ldots N \qquad (B2)$$

The four parameters in these equations were Co, $\bar{t}$, D and Vinv. Derivatives of equations (B1) and (B2) with respect to the parameters are:-

(a) Derivatives with respect to Co

Co is a linear scaling factor. Therefore;

$$\frac{\partial C_1}{\partial Co} = \frac{C_1}{Co} \qquad (B3a)$$

$$\frac{\partial C_i}{\partial Co} = \frac{C_i}{Co} \qquad (B3b)$$

(b) Derivatives with respect to $\bar{t}$

For equation (B1),

$$\frac{\partial C_1}{\partial \bar{t}} = \frac{V_1 Co\bar{t}}{2\ Vinv\ (t_1+t_o)}\left\{\frac{\partial}{\partial \bar{t}}\left[erf\left(\frac{t_1}{2\sqrt{D\bar{t}}} - \frac{1}{2\sqrt{D}}\right)\right]\right\} + \left\{\frac{\partial}{\partial \bar{t}}\left(\frac{V_1 Co\bar{t}}{2\ Vinv\ (t_1+t_o)}\right)\right\}\left\{erf\left(\frac{t_1}{2\sqrt{D\bar{t}}} - \frac{1}{2\sqrt{D}}\right) - erf\left(-\frac{1}{2\sqrt{D}}\right)\right\}$$

Now $\quad \frac{\partial}{\partial x}\{erf(f(x))\} = \frac{2}{\sqrt{\pi}}\left\{\exp\left[-(f(x))^2\right] \cdot \frac{\partial f(x)}{\partial x}\right\}$

So $$\frac{\partial}{\partial t}\left(\operatorname{erf}\left(\frac{t_1}{2\sqrt{Dt}}-\frac{1}{2\sqrt{D}}\right)\right)=\frac{2}{\sqrt{\pi}}\left(\exp\left[-\left(\frac{t_1}{2\sqrt{Dt}}-\frac{1}{2\sqrt{D}}\right)^2\right]\cdot\left(-\frac{t_1}{2\sqrt{D}t^2}\right)\right)$$

And $$\frac{\partial}{\partial t}\left(\frac{V_1 Co\,t}{2\ Vinv\ (t_1+t_o)}\right)=\frac{V_1 Co}{2\ Vinv\ (t_1+t_o)}$$

Therefore $$\frac{\partial C_1}{\partial t}=\frac{C_1}{t}\cdot\frac{V_1 Co\,t}{2\ Vinv\ (t_1+t_o)}\left(\frac{t_1}{\sqrt{D\pi}t^2}\right)\left(\exp\left[-\left(\frac{t_1}{2\sqrt{Dt}}-\frac{1}{2\sqrt{D}}\right)^2\right]\right) \qquad \text{(B4a)}$$

Similarly for equation (82),

$$\frac{\partial C_i}{\partial t}=\frac{V_i Co}{2\ Vinv\ (t_i-t_{i-1})}\left(\operatorname{erf}\left(\frac{t_i}{2\sqrt{Dt}}-\frac{1}{2\sqrt{D}}\right)-\operatorname{erf}\left(\frac{t_{i-1}}{2\sqrt{Dt}}-\frac{1}{2\sqrt{D}}\right)\right)+\frac{\partial C_{i-1}}{\partial t}\left(1-\frac{V_{i-1}}{Vinv}\right)+\frac{V_i Co\,t}{2\ Vinv\ (t_i-t_{i-1})}\cdot\frac{1}{\sqrt{D\pi}t^2}\left(t_{i-1}\cdot\exp\left[-\left(\frac{t_{i-1}}{2\sqrt{Dt}}-\frac{1}{2\sqrt{D}}\right)^2\right]-t_i\cdot\exp\left[-\left(\frac{t_i}{2\sqrt{Dt}}-\frac{1}{2\sqrt{D}}\right)^2\right]\right) \qquad \text{(B4b)}$$

(c) Derivatives with respect to D

For equation (81),

$$\frac{\partial C_1}{\partial D}=\frac{V_1 Co\,t}{2\ Vinv\ (t_1+t_o)}\left(\frac{\partial}{\partial D}\left[\operatorname{erf}\left(\frac{t_1}{2\sqrt{Dt}}-\frac{1}{2\sqrt{D}}\right)\right]-\frac{\partial}{\partial D}\left[\operatorname{erf}\left(-\frac{1}{2\sqrt{D}}\right)\right]\right)$$

Now $$\frac{\partial}{\partial D}\left[\operatorname{erf}\left(\frac{t_1}{2\sqrt{Dt}}-\frac{1}{2\sqrt{D}}\right)\right]=\frac{2}{\sqrt{\pi}}\left(\exp\left[-\left(\frac{t_1}{2\sqrt{Dt}}-\frac{1}{2\sqrt{D}}\right)^2\right]\cdot\left(\frac{1}{4D^{3/2}}-\frac{t_1}{4tD^{3/2}}\right)\right)$$

And $$\frac{\partial}{\partial D}\left[\operatorname{erf}\left(-\frac{1}{2\sqrt{D}}\right)\right]=\frac{2}{\sqrt{\pi}}\left(\exp\left(-\frac{1}{4D}\right)\cdot\left(\frac{1}{4D^{3/2}}\right)\right)$$

So $$\frac{\partial C_1}{\partial D}=\frac{V_1 Co\,t}{2\ Vinv\ (t_1+t_o)}\left[\frac{2}{\sqrt{\pi}}\left(\left(\frac{1}{4D^{3/2}}-\frac{t_1}{4tD^{3/2}}\right)\cdot\exp\left[-\left(\frac{t_1}{2\sqrt{Dt}}-\frac{1}{2\sqrt{D}}\right)^2\right]-\left(\frac{1}{4D^{3/2}}\right)\cdot\exp\left(-\frac{1}{4D}\right)\right)\right] \qquad \text{(B5a)}$$

Similarly for equation (B2),

$$\frac{\partial C_i}{\partial D} = \frac{V_i C o \bar{t}}{2\ Vinv\ (t_i - t_{i-1})}\left[\frac{2}{\sqrt{\pi}}\left(\frac{1}{4D^{3/2}} - \frac{t_i}{4\bar{t}D^{3/2}}\right)\cdot exp\left[-\left(\frac{t_i}{\sqrt{D\bar{t}}} - \frac{1}{2\sqrt{D}}\right)^2\right] - \left(\frac{1}{4D^{3/2}} - \frac{t_{i-1}}{4\bar{t}D^{3/2}}\right)\cdot exp\left[-\left(\frac{t_{i-1}}{2\sqrt{D\bar{t}}} - \frac{1}{2\sqrt{D}}\right)^2\right]\right] + \frac{\partial C_{i-1}}{\partial D}\left(1 - \frac{V_{i-1}}{Vinv}\right) \qquad (B5b)$$

(d) Derivatives with respect to Vinv

For equation (B1),

$$\frac{\partial C_1}{\partial Vinv} = \frac{C_1}{Vinv} \qquad (B6a)$$

For equation (B2)

$$\frac{\partial C_i}{\partial Vinv} = \frac{V_i C o \bar{t}}{2\ Vinv^2\ (t_i - t_{i-1})}\left(erf\left(\frac{t_i}{2\sqrt{D\bar{t}}} - \frac{1}{2\sqrt{D}}\right) - erf\left(\frac{t_{i-1}}{2\sqrt{D\bar{t}}} - \frac{1}{2\sqrt{D}}\right)\right) + \left(1 - \frac{V_{i-1}}{Vinv}\right)\cdot\frac{\partial C_{i-1}}{\partial Vinv} + C_{i-1}\left(\frac{V_{i-1}}{Vinv^2}\right) \qquad (B6b)$$

For single input experiments equation. (B1) to (B6) were used in SOFSQ.

B.1.2. Multi-input experiments

For these experiments the equations used to describe the residence time distributions were;

$$C_1 = \sum_{k=1}^{m} C_{1,k} \qquad m \leq 4 \qquad (B7)$$

$$C_i = \sum_{k=1}^{m} C_{i,k} \qquad m \leq 4 \qquad 3)$$

where $C_{1,k}$ and $C_{i,k}$ were given by equations (B1) and (B2) respectively using the relevant values of $\bar{t}k$.

The derivatives of these equations with respect to the parameters are;

$$\frac{\partial C_1}{\partial Co} = \sum_{k=1}^{m} \frac{C_{1,k}}{Co} \qquad m \leq 4 \qquad \text{(B9a)}$$

$$\frac{\partial C_i}{\partial Co} = \sum_{k=1}^{m} \frac{C_{i,k}}{Co} \qquad m \leq 4 \qquad \text{(B9b)}$$

$$\frac{\partial C_1}{\partial \bar{t}k} = \frac{\partial C_{1,k}}{\partial \bar{t}k} \quad k = 1, \ldots, m; \quad m \leq 4 \qquad \text{(B10a)}$$

$$\frac{\partial C_i}{\partial \bar{t}k} = \frac{\partial C_{i,k}}{\partial \bar{t}k} \quad k = 1, \ldots, m; \quad m \leq 4 \qquad \text{(B10b)}$$

where equations (B4a) and (B4b) give the values for $\frac{\partial C_{1,k}}{\partial \bar{t}k}$ and $\frac{\partial C_{i,k}}{\partial \bar{t}k}$ respectively using the relevant values of $\bar{t}k$.

$$\frac{\partial C_1}{\partial D} = \sum_{k=1}^{m} \frac{\partial C_{1,k}}{\partial D} \qquad m \leq 4 \qquad \text{(B11a)}$$

$$\frac{\partial C_i}{\partial D} = \sum_{k=1}^{m} \frac{\partial C_{i,k}}{\partial D} \qquad m \leq 4 \qquad \text{(B11b)}$$

where values of $\frac{\partial C_1,k}{\partial D}$ and $\frac{\partial C_i,k}{\partial D}$ are given by equations (B5a) and (B5b) respectively using the relevant values of $\bar{t}k$.

$$\frac{\partial C_1}{\partial Vinv} = \sum_{k=1}^{m} - \frac{C_1,k}{Vinv} \qquad m \leq 4 \qquad \text{(B12a)}$$

$$\frac{\partial C_i}{\partial Vinv} = \sum_{k=1}^{m} \frac{\partial C_i,k}{\partial Vinv} \qquad m \leq 4 \qquad \text{(B12b)}$$

where values of $\frac{\partial C_i,k}{\partial Vinv}$ are given by equation (B6b) using the relevant values of $\bar{t}k$. Equations (B7) to (B12) were used to calculate the values required by SOFSQ and for multi-input experiments.

B.1.3. Single input experiments to beneath electrode tips

$$C_1 = \frac{Co}{Vinv} \qquad \text{(B13)}$$

$$C_i = C_{i-1}\left(1 - \frac{V_{i-1}}{Vinv}\right) \qquad \text{(B14)}$$

The derivatives of these equations with respect to the parameters are;

$$\frac{\partial C_1}{\partial Co} = \frac{1}{Vinv} \qquad \text{(B15a)}$$

$$\frac{\partial C_i}{\partial Co} = \frac{\partial C_{i-1}}{\partial Co}\left(1 - \frac{V_{i-1}}{Vinv}\right) \qquad \text{(B15b)}$$

$$\frac{\partial C_1}{\partial Vinv} = - \frac{Co}{Vinv^2} \tag{B16a}$$

$$\frac{\partial C_i}{\partial Vinv} = \frac{\partial C_{i-1}}{\partial Vinv}\left(1 - \frac{V_{i-1}}{Vinv}\right) + C_{i-1}\left(\frac{V_{i-1}}{Vinv^2}\right) \tag{B16b}$$

Equations (B13) to (B16) were used in the calculations performed by SOFSQ for these experiments.

For each of the three types of experiments described above a different variation of SOFSQ was used. However, in each case SOFSQ performed the same functions, namely;

(i) To return values for the sum of squares and coefficient matrix when called by LBREG to do so.

(ii) To call the subroutine ANSWER when regression analysis was complete.

B.2. Main program MAIN

The purposes of this program were for the input of data and for the calling of LBREG. The input of the following data was achieved via MAIN for all applications of the computer program;

(i) The number of experimental points.

(ii) At each experimental point;

(a) Time lapse after radio-tracer input.

(b) The corrected counts recorded.

(c) The mass tapped. This was used to calculate the volume tapped (V_j).

(iii) The time lapse between the tapping immediately prior to radio-tracer input and radio-tracer input (t_o).

(iv) The maximum iterations to be performed by LBREG for each set of initial parameter values.

(v) The number of sets of initial parameter values to be regressed upon.

(vi) For multi-input experiments the number of $\bar{t}$'s to be considered. (To a maximum of 4).

(vii) The values of the initial parameters in each set of initial parameter values.

In experiments where the measured residence time distributions were truncated at the start of the distribution additional data input via MAIN was the times of tappings at which no counts were available

the volumes tapped at these tappings. The computer program was then used to predict the counts at these points.

In addition to performing an input function and calling LBREC, MAIN was used for the output of the final parameter values obtained for each set of initial values.

A copy of the actual computer program follows.

```
L.0001      DIMENSION B(10),TCL(10),X(10),B(10),C(10,11),E(11)
L.0002      DIMENSION T(40),F(40),D(40)
L.0003      COMMON T,F,C,NUM,TO,NEM,PEN,IR1
L.0004      NEM=0
L.0005      PEN=0
L.0006      READ(5,1) NUM
L.0007    1 FORMAT(I2)
L.0008      DO 2 I=1,NUM
L.0009    2 READ(5,3) T(I),F(I),D(I)
L.0010    3 FORMAT(3E12.4)
L.0011      READ(5,4) TO
L.0012    4 FORMAT(E12.6)
L.0013      NIM=NEM+1
L.0014      BETA=0.25
L.0015      ICPT=-1
L.0016      NEN=2
L.0017      ICUT=6
L.0018      MAX=100
L.0019      READ(5,9) M
L.0020    9 FORMAT(I1)
L.0021      TOL(1)=1.
L.0022      TOL(2)=.001
L.0023      TOL(3)=.000001
L.0024      TOL(4)=.001
L.0025      TOL(5)=.001
L.0026      TOL(6)=.001
L.0027      TOL(7)=.001
L.0028      DO 5 J=8,10
L.0029    5 TOL(J)=1.0E-25
L.0030      DO 6 K=1,11
L.0031    6 E(K)=1.0E-25
L.0032      READ(5,7) IR1
L.0033    7 FORMAT(I1)
L.0034      IR2=10*IR1
L.0035      DO 2004 JY=1,IR2
L.0036 2004 READ(5,2005) B(JY)
L.0037 2005 FORMAT(E12.6)
L.0038      CALL LBRBGI(BETA,B,TCL,M,ICPT,NEN,E,ICUT,MAX)
L.0039      STOP
L.0040      END
```

```
      SUBROUTINE LBREG(BETA,B,TOL,M,ICPT,NEWT,E,ICUT,MAX)
C     MODIFICATION 1   19/8/68    USE COCRT  MOD 1
      DIMENSION B(10),TOL(10),X(10),BI(10),C(10,11),E(11)
      ALPHA=1.0
      ITNO=1
      LAB = 0
   23 MATRX = 1
      CALL SCFSQ(LAB,MATRX,C,SA,B)
   24 SAI = SA
      IF(ITNO - MAX)124,124,34
  124 CALL COCRT (C,X,M,P)
      DT = 0.0
      WRITE (IOUT,301) ALPHA
  301 FORMAT (11H  ALPHA WAS,E16.7,15H LAST ITERATION)
      WRITE(IOUT,204)SA,ITNO
  204 FORMAT(18H SUM OF SQUARES IS,E11.4,22H AT START OF ITERATION,  I4)
      ITNO = ITNO + 1
      WRITE(IOUT,202)
  202 FORMAT (33H PARAMETERS AND PREDICTED CHANGES)
      DO 25 K=1,M
      DT = X(K)*C(K,M+1)+DT
      WRITE(IOUT,205)P(K),X(K)
   25 BI(K) = X(K)
      DT = NEWT*SA-(1-NEWT)*IOPT*DT
      ALPHA = 1.0
      IF(DT)26,128,128
   26 DO 27 K=1,M
   27 X(K) = -X(K)
      DT = -DT
  128 CONTINUE
      DO 29 K=1,M
   29 BI(K) = BI(K)+ALPHA*X(K)
      CALL SCFSQ(LAB,MATRX,C,SA,B)
      S = SA
      DELSA = IOPT*(SA-SAI)
      IF(DELSA -BETA*DT*(2.0*ALPHA-ALPHA*ALPHA))30,31,31
   30 ALPHA = ALPHA/ALOG(SA/SAI+7.5)
      MATRX = 0
      DO 40 K=1,M
      IF(ABS(ALPHA*X(K))-ABS(1.0E-07*BI(K)))40,40,128
   40 CONTINUE
      WRITE(IOUT,206)
  206 FORMAT (29H NO IMPROVEMENT IN ALPHA LOOP)
      GO TO 34
   31 DO 33 K=1,M
      IF(ABS(X(K))-TOL(K))32,33,33
   32 IF(MATRX)23,23,24
   33 CONTINUE
C     OUTPUT PHASE
   34 LAB = 1
      MATRX = 1
      CALL SCFSQ(LAB,MATRX,C,SA,B)
      WRITE(IOUT,205)
      DO 15 K=1,M
```

```
L.0055     15 WRITE(IOUT,216)P(K),TOL(K),X(K)
L.0056        WRITE(IOUT,209)
L.0057        WRITE(IOUT,306)SA,ALPHA
L.0058        WRITE(IOUT,210)
L.0059        L=M+1
L.0060        DO 16 I=1,M
L.0061     16 WRITE(IOUT,214)(C(I,J),J=1,M)
L.0062        CALL CORRT (C,X,M,F)
L.0063        FINF = F(M+1)/SA
L.0064        WRITE(IOUT,212)FINF
L.0065        WRITE(IOUT,211)
L.0066        DO 17 I=1,M
L.0067     17 WRITE(IOUT,214)(C(I,J),J=1,M)
L.0068    214 FORMAT (2HO ,8E15.7)
L.0069    209 FORMAT(2E15.7)
L.0070    216 FORMAT(E16.7,F14.4,F26.7)
L.0071    306 FORMAT(E15.7,F12.4)
L.0072    208 FORMAT (1HO,50H PARAMETERS  TOLERANCES REQD.  TOLERANCES ACHIEVED)
L.0073    209 FORMAT(1HO,24H SUM OF SQUARES     ALPHA)
L.0074    210 FORMAT(1HO,19H INFORMATION MATRIX)
L.0075    211 FORMAT(1HO,17H VAR. COV. MATRIX)
L.0076    212 FORMAT(/34H INFORMATION PER OBSERVATION POINT,E16.7)
L.0077        RETURN
L.0078        END
L.0079        SUBROUTINE CORRT(C,X,N,TOL)
L.0080        DIMENSION  C(10,11),X(10),LLL(11),A(10,11),TOL(11)
L.0081 C      MOD 2  INTERCHANGES ROWS AND COLUMNS IF MATRIX IS SINGULAR
L.0082        F=TOL(10)
L.0083        NN=N+1
L.0084        DO 501 I=1,N
L.0085    501 LLL(I)=1
L.0086        DO 502 I=1,N
L.0087        DO 502 J=1,NN
L.0088    502 A(I,J)=C(I,J)
L.0089        LL=0
L.0090        L=1
L.0091    503 IF(L-1)506,504,506
L.0092    504 IF(ABS(A(1,1))-F) 521,521,505
L.0093    505 LL=0
L.0094        L=L+1
L.0095    506 DO 507 JJ=1,N
L.0096        J=N+2-JJ
L.0097    507 A(1,J)=A(1,J)/A(1,1)
L.0098        JJ = N + 1
L.0099    508 NN=J-1
L.0100        JJ=JJ-1
L.0101        DO 509 II=2,JJ
L.0102        I=N+2-II
L.0103        DO 509 K=1,NN
L.0104    509 A(I,J)=A(I,J)-A(1,K)*A(K,J)
L.0105        IF (L - J) 412,510,412
L.0106    510 IF (ABS(A(J,J))-F) 521,521,511
L.0107    511 LL=0
L.0108        L=L+1
L.0109    412 II = JJ + 1
L.0110        II = II - 2
L.0111        DO 514 JJ=1,II
L.0112        J=N+2-JJ
L.0113        DO 513 K=1,NN
```

```
L.C114    513 A(I,J)=A(I,J)-A(I,K)*A(K,J)
L.C115    514 A(I,J)=A(I,J)/A(I,I)
L.C116        JJ = II + 1
L.C117        IF(J-(N+1))509,516,516
L.C118    516 LL=LL+2
L.C119        DO 517 II=LL,N
L.C120        I=N+1-II
L.C121        NN=I+1
L.C122        DO 517 K=NN,N
L.C123    517 A(I,N+1)=A(I,N+1)-A(I,K)*A(K,N+1)
L.C124        DO 520 I=1,N
L.C125        K=1
L.C126    518 IF(LLL(K)-I)519,520,519
L.C127    519 K=K+1
L.C128        GOTO 518
L.C129    520 X(I)=A(K,N+1)
L.C130        GOTO 532
L.C131 C       SPECIFY APPROPRIATE OUTPUT DEVICE NUMBER-------
L.C132 C       THE NUMBER 3 IN STATEMENT NO. 521 IS THE IBM 1130 PRINTER------
L.C133    521 WRITE(3,528) L,L,A(L,L)
L.C134        IF(LL-N+1)527,522,527
L.C135    522 DO 523 I=L,N
L.C136        A(I,I) = 0.0
L.C137    523 A(I,N+1)=0.0
L.C138        GOTO 516
L.C139    527 NN=N+1
L.C140    528 FORMAT(3H A(,I2,I2,2H)=,E13.5)
L.C141        DO 529 I=1,N
L.C142        LLL(I)=I
L.C143        DO 529 J=1,NN
L.C144    529 A(I,J)=C(I,J)
L.C145        NN=N-1
L.C146        DO 530 I=1,N
L.C147        A(I,L)=C(I,NN)
L.C148    530 A(I,NN)=C(I,L)
L.C149        K = N + 1
L.C150        DO 540 J=1,K
L.C151        TOL(I)=A(NN,J)
L.C152        Z(NN,J) = A(L,J)
L.C153    540 A(L,J ) = TOL(I)
L.C154        LLL(L)=NN
L.C155        LLL(NN)=L
L.C156        LL=LL+1
L.C157        GOTO 503
L.C158    532 CONTINUE
L.C159        TOL(N+1)=1.0
L.C160        DO 533 J = 1,N
L.C161    533 TOL(N+1) = TOL(N+1)*A(J,J)
L.C162        RETURN
L.C163        END
L.C164        SUBROUTINE SOESO(LAP,MATRX,C,SA,B)
L.C165        DIMENSION C4(40),T1(40),O2(40),C3(40),D4(40)
L.C166        DIMENSION T(40),F(40),D(40)
L.C167        DIMENSION Z(40)
L.C168        COMMON T,F,D,NUM,TO,MEM,MEN,IR1
L.C169        MEM=MEM+1
L.C170        DIMENSION B1(40),B2(40),B3(40),C1(40),C2(40),C3(40)
L.C171        DIMENSION VAL(40),VAT(40),A1(40),A2(40),A3(40)
L.C172        DIMENSION B(10),VEL(10,11),A(10,40),C(10,11),SUM(40)
```

```
L.0114    513 A(I,J)=A(I,J)-A(I,K)*A(K,J)
L.0115    514 A(I,J)=A(I,J)/A(I,I)
L.0116        JJ = II + 1
L.0117        IF(J-(N+1))508,516,516
L.0118    516 LL=LL+2
L.0119        DO 517 II=LL,N
L.0120        I=N+L-II
L.0121        NN=I+1
L.0122        DO 517 K=NN,N
L.0123    517 A(I,N+1)=A(I,N+1)-A(I,K)*A(K,N+1)
L.0124        DO 520 I=1,N
L.0125        K=1
L.0126    518 IF(LLL(K)-I)519,520,519
L.0127    519 K=K+1
L.0128        GOTO 518
L.0129    520 X(I)=A(K,N+1)
L.0130        GOTO 532
L.0131 C       SPECIFY APPROPRIATE OUTPUT DEVICE NUMBER-------
L.0132 C       THE NUMBER 3 IN STATEMENT NO. 521 IS THE IBM 1130 PRINTER-------
L.0133    521 WRITE(3,528) L,L,A(L,L)
L.0134        IF(LL-N+L)527,522,527
L.0135    522 DO 523 I=L,N
L.0136        A(I,I) = 0.0
L.0137    523 A(I,N+1)=0.0
L.0138        GOTO 516
L.0139    527 NN=N+1
L.0140    528 FORMAT(3H A(,I2,I2,2H)=,E13.5)
L.0141        DO 529 I=1,N
L.0142        LLL(I)=I
L.0143        DO 529 J=1,NN
L.0144    529 A(I,J)=C(I,J)
L.0145        NN=N-LL
L.0146        DO 530 I=1,N
L.0147        A(I,L)=C(I,NN)
L.0148    530 A(I,NN)=C(I,L)
L.0149        K = N + 1
L.0150        DO 540 J=1,K
L.0151        TOL(I)=A(NN,J)
L.0152        A(NN,J) = A(L,J)
L.0153    540 A(L,J ) = TOL(I)
L.0154        LLL(L)=NN
L.0155        LLL(NN)=L
L.0156        LL=LL+1
L.0157        GOTO 503
L.0158    532 CONTINUE
L.0159        TOL(N+1)=1.0
L.0160        DO 533 J = 1,N
L.0161    533 TOL(N+1) = TOL(N+1)*A(J,J)
L.0162        RETURN
L.0163        END
L.0164        SUBROUTINE SOLSQ(LAB,MATRX,C,SA,P)
L.0165        DIMENSION C1(40),C1(40),C2(40),C3(40),D4(40)
L.0166        DIMENSION T(40),P(40),D(40)
L.0167        DIMENSION Z(40)
L.0168        COMMON T,P,D,SUM,TO,NEM,MEN,IRI
L.0169        NIM=NEM+1
L.0170        DIMENSION B1(40),B2(40),B3(40),C1(40),C2(40),C3(40)
L.0171        DIMENSION VAL(40),VRT(40),A1(40),A2(40),A3(40)
L.0172        DIMENSION B(10),VEL(10,11),A(10,40),C(10,11),SUM(40)
```

```
L.0173        IF(B(1)) 555,40,40
L.0174     40 IF(B(2)) 555,41,41
L.0175     41 IF(B(3)) 555,42,42
L.0176     42 IF(B(4)) 555,556,556
L.0177    556 P1=4.*ATAN(1.)
L.0178        N=NUM
L.0179        JR1=IR1+3
L.0180        DO 888 JR2=1,JR1
L.0181        DO 888 JR3=1,N
L.0182    888 A(JR2,JR3)=0.
L.0183        DO 702 IR4=1,N
L.0184    702 C4(IR4)=0.
L.0185        DO 700 IR2=1,IR1
L.0186        P2=SQRT(P1)
L.0187        P3=SQRT(B(1))
L.0188        P4=1./(4.*SQRT(B(3)*B(3)*B(3)))
L.0189        P5=1./(P2*P3*(B(3+IR2)**2))
L.0190        P6=-1./(2.*P3)
L.0191        CALL ERRINT(P6,B0,CC)
L.0192        DO 1 I=1,N
L.0193        A1(I)=T(I)/(2.*P3*B(3+IR2))+P6
L.0194        CALL ERRINT(A1(I),P1(I),C1(I))
L.0195        D1(I)=P(I)/6.**5
L.0196        A2(I)=(D1(I)*P(1))/(2.*B(3))
L.0197        C2(I)=(T(I)*P4)/E(3*IP2)
L.0198        B2(I)=(2./P2)*(P4-C2(I))
L.0199        D2(I)=(1.-(D1(I)/B(2)))
L.0200        D3(I)=D1(I)/(B(2)**2)
L.0201        C3(I)=((T(I)/(2.*P3*B(3+IR2)))+P6)**2
L.0202        B3(I)=EXP(-C3(I))
L.0203        M=I-1
L.0204        IF(M) 100,100,101
L.0205    100 VRT(I)=((B1(I)-B0)*A2(I)*B(3+IR2))/(T(I)+T0)
L.0206        C4(I)=C4(I)+VRT(I)
L.0207        GO TO 102
L.0208    102 IF(I-N) 1,1,103
L.0209    101 VRT(I)=(((B1(I)-B1(M))*A2(I)*B(3+IR2))/(T(I)-T(M)))
L.0210        VRT(I)=VRT(I)+VRT(M)*D2(M)
L.0211        C4(I)=C4(I)+VRT(I)
L.0212        GO TO 333
L.0213    333 IF(I-N) 1,1,103
L.0214    103 VAL(I)=P(I)-C4(I)
L.0215        GO TO 1
L.0216      1 CONTINUE
L.0217        IF(MAT+X) 3,3,2
L.0218      2 DO 4 J=1,N
L.0219        M=J-1
L.0220        IF(M) 104,104,105
L.0221    104 A(1,J)=A(1,J)+VRT(J)/P(1)
L.0222        A(3+IR2,J)=-(P*RT(J)*P3(J)*A2(J)*B(3+IR2))/(T(J)+T0)+VRT(J)/B(2)
L.0223        Z(J)=(D2(J)*B3(J)*A2(J)*B(3+IR2))/(T(J)+T0)
L.0224        A(3,J)=A(3,J)+Z(J)-(A2(J)*B(3+IR2)*P4*EXP(-1./4.*(B(J)))/(T(J)+T0))*(2./P2)
L.0225        A(2,J)=A(2,J)-VRT(J)/P(2)
L.0226        GO TO 4
L.0227    105 A(1,J)=A(1,J)+((P1(J)-P1(M))*A2(J)*P(3+IR2))/(B(1)*(T(J)-T(M)))
L.0228        A3(J)=(A2(J)*P(3+IP2)/(T(J)-T(M)))*(P5*(T(M)*B3(M)-T(J)*B3(J)))
L.0229        A(3+IR2,J)=A3(J)+A2(J)*(B1(J)-B1(M))/(T(J)-T(M))+A(2,M)*D2(M)
L.0230        C4(J)=(B2(J)*B3(J)-B2(M)*B3(M))*A2(J)*B(3+IR2)/(T(J)-T(M))
L.0231        A(3,J)=A(3,J)+D4(J)
```

```
L.0232          A(2,J)=A(2,J)-A2(J)*B(3+IR2)*(B1(J)-B1(M))/(B(2)*(T(J)-T(M)))
L.0233          IR3=IR2-IR1
L.0234          IF(IR3) 4,701,701
L.0235      701 A(1,J)=A(1,J)+A(1,M)*D2(M)
L.0236          A(3,J)=A(3,J)+A(3,M)*D2(M)
L.0237          A(2,J)=A(2,J)+A(2,M)*D2(M)+C4(M)*D3(M)
L.0238          GO TO 4
L.0239        4 CONTINUE
L.0240      700 CONTINUE
L.0241          IR5=3+IR1
L.0242          DO 5 K=1,IR5
L.0243          DO 5 L=1,IR5
L.0244          C(K,L)=0.
L.0245          DO 5 M=1,N
L.0246          VEL(K,L)=A(K,M)*A(L,M)+C(K,L)
L.0247        5 C(K,L)=VEL(K,L)
L.0248          DO 6 I=1,IR5
L.0249          SUM(I)=0.
L.0250          DO 6 J=NIM,N
L.0251          IF(J.EQ.MEN) GO TO 6
L.0252          C(I,IR5+1)=VAL(J)*A(I,J)+SUM(I)
L.0253        6 SUM(I)=C(I,)**+1)
L.0254          GO TO 3
L.0255        3 SO=0.
L.0256          DO 7 K=NIM,N
L.0257          IF(K.EQ.MEN) GO TO 7
L.0258          SA=VAL(K)**2+SO
L.0259        7 SO=SA
L.0260          IF(LAU) 4,8,9
L.0261        9 CALL ANSWER(T,F,VRT,N,NEM)
L.0262          GO TO 8
L.0263        8 RETURN
L.0264      555 SA=1.0E+74
L.0265          N=NUM
L.0266          IF(MATEX) 557,557,558
L.0267      558 IR4=IR5+1
L.0268          DO 559 I=1,IR4
L.0269          DO 559 J=1,IR4
L.0270      559 C(I,J)=C(I,J)
L.0271          GO TO 557
L.0272      557 IF(LAU) 560,560,561
L.0273      561 CALL ANSWER(T,F,C4-A,NEM)
L.0274          GO TO 560
L.0275      560 RETURN
L.0276          END
L.0277          SUBROUTINE ANSWER(T,F,C4,N,NEM)
L.0278          DIMENSION T(40),F(40),C4(40)
L.0279          WRITE(6,1)
L.0280        1 FORMAT(/20H  TIME     MEASURE  CALCULT)
L.0281          NIM=NEM+1
L.0282          IF(NEM) 6,6,7
L.0283        7 DO 4 J=1,NEM
L.0284        4 WRITE(6,5) T(J),C4(J)
L.0285        5 FORMAT(L9.3,12H    NONE      E14.8)
L.0286          GO TO 6
L.0287        6 DO 2 I=NIM,N
L.0288        2 WRITE(6,3) T(I),F(I),C4(I)
L.0289        3 FORMAT(E9.3,F12.6,E14.8)
L.0290          RETURN
```

```
L.C291          END
L.0292          SUBROUTINE ERPRT (X, ERF, ERFC)
L.C293          NBC=8
L.C294          NBM=23
L.0295          ONE=1.
L.0296          TWO=2.
L.0297          FOUR=4.
L.0298          ULPS=1.
L.C299          CONS=0.83
L.C300          TRRTPI=1.1283791671
L.C301          RNBC=NBC
L.C302          TOLER=TWO**(-NBM)
L.C303 C        TEST ON ZERO
L.0304          IF (X) 2,1,2
L.0305    1     ERF=0
L.0306          ERFC=ONE
L.0307          RETURN
L.0308        2 Y=ABS(X)
L.0309          YSQ=Y**2
L.0310          IF (Y-ULPS) 3,3,4
L.0311 C        MAXIMUM ARGUMENT
L.0312    4     C1=TWO** ((RNBC-ONE)/TWO)
L.0313          ULOF=CONS*C1
L.0314 C        SCALE FACTOR
L.0315          SCF=TWO**(C1**2-RNBC)
L.0316 C        LIMITING VALUE
L.0317          IF (Y-ULOF) 10,10,11
L.0318   11     ERF=ONE
L.0319          ERFC=0
L.0320          GO TO 7
L.0321 C        METHOD POWER SERIES
L.0322    3     SUM=0
L.0323          DN=ONE
L.0324          TN=ONE
L.0325          PWR=TWO*YSQ
L.0326    6     DN=DN+TWO
L.0327          TN=PWR*TN/DN
L.0328          SUM=TN+SUM
L.0329 C        TOLERANCE CHECK
L.0330          IF (TN-TOLER) 5,5,6
L.0331        5 ERF=(SUM+ONE)*TRRTPI*Y*EXP(-YSQ)
L.0332          ERFC=ONE-ERF
L.0333 C        NEGATIVE ARGUMENT
L.0334    7     IF (X) 8,9,9
L.0335    8     ERF=-ERF
L.0336          ERFC=TWO-ERFC
L.0337    9     RETURN
L.0338 C        METHOD=CONTINUED FRACTION
L.0339   10     FNM2=0
L.0340          GNM2=ONE
L.0341          FNM1=TWO*Y
L.0342          GNM1=TWO * YSQ+ONE
L.0343          PREV=FNM1/GNM1
L.0344          WN=ONE
L.0345          BN=GNM1+FOUR
L.0346   14     AN=-WN*(WN+ONE)
L.0347          FN=BN*FNM1+AN*FNM2
L.0348          GN=BN*GNM1+AN*GNM2
L.0349          F=FN/GN
```

```
L.0350 C      TOLERANCE CHECK
L.0351        IF(ABS(ONE-(F/PREV))-TOLER) 12,12,13
L.0352   13   IF (PREV-F) 17, 17, 18
L.0353 C      BOTH FN AND GN MUST BE TESTED IF ABS (X) .LT. .61
L.0354   17   IF (GN .LT. SCF) GO TO 16
L.0355 C      SCALING
L.0356   15   FN=FN/SCF
L.0357        GN=GN/SCF
L.0358        FNM1=FNM1/SCF
L.0359        GNM1=GNM1/SCF
L.0360   16   FNM2=FNM1
L.0361        GNM2=GNM1
L.0362        FNM1=FN
L.0363        GNM1=GN
L.0364        WN=WN+TWO
L.0365        GN=GN+FOUR
L.0366        PREV=F
L.0367        GO TO 14
L.0368   18   F=PREV
L.0369     12 EXFC=F*EXP(-YSQ)*TWOPI/TWO
L.0370        ERF=ONE-EXFC
L.0371        GO TO 7
L.0372        END
```

APPENDIX C. Estimation of mass capacity of furnaces M10 and M11

The inside furnace volume calculated from furnace dimensions is 402,7 m^3. This volume is occupied by the electrodes, the solid burden, the molten alloy, and the molten slag. The volume occupied by the electrodes may be calculated from the electrode diameter, the hearth floor to stockline distance, and the electrode tip to hearth floor distance. Assuming hemispherical electrode tips this volume is,

$$3 \cdot \pi \times 0,95^2 \{(4,95-2,61 - 0,95) + 0,95 \times 2/3\} = 17,1 \ m^3$$

where, 0,95 m = electrode radius
4,95 m = typical hearth floor to stockline distance
2,61 m = typical electrode tip to hearth floor distance.

Remaining furnace volume is therefore 385,6 m^3.

The permanent alloy inventory is estimated to be 325 tonnes.[74] The density of the alloy (containing 78 mass per cent Mn and 22 mass per cent Fe) is taken as 6,65 tonnes/m^3. This value is calculated by interpolation between the densities of pure Fe and Mn at 20°C and then by assuming that the per cent decrease in density between 20°C and 1600°C for the alloy is the same as that for pure Fe. Values for the densities of pure Fe and Mn at 20°C and for the density of pure Fe at 1500°C are available.[73] The volume occupied by alloy is therefore 48,42 m^3. The remaining furnace volume is therefore 336,28 m^3. The depth of the permanent slag bath in the furnace is estimated to be 0,43 m.[74] The volume occupied by this slag bath can be calculated from inside furnace dimensions (shown in Figure C1) to be

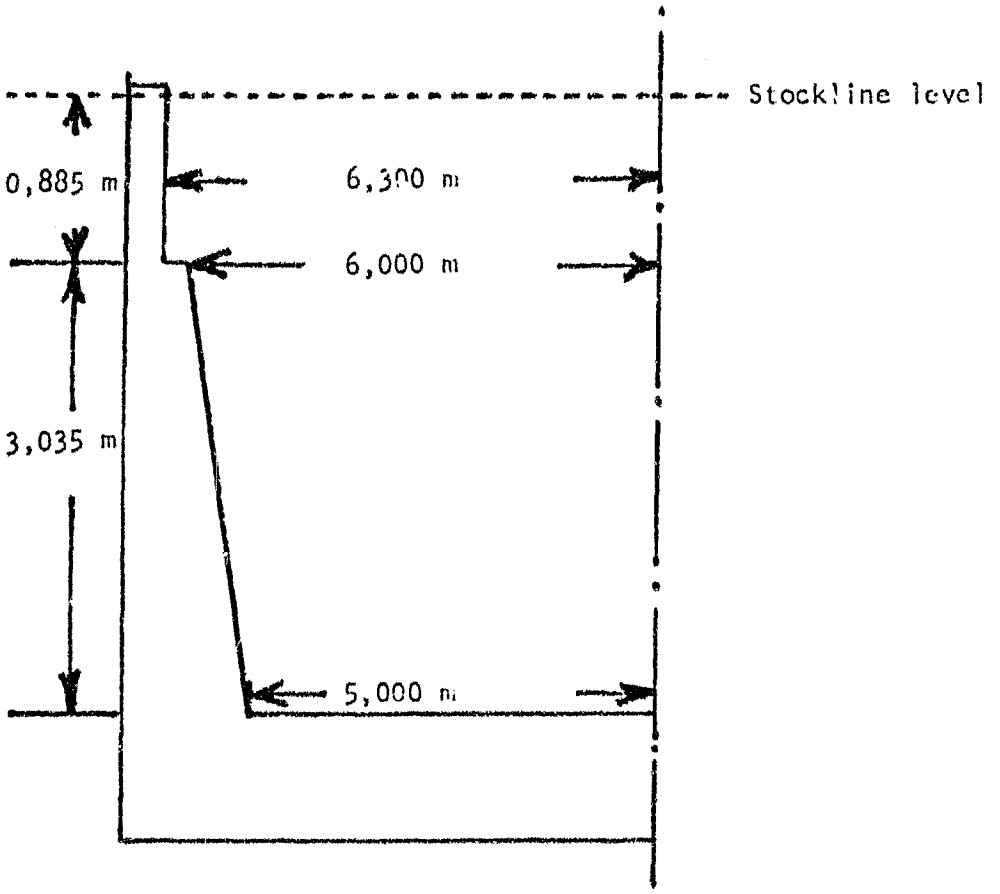

Figure C1. Inside furnace dimensions

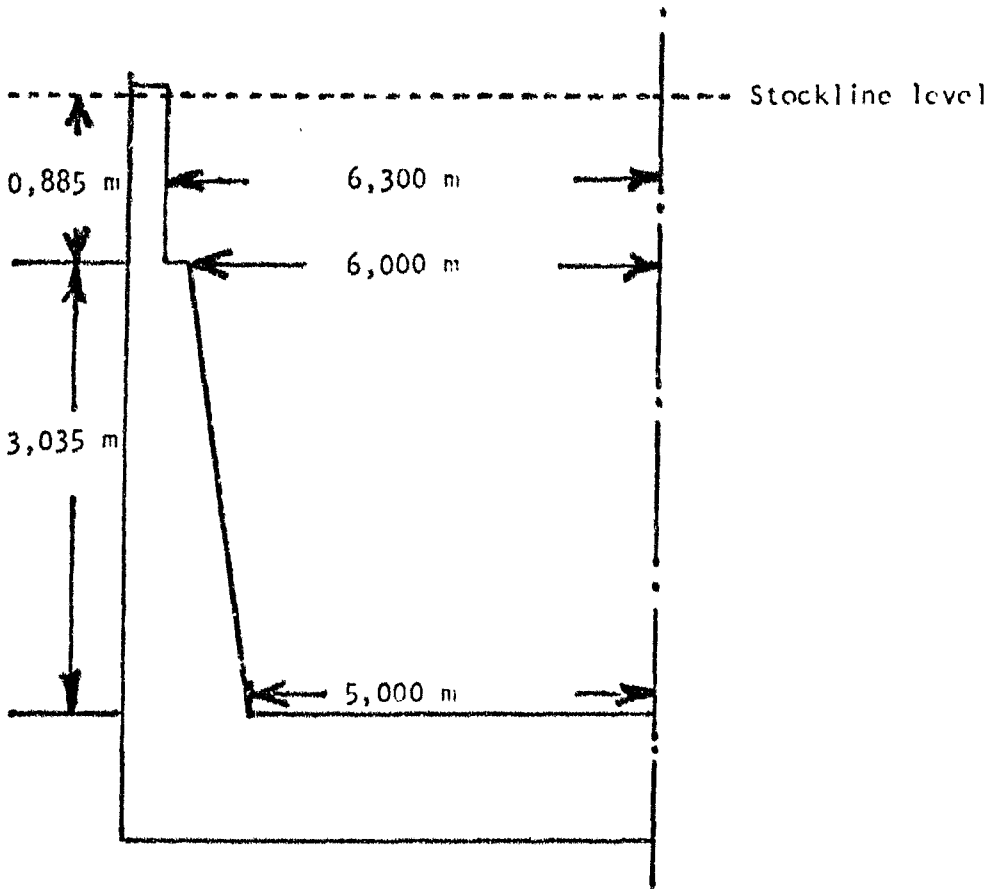

Figure C1. Inside furnace dimensions

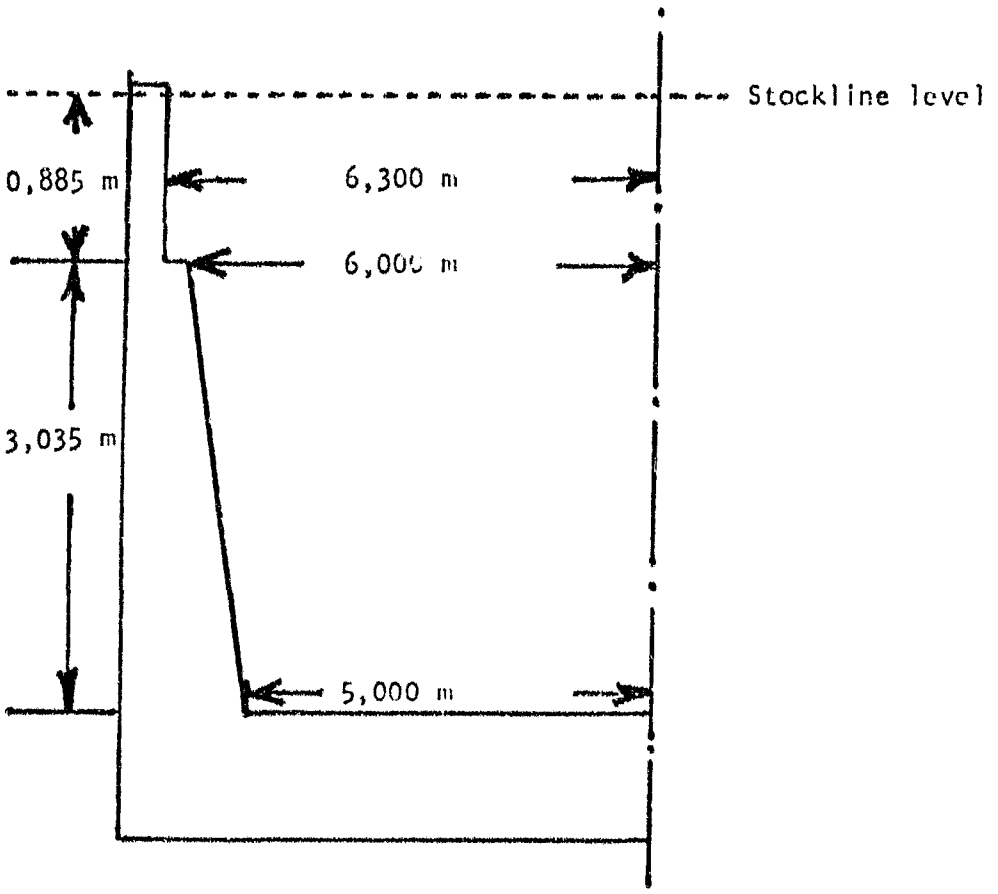

Figure C1. Inside furnace dimensions

39,02 m^3. Assuming the slag density to be that of a melt containing in mass per cent, 34 CaO, 30 Al_2O_3, and 36 SiO_2, at 1500 C the slag density is 2,79 tonnes/m^3. The mass of slag in the furnace is therefore 108,87 tonnes.

The volume remaining is 297,26 m^3. This volume is occupied by solid burden. The density of the solid burden is calculated to be 1,96 tonnes/m^3. This is based on a burden made up of the following components in mass per cent; 45,2 Mamatwan ore, 22,4 Hotazel ore, 11,1 coal, 5,7 coke, 6,8 return slag, 5,7 quartz and 3,1 fine ferromanganese. The following silo design bulk densities are used:-[74]

Hotazel	2,21 tonnes/m^3
Mamatwan	1,76 tonnes/m^3
Coal	0,74 tonnes/m^3
Coke	1,22 tonnes/m^3
Quartz	1,50 tonnes/m^3

The apparent densities of fine solid alloy and fine solid slag were measured to be 7,14 tonnes/m^3 and 3,00 tonnes/m^3 respectively.

Consequently the mass of solid burden in the furnace is taken to be 581,41 tonnes. The mass capacity of the furnace is therefore 1015,28 tonnes.

REFERENCES

1. Mikolajczak, L. Ferro-manganese review. A world Analysis. *Metal Bulletin Monthly* No. 40, April, 1974: pp. 21-23.

2. Volkert, G., *et al.* Ferromanganese and Manganese Metal. The Metallurgy of Ferroalloys. Editors: Volkert, G. and Frank, K.D. Berlin, 1972. 2nd Edition: pp. 393-431. N.I.M. Translation 516, Rep. of South Africa.

3. Hooper, R.T. The production of Ferromanganese. *Elec. Furnace Conf. Proc.* 1967. Ferroalloys pp. 141-145.

4. Selmer-Olsen, S. Trends in Ferro-alloy production. *J., S. Afr. Inst. Min. Met.* May, 1971: pp. 210-214.

5. Woollacott, L.C., *et al.* The viscosities and electrical conductivities of slags associated with the production of high-carbon ferromanganese alloys *1st Internat. Ferroalloy Conf. "Infacon 74"., Proc.*, Johannesburg, April, 1974. Editor: Glenn, H.: pp. 227-232.

6. Warren, G.F., *et al.* Liquidus temperatures and the activities of manganese (II) oxide in slags associated with the production of high-carbon ferromanganese alloys. *Ibid.* pp. 175-185

7. Driller, A. The electrical side of ferroalloy furnaces. The Metallurgy of Ferroalloys. Editors: Volkert, G. and Frank, K.D. Berlin, 1972. 2nd Edition: pp. 130-131. N.I.M. Translation 415, Rep. of South Africa.

8. Olsen, L., *et al.* Temperature distribution in Soderberg electrodes. *Elektrowärme Internat.* Vol. 31, No. B3, June, 1973: pp. B128-B131.

9. van der Walt, Z., Gericke, W.A. The effect of magnitude of scale on various operating characteristics in the production of high carbon ferromanganese in electric smelting furnaces. Presented at the Latin American Seminar on Ferroalloys, Salvador de Bahia (Brazil), June, 1975.

10. King, S.G. Electric smelting furnaces in Southern Africa. *1st Internat. Ferroalloy Conf. "Infacon 74." Proc.* Johannesburg, April, 1974. Editor: Glenn, H.: pp. 135-142.

11. Featherstone, R.A. Applications of Mamatwan manganese ore. *Ibid:* pp. 263-273.

12. Selmer-Olsen, S. Slag-metal relationship in Metalloys high carbon ferro-manganese furnaces. *Ibid:* pp. 209-216.

13. Dewar, K., Koursaris, A. High carbon ferromanganese production at Metalloys Ltd., Meyerton *N.I.M. Technical Mem., No. 10076,* Nov., 1975. Rep. of South Africa.

14. Coetzee, J.J., Smit, N. The production of Ferroalloys. *7th Comm. Min. and Met. Congress*, 1961: pp. 1044-1052.

15. Erwall, Lars-G., Ljunggren, K. Recent uses of Radioisotopes in Technological Research and Control in Sweden. *Proc. 2nd U.N. Internat. Conf.* PUAE, Vol. 19 (1958): pp.3-12.

16. Wildblood, A.M. Investigation of material velocities in continuous process plants by radioisotopes. *Chemistry and Industry*, March 23, 1957: p. 364.

17. Akerman, K., *et al.* Mechanism and rate of passage of materials in rotary kilns. *British Chem. Engineering*, Vol. 11, No. 1, Jan., 1966: pp. 26-29.

18. Rutle, J. Investigation of Material Transport in Wet-Process Rotary Kilns by Radioisotopes. *Pit and Quarry*, Vol. 48, No. 1, 1955: pp. 120-136.

19. Fries, B.A. Residence time of particles in a rotary kiln. 2nd Annual Oak Ridge Conf. April, 1964. *USAEC Rep. TID-7689* (1964) 113: pp. 133-136.

20. Gruzin, P.L., *et al.* Investigation of the blast-furnace process with the aid of radioactive isotopes and radiation. *Stal in English*, April, 1959: pp. 251-256.

21. Pavlik, W.R. Radioisotopes in Blast-Furnace Iron-making Operations *Isotopes and Radiation Technology*. Vol. 9, No. 1, 1971: pp. 8-21.

22. Gudenko, V.N., *et al.* Radioisotope monitoring of the blastfurnace stockline. *Steel in the U.S.S.R.*, July, 1972: pp. 509-511.

23. Polovchenko, I.G. Discussion on the study of blast-furnace materials with radioactive isotopes. *Stal in English*, Sept., 1959: pp. 651-658.

24. Gulyga, D.V., *et al.* Study of the movement of the charge materials in a blast-furnace during the smelting of Kamysh Burun Sinter. *Stal in English*, Aug., 1973: pp. 595-598.

25. Dara, S.S., Misra, V.N. Applications of Radio-isotopes in Metallurgy. *J., Scientific and Industrial Research*, Vol. 29, Sept., 1970: pp. 403-412.

26. Miyagawa, K., *et al.* Applications of Radioisotopes in Steel Works. *Trans., Iron and Steel Inst. of Japan.* Vol. 9, No. 5, 1969: pp. 423-431.

27. Babarykin, N.N., *et al.* Movement of pig iron and slag in the blast-furnace hearth. *Steel in the U.S.S.R.*, Jan., 1960: pp. 16-19.

28. Libby, W.F. Industrial uses of isotopes. *Annual Review of Nuclear Science.* Editor: Segrè, E. Vol. 11, 1961: pp. 461-482.

29. Booth, F. Radioisotopes in the Steel Industry. *Atomic Energy in Australia*, July, 1968: pp. 9-12.

30. Szekely, J. Experimental study of the rate of metal mixing in an open-hearth furnace. *J., Iron and steel Inst.* Vol. 202, June, 1964: pp. 505-508.

31. Balasubramanian, V., Djiakonov, A.I. Investigation of melting and mixing processes during open hearth steelmaking by radiotracer techniques. *Trans., The Indian Inst. of Metals*, June, 1966: pp. 103-107.

32. Engh, T.A., *et al.* Measurement of the residence time distribution for the Worcra steel refiner. *Jernkout. Ann.*, Vol. 155, 1971: pp. 93-97.

33. Jenkins, T.W., *et al.* Application of the Levenspiel Dispersion Model to Metal Flow in Pilot Plant Worcra Continuous Steelmaking Furnace. *Metallurgical Transactions*, Vol. 2, 1971: pp. 1258-1259.

34. Engh, T.A., *et al.* Determination of flow characteristics for a continuous slag-metal reactor. *Nuclear Techniques in the Base Metal Industries; Symp., Proc.* IAEA., Vienna, 1973. pp. 251-264.

35. Nakanishi, K., *et al.* Experimental and theoretical investigation of mixing phenomena in the RH-vacuum process. *Ironmaking and Steelmaking*, 1975, No. 2: pp. 115-124.

36. Nakanishi, K., *et al.* Stirring and its effect on Aluminium Deoxidation of Steel in the ASEA-SKF Furnace: Part 1. Plant Scale Measurements and Preliminary Analysis. *Metallurgical Transactions B.*, Vol. 6B, Mar., 1975: pp. 111-118.

37. Themelis, N.J., Spira, P. Flow Phenomena in Reverberatory Smelting. *Transactions of the Metallurgical Society of AIME*, Vol. 236, June, 1966: pp. 821-828.

38. Urquhart, R.C., *et al.* The smelting of copper-nickel concentrates in an electric furnace. *N.I.M. Report No. 1664*, Sept., 1974. Rep. of South Africa.

39. Kuoppamäki, R., *et al.* Use of activated process materials as tracers in smelter process studies. *Nuclear Techniques in the Base Metal Industries; Symp., Proc.* IAEA., Vienna, 1973: pp. 227-236.

40. Kulcsár, M. Study of chemical processes by isotope tracer techniques. *Radioisotope Tracers in Industry and Geophysics.* IAEA., Vienna, 1967: pp. 425-426.

41. Lewis, C.H. The Measurement of Coal Travel in Continuous Vertical Retorts by means of Radioactive Tallies. *The Gas World*, Vol. 134, Dec., 1951: pp. 505-510.

42. Akerman, K., *et al.* Radioactive-Tracer Studies of the Behaviour of Arsenic and Thallium during Fractional Distillation of Cadmium-Bearing Materials. *J., Inst. Metals*, Vol. 94, 1966: pp. 72-73.

43. Kato, M., *et al.* Application of radioisotopes in the aluminium industry in Japan. *Nuclear Techniques in the Base Metal Industries; Symp., Proc.* IAEA., Vienna, 1973: pp. 37-47.

44. Perko, J.F., Spirko, E.J. Blast furnace refractory lining wear. Status using radioactive sources, Part 2. *Industrial Heating*, Vol. 42, No. 7, 1975: pp. 47-57.

45. Berg, S., *et al.* Continuous Measurement of Lining Wear in Steel Furnaces with Radioisotopes. *J., of Metals*, Vol. 21, No. 2, 1969: pp. 19-22.

46. Booth, E., Pepper, M.D. Determination of blast furnace lining wear by radioisotopes. *BHP Technical Bull.*, Vol. 15, No. 2, 1971: pp. 8-13.

47. Dyason, G.J. Radio-tracer techniques for investigation of bulk flow phenomena in pyrometallurgical processes. *N.I.M. Technical Memo. No. 1, Divisional No. 16082*, Jan., 1976. Rep. of South Africa.

48. Danckwerts, P.V. Continuous flow systems. Distribution of residence times. *Chem. Eng. Sci.*, Vol. 2, No. 1, Feb. 1953: pp. 1-13.

49. Levenspiel, O. Chemical Reaction Engineering. 2nd Edition. Published: John Wiley and Sons, Inc., New York, 1972: Ch. 9. pp. 253-325.

50. Ljunggren, K. Review of the use of radioactive tracers for evaluating parameters pertaining to the flow of material in plant and natural systems. *Radioisotope Tracers in Indust and Geophysics*. IAEA., Vienna, 1967: pp. 308-348.

51. Szekely, J., Themelis, N.J. Rate Phenomena in Process Metallurgy. Published: Wiley-Interscience, New York, 1971: Ch. 15. pp. 515-556.

52. Bullock, R.M., *et al.* Some examples of residence time distribution studies in large scale chemical processes by using radiotracer techniques. *Radioisotope Tracers in Industry and Geophysics.* IAEA., Vienna, 1967: pp. 393-409.

53. Fries, B.A. Solving process engineering problems with radiotracers: Mass transfer. *Chem. Eng. Process Symp. Series,* Vol. 66, No. 106, 1970. Applications of radioisotopes nuclear engineering - Part XXII. pp. 1-6.

54. Levenspiel, O., Smith, W.K. Notes on the diffusion-type model for the longitudinal mixing of fluids in flow. *Chem. Eng. Sci.,* Vol. 6, 1957: pp. 227-233.

55. Östedt, T. Computer evaluation of tracer investigations on systems when output flow is recirculated to the inlet. *Mathematics and Computing Machinery Series,* No. 17, 1969: pp. 1-19. Reproduced: The Clearinghouse for Federal Scientific and Technical Information, Springfield, Virginia 22151.

56. Levenspiel, O. Mixed Models to Represent Flow of Fluid through Vessels. *The Canadian J. of Chem. Eng.,* Vol. 40, Aug., 1962: pp. 135-138.

57. Westly, J. The electrical characteristics of a submerged arc furnace - Resistance and heat distribution. *1st Internat. Ferroalloy Conf. "Infacon 74." Proc.*, Johannesburg, April 1974. Editor: Glenn, H.: pp. 121-127.

58. Andreae, F.V. Design and Control of Ferroalloy Furnaces. *A.I.E.E., Trans.*, Vol. 69, 1950: pp. 557-562.

59. Westly, J. Critical parameters in design and operation of the submerged arc furnaces. *Elec. Furnace Conf.* 1975.

60. Driller, A. The electrical side of ferroalloy furnaces. The Metallurgy of Ferroalloys. Editors: Volkert, G. and Frank, K.D. Berlin, 1972. 2nd Edition: pp. 131-145. M.I.M. Translation 415. Rep. of South Africa.

61. Fitzgerald, A.E., *et al.* Basic Electrical Engineering International Student Edition, 3rd Edition. Published: McGraw-Hill Book Company, New York. Ch. 6.

62. Urquhart, R.C. The dissipation of electrical power in the burden of a submerged-arc furnace. *N.I.M. Report No. 1521*, Feb., 1973. Rep. of South Africa.

63. Semenovich, B.V., Stefanovich, M.A. Energy balance of a furnace in the melting of ferrosilicon. *Steel in the U.S.S.R.* Jan., 1972: pp. 41-43.

64. Otani, Y., *et al.* The inner structure of the submerged arc furnace. *6th Internat. Congress on Electro-heat*, Brighton, 1968. Paper No. 112.

65. Müller, M.B., *et al.* Heat and Mass Transfer in the ferrosilicon Process. *Scandinavian J. of Metallurgy*, Vol. 1, 1972: pp. 145-155.

66. Yamagishi, K., *et al.* A comprehensive analysis of the furnace interior for high carbon ferro-chromium. *1st Internat. Ferroalloy Conf. "Infacon 74."*, *Proc.*, Johannesburg, April, 1974. Editor: Glenn, H.: pp. 143-147.

67. Andersen, H.C. Some Significant Metallurgical Aspects of the Smelting of Pig Iron in Electric Furnaces. *Canadian Min. and Met. Bull.*, July, 1963: pp. 509-516.

68. Channon, W.P., *et al.* The mode of current transfer between electrode and slag in the submerged-arc furnace. *J., S. Afr. Inst. Min. Met.*, Aug., 1974: pp. 4-7.

69. Beek, W.J., *et al.* Residence-time distributions in lamilar flows and during the passage of granular solids through rotary kilns. *Radioisotope Tracers in Industry and Geophysics.* IAEA., Vienna, 1967: pp. 537-549.

70. NG., E.W., Geller, M. A table of integrals of the error function. *J. of Research - National Bureau of Standards - B. Mathematical Sciences*, Vol. 73B, No. 1, 1969: pp. 1-18.

71. Chatfield, C. Statistics for technology. Published: Penguin Books: Penguin Education Studies in applied statistics. General editor: Vesselo, I.R.: Ch. 7. pp. 134-165.

72. King, R.P. Private communication. University of the Witwatersrand, Rep. of South Africa. June-Sept., 1976.

73. The Making, Shaping and Treating of Steel, Ch. 13, part II, p. 338 and Appendix B, p. 1306. Ed. H.E. McGannon. Published: United States Steel, Dec., 1970.

74. Hennessey, D. Private communication. Metalloys (Pty) Limited, Meyerton, Rep. of South Africa, Nov., 1975.

Author Dyason G J
Name of thesis A study of burden movement in Submerged-Arc Furnaces 1977

PUBLISHER:
University of the Witwatersrand, Johannesburg
©2013

LEGAL NOTICES:

Copyright Notice: All materials on the University of the Witwatersrand, Johannesburg Library website are protected by South African copyright law and may not be distributed, transmitted, displayed, or otherwise published in any format, without the prior written permission of the copyright owner.

Disclaimer and Terms of Use: Provided that you maintain all copyright and other notices contained therein, you may download material (one machine readable copy and one print copy per page) for your personal and/or educational non-commercial use only.

The University of the Witwatersrand, Johannesburg, is not responsible for any errors or omissions and excludes any and all liability for any errors in or omissions from the information on the Library website.